

UiT

THE ARCTIC
UNIVERSITY
OF NORWAY

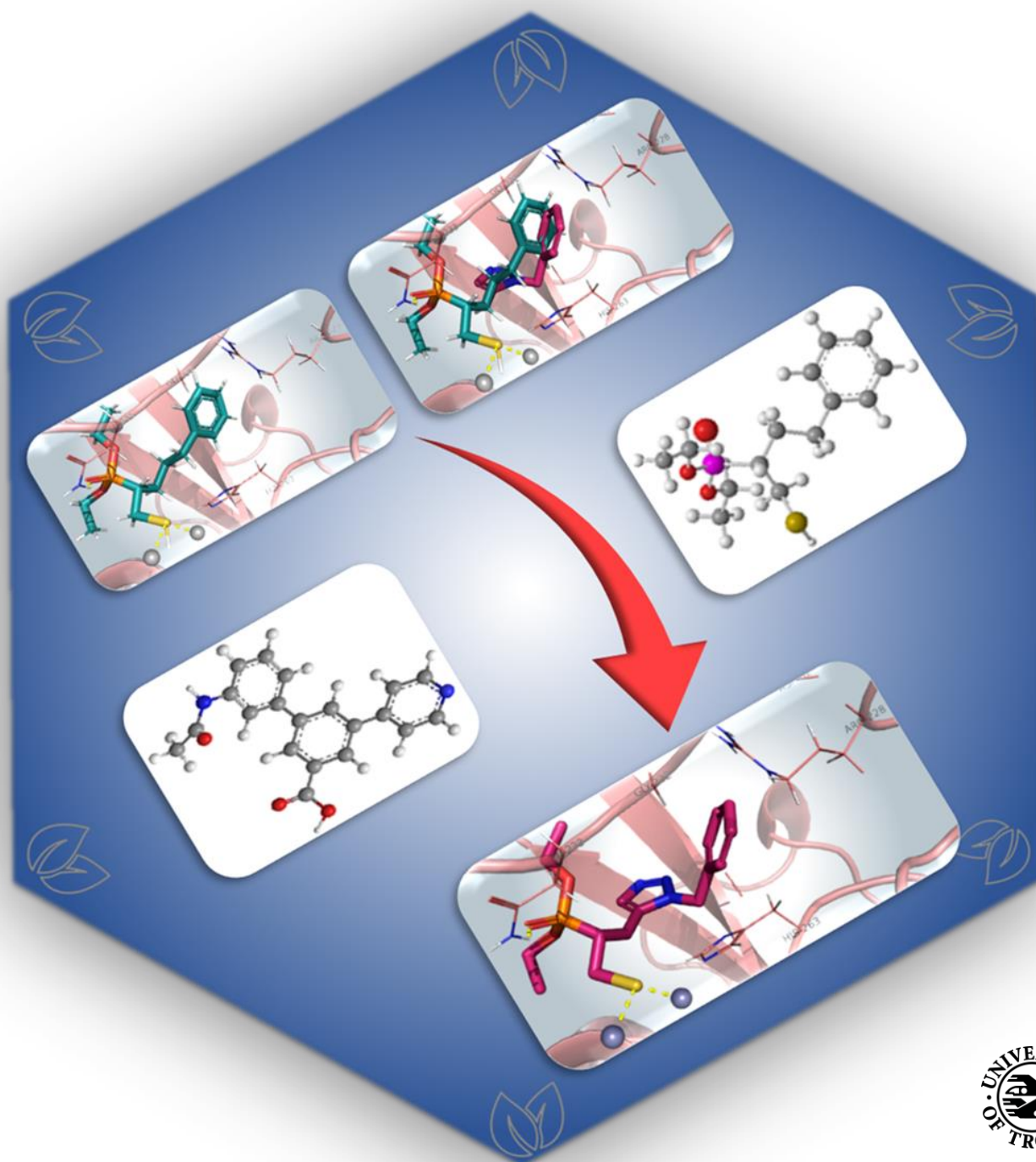
Faculty of Science and Technology

Department of Chemistry

Synthesis and inhibitor design of carbapenemase inhibitors

Sundus Akhter

A dissertation for the degree of Philosophiae Doctor – March 2018



Abstract

The efficiency of bacteria in acquiring resistance for their survival ensures a never-ending war against resistance. The only tactic to curtail the resistance crisis is to keep pace with it, e.g. by continuous development of new antibiotics with activity against resistant bacteria or revival of existing agents by inhibiting the mechanisms of resistance. β -lactams are the largest and most widely used group of antibiotics and can be divided into four main groups penicillins, cephalosporins, monobactams and carbapenems. In response to β -lactams, bacteria can produce β -lactamases (BLs), enzymes that are responsible for hydrolysis and inactivation of β -lactam antibiotics. BLs are the major factor for the resistance towards β -lactam antibiotics. Mechanistically BLs can be divided into two main families – the serine- β -lactamases (SBLs) and metallo- β -lactamases (MBLs). Currently, the main concern is BLs with activity against carbapenems, which is our most important group of β -lactams for the treatment of serious and life-threatening infections. In addition to inactivating carbapenems, these carbapenemases can hydrolyze almost all groups of β -lactams.

The combination of antibiotics with inhibitors is a proven strategy for revival of β -lactams against BLs. Several inhibitors against serine carbapenemase have recently been approved or are in late stage clinical development, however, for MBLs there are no inhibitors on the market. In order to understand and design improved BL inhibitors that could become a potential starting point for the search for broad-spectrum inhibitors, we designed and synthesized mercaptocarboxylate inhibitors using bioisosteric approach and *NH*-triazole based inhibitors targeting the MBLs VIM-2, NDM-1 and GIM-1. In addition, various fragments were also synthesized to explore the active site of the serine carbapenemase OXA-48. Our inhibitors gave different levels of inhibition towards the carbapenemases tested during the course of the study. Overall, the studies described in the thesis identified potent thiol-based and *NH*-triazole based VIM-2 inhibitors, in addition, to various fragments and their improved analogs against OXA-48. Moreover, the X-ray crystal structures of the enzyme-inhibitor complexes, reveal information relevant for further development of the inhibitors, thus providing valuable starting points for design of potent BL inhibitors.

List of Papers

This thesis is based on the following papers:

Paper 1 **Metallo- β -lactamase inhibitors by bioisosteric replacement: Preparation, activity and binding**

Susann Skagseth[#], **Sundus Akhter[#]**, Marianne H. Paulsen, Zeeshan Muhammad, Ørjan, Samuelsen, Hanna-Kirsti S. Leiros, Annette Bayer.
European Journal of Medicinal Chemistry, **2017**, *135*, 159–173.

[#] These authors contributed equally to the paper.

Paper 2 **Triazole inhibitors with promising inhibitory effects against antibiotic resistant metallo- β -lactamases**

Zeeshan Muhammad, Susann Skagseth, **Sundus Ahkter**, Christophe Fröhlich, Tony Christopheit, Annette Bayer, Hanna-Kirsti S. Leiros.

Manuscript.

Paper 3 **A focused fragment library targeting the antibiotic resistance enzyme - Oxacillinase-48: Synthesis, structural evaluation and inhibitor design**

Sundus Ahkter[#], Bjarte Aarmo Lund[#], Aya Ismael, Manuel langer, Johan Isaksson, Tony Christopheit, Hanna-Kirsti Schrøder Leiros, Annette Bayer.

European Journal of Medicinal Chemistry, **2018**, *145*, 634–648.

[#] These authors contributed equally to the paper.

Contribution Report

- Paper 1** I contributed in the development of the synthetic methodology and synthesized, purified and analyzed many of the included compounds. I contributed to the data analysis and wrote parts of the paper.
- Paper 2** I contributed towards the organic synthesis, analysis of the data, design of inhibitors and writing of the manuscript.
- Paper 3** I planned and performed or supervised the synthesis of the compounds. I contributed towards the structure-guided design of the compounds, the interpretation of the results, analysis of the data and wrote parts of the manuscript.

Related publication, not included in this thesis:

Structural insights into TMB-1 and the role of residues 119 and 228 in substrate and inhibitor binding.

Susann Skagseth, Tony Christopeit, **Sundus Akhter**, Annette Bayer, Ørjan, Samuelsen, Hanna-Kirsti S. Leiros.

Antimicrobial Agents and Chemotherapy, **2017**, *61*, e02602–16.

Table of Contents

Abstract.....	i
List of Papers.....	ii
Contribution Report.....	iii
Table of Contents.....	iv
Abbreviations.....	vii
Acknowledgements.....	x
Dedication.....	xi
1. Introduction.....	1
1.1 Aims of the study.....	1
1.2 Outline of the thesis.....	2
2. Relevant background for the thesis.....	3
2.1 History of antibiotics.....	4
2.2 Classification of antibiotics.....	4
2.2.1 β -Lactam antibiotics.....	5
2.3 Antibiotic resistance.....	6
2.3.1 Different modes of bacterial defense mechanisms.....	7
2.3.1.1 Enzymatic β -lactam inactivation.....	7
2.4 β -Lactamases (BLs).....	8
2.4.1 Carbapenemases.....	8
2.4.1.1 Metallo- β -lactamases (MBLs).....	9
2.4.1.1.1 Mechanism of action of MBLs.....	9
2.4.1.2 Serine- β -lactamases (SBLs).....	10
2.4.1.2.1 Mechanism of action of SBLs.....	11
2.5 β -Lactamase inhibitors.....	12
2.5.1 Metallo- β -lactamase inhibitors.....	12

2.5.2	Serine- β -lactamase inhibitors	15
2.6	Drug development.....	18
2.6.1	Structure- and ligand-based drug design	18
2.6.2	Hit generation strategies	18
2.6.2.1	Fragment-based drug design (FBDD).....	19
2.6.3	Bioisosteric replacement.....	21
3.	Metallo-β-lactamase inhibitors by bioisosteric replacement	22
3.1	Rationale for design of bioisosters.....	22
3.2	Reactions utilized in the synthesis	23
3.3	Results and discussion	24
3.3.1	Synthesis.....	24
3.3.2	Evaluation of inhibitors against VIM-2, GIM-1, and NDM-1.....	27
3.4	Conclusion	30
4.	Triazole inhibitors against metallo-β-lactamases	31
4.1	Rationale for the choice and design of triazole based inhibitors.....	31
4.2	Banert cascade (BC) reaction.....	32
4.3	Results and discussion	32
4.3.1	Synthesis.....	32
4.3.2	Evaluation of inhibitors against VIM-2, GIM-1, and NDM-1.....	36
4.4	Conclusion	38
5.	Focused fragment library targeting OXA-48.....	39
5.1	Rationale for the design of fragments	39
5.2	Suzuki-Miyaura coupling reaction (SMC).....	40
5.3	Results and discussion	41
5.3.1	Synthesis.....	41
5.3.1.1	3-Substituted benzoic acid derivatives.....	41
5.3.1.2	Synthesis of 3,5-disubstituted benzoic acid derivatives.....	45
5.3.2	Evaluation of the fragments against OXA-48.....	48
5.4	Conclusion	52
6.	Inhibitor design and future perspective.....	53
6.1	Towards 2 nd generation of thiophosphonate- and triazole-based inhibitors.....	53
6.1.1	2 nd Generation of mercaptophosphonate compounds	53

6.1.2	2 nd Generation of triazole inhibitors	57
6.2	Literature based search for scaffolds directed towards inhibitor development.....	60
6.2.1	Inhibitors active across different subclasses in MBLs.....	61
6.2.1.1	Bisthiazolidines (BTZs)	61
6.2.2	Inhibitors with dual action targeting both SBLs and MBLs.....	63
6.2.2.1	Rhodanine-based inhibitors.....	63
6.2.2.2	Cyclic boronates.....	65
6.2.3	Inhibitors targeting class D SBLs	67
6.2.3.1	Penicillanic acid sulfone-based inhibitors; a possibility to achieve additional interactions	67
6.3	Conclusion	68
7.	Concluding remarks	69
8.	References	70
	Appendix.....	83

Abbreviations

Ala	Alanine
AmpC	Class C β -lactamase
Arg	Arginine
Asn	Asparagine
BL	β -lactamase
BcII	<i>Bacillus cereus</i> metallo- β -lactamase
BC	Banert cascade
BTZ	Bisthiazolidines
CB	Cyclic boronate
CphA	<i>Aeromonas</i> carbapenem-hydrolyzing β -lactamase
Da	Dalton
DMAP	4-Dimethylaminopyridine
DMF	Dimethylformamide
DMSO	Dimethyl sulfoxide
DNA	Deoxyribonucleic acid
EDTA	Ethylemediaminetetraacetic acid
ESBL	Extended Spectrum β -lactamase
Equiv	Equivalent
FBDD	Fragment based drug design
FDA	Food and drug administration
GIM	German imipenemase metallo- β -lactamase
His	Histidine
HPLC	High-performance liquid chromatography
HRMS	High resolution mass spectrometry
HTS	High throughput screening
IC ₅₀	Half maximal inhibitory concentration
Ile	Isoleucine

IMP	Imipenemase
ImiS	Imipenem hydrolyzing metallo- β -lactamase
IPM	Imipenem
K_i	Inhibitory constant
KPC	<i>Klebsiella pneumoniae</i> carbapenemase
L1	<i>Stenotrophomonas maltophilia</i> L1 (β -lactamase 1)
LBDD	Ligand based drug design
L.E	Ligand efficiency
Leu	leucine
lys	Lysine
MBL	Metallo- β -lactamase
MDR	Multidrug resistance
MEM	Meropenem
MIC	Minimum inhibitory concentration
MS	Mass spectrometry
MRSA	Methicillin-resistant <i>Staphylococcus aureus</i>
MW	Micro waves
NDM	New Delhi metallo- β -lactamase
NCF	Nitrocefin
NMR	Nuclear magnetic resonance
Nu	Nucleophile
OXA	Oxacillinase
PBP	Penicillin binding protein
PDB	Protein Data Bank
rt	Room temperature
SAR	Structure activity relationship
SBDD	Structure based drug design
SBL	Serine- β -lactamase

Ser	Serine
Sfh	<i>Serratia fonticola</i> hydrolase
SMC	Suzuki-Miyaura Coupling
SPR	Surface Plasmon Resonance
TB	Tuberculosis
THF	Tetrahydrofuran
Thr	Threonine
TMB	Tripoli metallo- β -lactamase
Trp	Tryptophan
Tyr	Tyrosine
Val	Valine
VIM	Verona integron-encoded metallo- β -lactamase
WHO	World health organization

Acknowledgements

My first and foremost gratitude is to my supervisor Assoc. Prof. Annette Bayer for steering me through the crest and troughs of the PhD path. Thanks for showing trust in my skills and accepting me as your PhD student. Your vision, skills, valuable discussion, encouragement and continuous support specially during the thesis writing process has paved my way to reach towards the completion of my PhD.

I am also obliged to my co-supervisors Dr. Hanna-Kirsti Leiros and Ørjan Samuelson for making me part of their studies and sharing their knowledge with me giving me constant encouragement and support. I owe my appreciation to all the co-authors for the valuable discussions and fantastic input in our publications it has been great working with you all.

My thanks go to the engineers who make our work easy, Truls Ingebrigtsen, Jostein Johansen and specially Arnfinn Kvarsnes for helping me with phosphorus NMR. I am also thankful to Ms. Valentina Vollan and the administrative staff at the Department of Chemistry for providing good working environment.

I am really thankful to Mr. Frederick Leeson for proofreading my thesis and for the interesting talks during the teaching duties. Furthermore, I highly appreciate Marianne H. Paulsen for giving a good start to the MBL project and providing valuable suggestions, thorough proofreading and input for my thesis. I would also like to thank Dr Åsmund Kaupang and Illimar Hugo Rekand at the Department of Chemistry, University of Bergen for their valuable suggestions and proofreading of Chapter 6 of my thesis.

I am truly grateful to Aya Ismael, Fatemeh Shouli Pour, Urna and Amudha for providing a great friendly environment and ‘smart’ discussions in these years. I am also thankful to all my former and present group members and Yngve for introducing me to the love of my life “automated flash system—the Biotage”. All of you made my stay memorable.

Finally, I would like to thank my Mom Shaista, my younger sisters Sana, Vana and my mother and father in law Shehzad Begam and Muhammad Arif and all family members. Your constant support and prayers blessed me with vigor, audacity, and comprehension to successfully complete this project to which I have sacrificed a world of love, passion, and endeavour.

Last but not least deep gratitude goes to my beloved husband Zeeshan and my precious son Owais, to whom I express my profound gratitude for their unconditional support at each and every step, for their prayers, constant love and care that encouraged me to finish this thesis.

Sundus Akhter

Tromsø, March 2018

Dedication

*To my beloved Mom Shaista,
Zeeshan and Owais*

1. Introduction

Carbapenems are broad-spectrum β -lactam antibiotics that are considered as the best drugs and the last hope against many multi-drug resistant bacteria. In the last few years, we have seen the global spread of carbapenem resistance among Gram-negative bacteria. (1-3) Bacterial production of enzymes that are able to hydrolyze the β -lactam ring of the carbapenems, causing the β -lactam antibiotics to become inactive, appears to be the most prevalent cause of carbapenem resistance. Those enzymes are called carbapenemases and belong to the β -lactamases (BLs). Carbapenemases have been identified among three classes of β -lactamases, class A and D (serine-BLs), and class B (metallo-BLs) (for more details see Section 2.4, Chapter 2). One way to combat this mechanism of antibiotic resistance is to develop BL inhibitors, which can restore the activity of the β -lactam antibiotics.

1.1 Aims of the study

In this project, we endeavored to search for potent inhibitors that could target a broad-spectrum of BLs and restore antibiotic activity. We focused our work on carbapenemases belonging to the metallo- β -lactamases such as Verona integron-encoded metallo- β -lactamase-2 (VIM-2), German imipenemase metallo- β -lactamase-1 (GIM-1), New Delhi metallo- β -lactamase-1 (NDM-1), Imipenemase (IMP) and the serine-carbapenemase oxacillinase-48 (OXA-48), which are geographically spread and effectively hydrolyze carbapenems. (4) Our goal was to find inhibitors active against one or several enzymes and to further develop these by structure-based design with the help of X-ray structures of enzyme-inhibitor complexes. To achieve our goal, we focused on the following individual objectives:

- Synthesize and investigate a library of thiol-based compounds as inhibitors against the MBLs VIM-2, NDM-1, and GIM-1 and to get insight into the binding mode with the help of X-ray structures of enzyme inhibitor complexes.
- Gain insight into the binding mode of known triazole-based inhibitors in complex with different MBLs and design new improved inhibitors. Based on the information gained,

synthesize a small library of compounds and evaluate their inhibition potential against VIM-2, NDM-1, and GIM-1. Furthermore, evaluate the activity of the hits against clinical isolates harboring individual enzymes.

- Identify fragments and develop new inhibitors for the clinically relevant OXA-48 enzyme with the help of hits from a fragment library search, backed up by insight obtained from fragment-OXA-48 complex crystal structures.

1.2 Outline of the thesis

The thesis comprises of 8 Chapters, where Chapter 1, gives a short introduction about the thesis and the aim of the study. Chapter 2 discusses briefly antibiotics and resistance against antibiotics, followed by a short overview of β -lactamases, β -lactamase inhibitors, and finally drug design. Chapter 3, 4 and 5 cover the synthetic strategies, biological results and discussions that are presented in Papers 1, 2 and 3, respectively.

To help the reader, the compound numbers from the Papers are used in the thesis with the addition of prefix P1, P2, or P3 before the compound numbers. Thus compound **1** presented in Paper 1, becomes P1-**1** in the Chapter 3 and so on. Chapter 6, presents design of inhibitors and future perspective of the studies. Chapter 7, provides the concluding remarks.

2. Relevant background for the thesis

Pathogenic bacteria are responsible for diseases such as diarrhea, tuberculosis and pneumonia and are the main cause of large-scale death and disability. In a study from 2013, pneumonia and diarrheal disease caused annual deaths of 935 000 adults and 760 000 children under 5 years. Furthermore, tuberculosis (TB) killed 1.5 million adults in the same year. (5-7)

Due to negligence and misuse of antibiotics over the past decades, antibiotic resistance has become a major global healthcare problem of the 21st century. Resistant pathogens belonging to Gram-positive bacteria, like Methicillin-resistant *Staphylococcus aureus* (MRSA) and multiple drug-resistant (MDR) *Mycobacterium tuberculosis*, and Gram-negative bacteria producing extended-spectrum β -lactamases (ESBLs) or carbapenemases are examples of drug-resistant bacteria that are a major concern for the whole world. (8) The human race may not be able to enjoy the blessings of antibiotics for very much longer due to development of bacterial resistance towards antibiotics. This disastrous situation poses one of the most serious threat to human health. (9)

It is therefore vital that apart from development of new antibiotics a global initiative is upheld to address and communicate this crisis. It is very important to increase awareness amongst health-care professionals and people in general regarding the practice of good hygiene, as well as to have access to an efficient global surveillance program. In many parts of the world, antibiotics are still inappropriately taken and prescribed resulting in the misuse of antibiotics. Misuse of antibiotics can harm not just the infected patient but also the broader community. Change in our behavior towards use and prescription of antibiotics is extremely important. Moreover, fast and efficient diagnostic tools are needed to prevent mistreatment. Lastly, but vitally, it is important to facilitate and attract basic and advanced research to better understand and tackle the resistant bacteria. (10)

2.1 History of antibiotics

The discovery of the β -lactam penicillin in 1928 by Sir Alexander Fleming was the result of serendipity and marks a turning point in the history of medicine. Fleming did not, however, had the capacity to develop and produce penicillin on large scale as a medicine. This was later done by Sir Howard Walter Florey and Ernst Boris Chain, for which they all shared the Noble prize. In the same year, penicillin G (Figure 2.1), was made commercially available in the USA. Penicillin was found effective against bacteria, which were resistant to the sulfonamides, the only other antibiotic therapy available at that time. (11,12) The success of the first β -lactam, penicillin G (benzylpenicillin or penicillin G, Figure 2.1) initiated extensive development of other derivatives to find potent antibiotics, starting from the 1940s. This quest identified many β -lactam antibiotics, e.g. penicillins, cephalosporins, monobactams and carbapenems that are in clinical use today. Resulting in a marked decrease in the mortality rate during 1940-1980 in the USA. (13) At that time it was assumed that the fatal diseases such as meningitis, tuberculosis (TB) and pneumonia would be wiped out solely with the help of antibiotics. This assumption could not be more wrong.

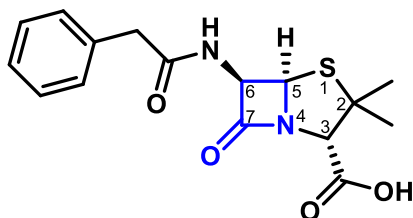
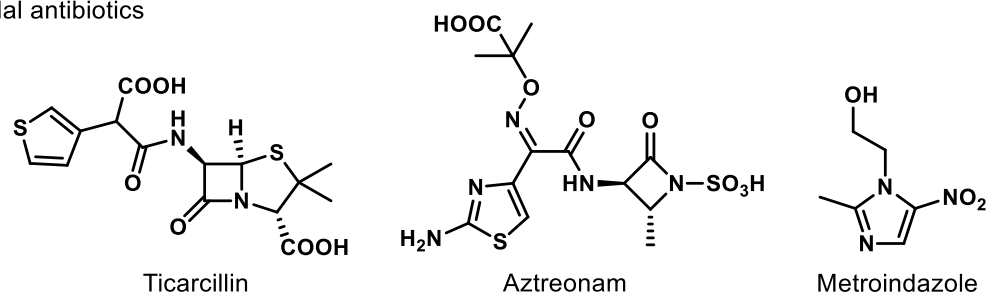


Figure 2.1. The chemical structure of β -lactam antibiotic, penicillin G. (5)

2.2 Classification of antibiotics

Based on their mechanism of action, antibiotics are classified as bactericidal or bacteriostatic. Bactericidal antibiotics such as β -lactam antibiotics (Figure 2.2) kill bacteria, whereas bacteriostatic antibiotics such as tigecycline and spectinomycin (Figure 2.2) limit bacterial growth. (14,15) On the basis of their chemical structures, antibiotics are classified as β -lactams (being the major class), and others such as tigecycline, tetracyclines, aminoglycosides, sulfonamides, quinolones, macrolides etc. However, our focus in this thesis will be the β -lactams.

Bactericidal antibiotics



Bacteriostatic antibiotics

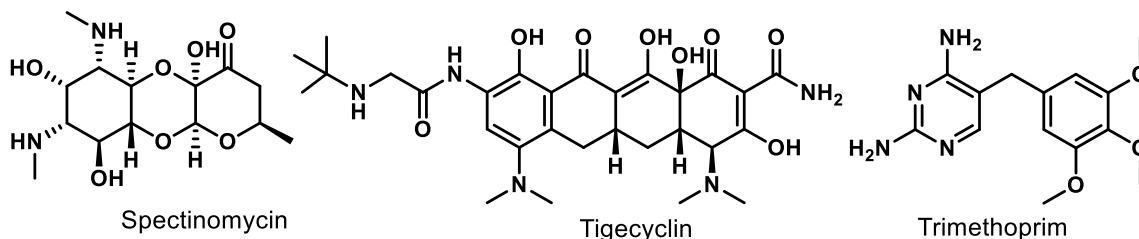


Figure 2.2. Structures of some of the bactericidal and bacteriostatic antibiotics

2.2.1 β -Lactam antibiotics

In the US, more than 65% of the prescriptions of antibiotics consist of β -lactams. (16) The β -lactam ring is the main part of the pharmacophore of β -lactam antibiotics. β -lactams have a broad-spectrum of activity against Gram-positive and Gram-negative bacteria making them valuable drugs. (6,7) Classes of β -lactam antibiotics include penicillins, cephalosporins, carbapenems and monobactams (Figure 2.3). (16-23)

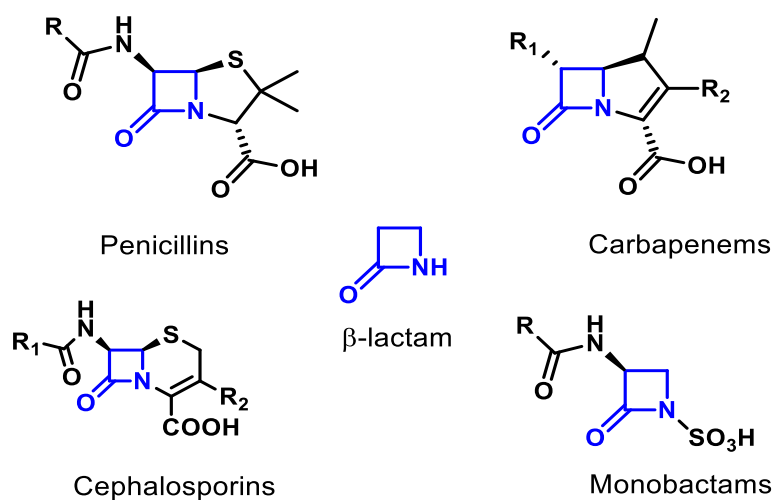


Figure 2.3. Structures of common classes of β -lactam antibiotics

2.3 Antibiotic resistance

Antibiotic resistance was present even before the introduction of modern antibiotics, but the mass-production and accessibility of antibiotics during the 1940s exerted a strong evolutionary pressure on bacteria. Which resulted in the emergence resistant bacterial strains. This was already predicted by Alexander Fleming who gave a prophetic statement in 1945 during an interview with New York Times about the future of the miracle drug:

“... the public will demand [penicillin] ...then will begin an era...of abuses. The microbes are educated to resist penicillin and a host of penicillin-fast organisms is bred out which can be passed to other individuals and perhaps from there to others until they reach someone who gets a septicemia or a pneumonia which penicillin cannot save. (11)

Antibiotic resistance is rising to dangerously high levels in all parts of the world while the development of new antibiotics has slowed considerably down (Figure 2.4). (24) As of now there is an inaccurate and probably very low estimate that 700,000 lives are lost each year due to resistant strains of bacteria. If this problem remains unattended it is estimated that, by 2050 deaths due to infection caused by resistant bacterial resistance could reach up to 10 million per year. (25) Consequently dealing with antibiotic resistance is a high priority for the World Health Organization (WHO). (4)

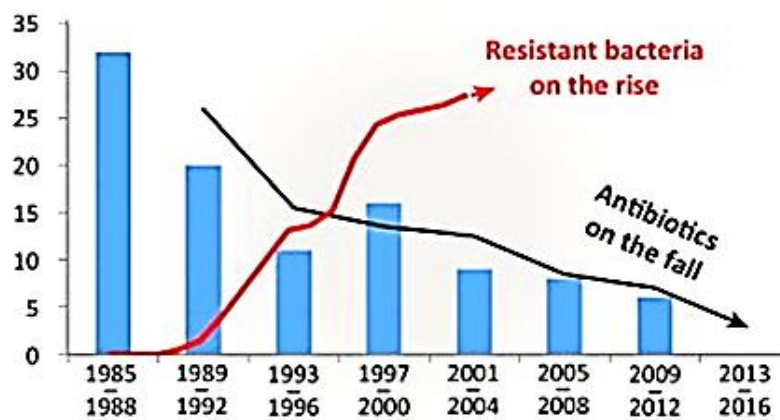


Figure 2.4. Development of new antibiotics with respect to the rise of the resistant bacteria. X-axis describes timeline, Y-axis describes number of antibiotics, blue bars exhibit the number of antibiotics launched; red line represents rise of resistant bacteria, black line represents decrease in the production of new antibiotics. Figure reprinted with permission from Schäberle et al. (24)

Currently, growing list of common nosocomial infections acquired as a result of minor injuries or surgeries are becoming harder to treat, and without urgent action, we are entering a scenario where common infections and minor injuries can once again kill. (4)

2.3.1 Different modes of bacterial defense mechanisms

There are different modes of resistance that can be adopted by bacteria in order to make antibiotics inactive. (26) Among others, bacteria can replace or modify the drug target (27) reduce the drug uptake, (28) activate efflux pumps, which can help pump out drugs from the bacterial cell, (29,30) increase production of the substrate for the targeted enzyme and enzymatic inactivation of antibiotics. (28)

2.3.1.1 Enzymatic β -lactam inactivation

The focus and emphasis will be on the enzyme mediated drug inactivation mechanism by metallo and serine β -lactamases. As biological evaluation was carried out on VIM-2, GIM-1, and NDM-1 (MBLs) and OXA-48 (SBL).

Various Gram-positive and Gram-negative bacteria produce enzymes capable of hydrolyzing the β -lactam ring of the β -lactam antibiotics thus rendering the drug molecules inactive (Figure 2.5), such enzymes are called β -lactamases (BLs). (31)

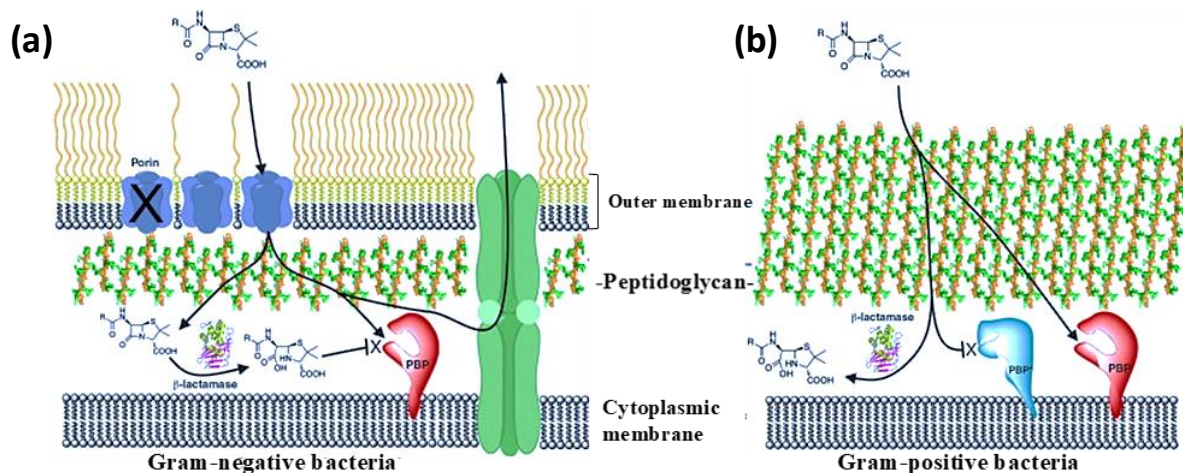


Figure 2.5. Mechanism of β -lactam inhibition, and schematic representation of β -lactam resistance by (a) Gram-negative and (b) Gram-positive bacteria. Figure acquired with permission from Llarull et al. (32)

2.4 β -Lactamases (BLs)

BLs were observed before the introduction of the penicillin in the market in 1940, and by 1950s, 50% *Staphylococcus aureus* had become resistant. (28) BLs are divided into four major classes namely A, B, C, and D (Figure 2.6). Classes A, C, and D are SBLs that contain a conserved serine residue in the active site, which is responsible for the nucleophilic attack on the C=O carbon of the β -lactam ring. Class B BLs contain one or two divalent zinc cations (Zn^{2+}) that are responsible for the activation of a water molecule that hydrolyzes the β -lactam. (31)

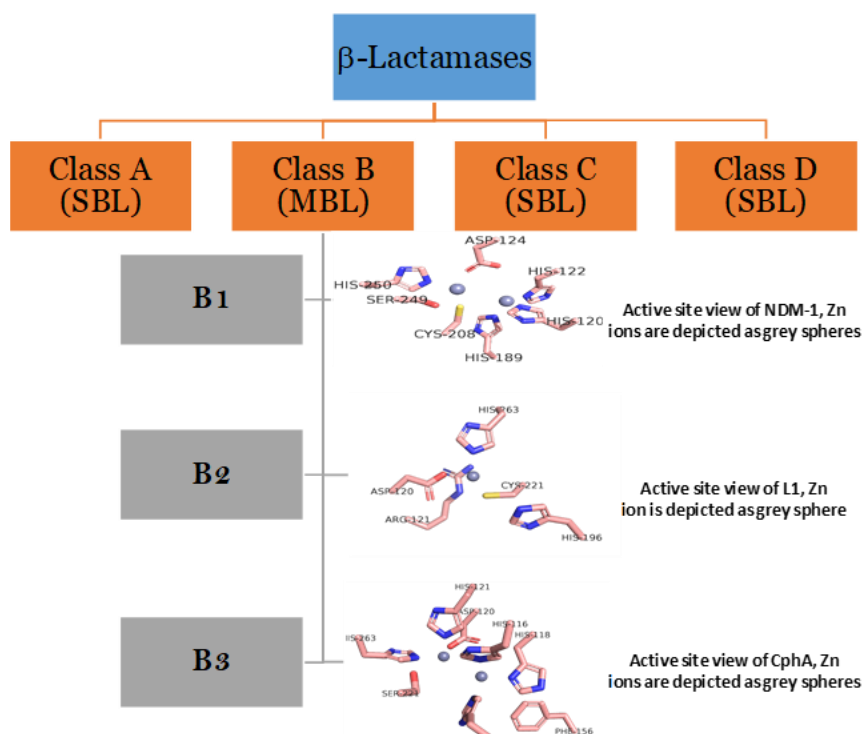


Figure 2.6. Amber and Bush-Jacoby classification of BLs. (31)

Figure is prepared using PyMOL for enzymes NDM-1 (PDB ID: 3SPU), L1 (PDB ID: 2FM6) and CphA (PDB ID: 1X8G).

2.4.1 Carbapenemases

BLs that are able to hydrolyze carbapenems are called carbapenemases. All the enzymes evaluated in this study are carbapenemases.

2.4.1.1 Metallo- β -lactamases (MBLs)

The class B MBLs, are part of a superfamily of metallohydrolase enzymes. (33) MBLs are able to deactivate a broad-spectrum of β -lactam antibiotics, including penicillins, cephalosporins and carbapenems. Furthermore, some MBLs are reported to even hydrolyze SBL inhibitors such as sulbactam and tazobactam. (34) MBLs use a hydroxyl group bound to the zinc ion in the active site as the nucleophile.

Bush categorized the MBLs into B1, B2, and B3 subclasses (Figure 2.6) and later updated the scheme as more MBL enzymes were discovered. (35,36) Examples of B1 subclass MBLs are the VIM, GIM and NDM. B1 enzymes have two zinc ions in the active site. The B2 subclass MBLs, for example imipenem hydrolyzing metallo- β -lactamase (ImiS), require one zinc ion for their activity. B3 subclass MBLs such as the *Stenotrophomonas maltophilia* β -lactamase 1 (L1) enzyme need two zinc ions in the active site to hydrolyze β -lactam rings in antibiotics. The sequence identity between subclasses can be very low and in some case only 10%. Therefore, it is very difficult to design an inhibitor that can target all classes but recently some examples of inhibitors targeting several classes are starting to emerge in the literature. (37,38)

2.4.1.1.1 Mechanism of action of MBLs

In this section, the mechanism of action of meropenem hydrolysis by the NDM-1 enzyme, that belongs to subclass B1 of MBLs is described (Figure 2.7). NDM-1 exhibits broad-spectrum hydrolytic activity against β -lactams including the last resort carbapenems such as meropenem. The mechanistic studies described here are consistent with X-ray structures as well as a recently published study based on NDM-1. (39,40)

In the first step negatively charged oxygen from hydroxide ion bridging the two Zn ions attacks the electron deficient carbonyl carbon of the β -lactam ring (Figure 2.7, **a**), as a result of which the C-N bond is cleaved, whilst the negative charge on the nitrogen is stabilized by Zn^{+2} after cleavage of the ring. This coordination between nitrogen and Zn^{+2} is supported and confirmed by earlier X-ray crystal structures studies of NDM-1 or other MBLs in complex with the cleaved β -lactam ring of the drug. (41,42) Next a proton transfer occurs from bridging OH⁻ to Asp120 (**a**→**b**), followed by the entry of water molecules, into the active site (enzyme inhibitor, EI complex, **c**; Figure 2.7) that eventually (**c**→**f**) takes the place

of the bridging hydroxyl shown in complex **a**. (40,43,44) This is also in agreement with previous studies and observations and is the case for mono zinc based MBLs as well. (45) In the final step, these water molecules serve as the source of protons, during the proton transfer to the nitrogen resulting in the hydrolysis of the β -lactam ring. As a result, following path; **f**→**E+P**, the catalytic center is reformed, followed by the removal of the hydrolyzed meropenem.

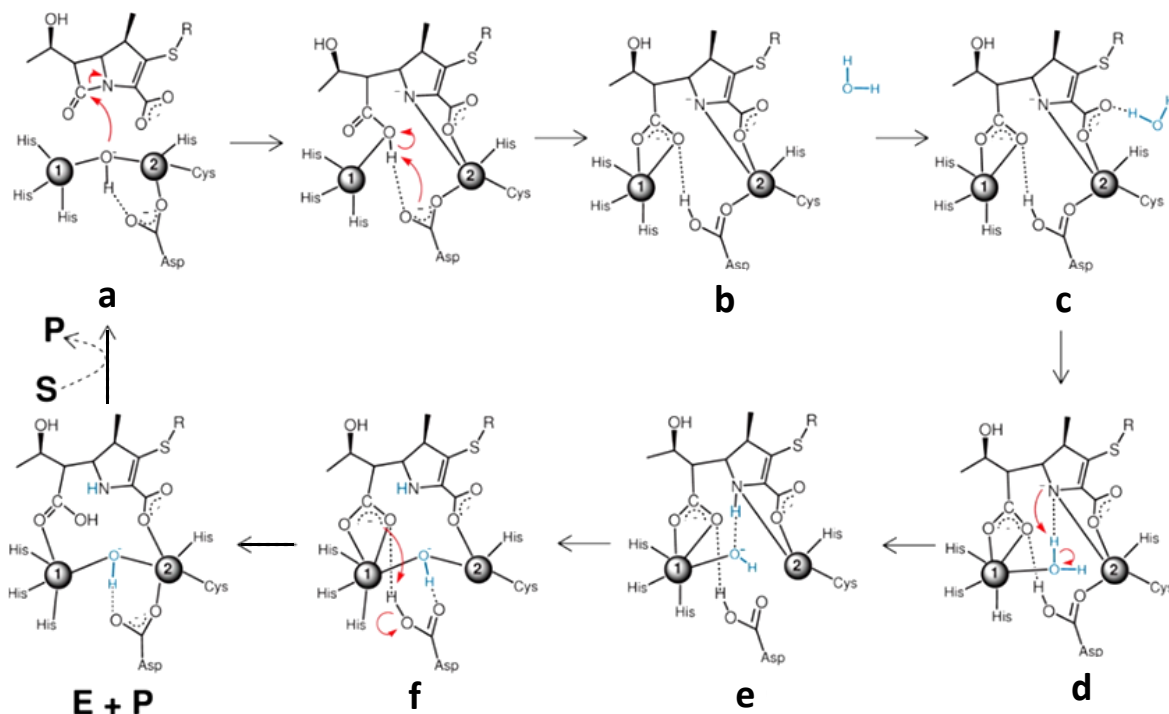


Figure 2.7. Mechanism of hydrolysis of meropenem by the enzyme NDM-1. Zn ions are denoted by the numbers 1 and 2 inside the grey spheres. Where Zn1 is shown to coordinate with residues His116, 118, and 196, while Zn2 is in coordination with residues His263, Asp120 and Cys221. Figure acquired with permission from Tripathi et al. (40)

2.4.1.2 Serine- β -lactamases (SBLs)

Serine carbapenemases were first discovered in 1985 in *Acinobacter baumannii* multidrug-resistant strain and reported in 1993 by Paton et al. (46) Among the SBLs, serine carbapenemases have been described in class A and class D (oxacillinases) BLs. SBLs contain a serine residue in their active sites, which acts as a nucleophile and plays a vital role in the inactivation of antibiotics. (31)

OXA-48 is the most efficient class D carbapenemase and can inactivate imipenem readily as compared to other class D carbapenemases. The overall structure of OXA-48 is similar to other class D BLs such as OXA-1, OXA-10, and OXA-13 whereas OXA-181 differs only by a single point mutation from OXA-48. Figure 2.8 gives an idea about the global presence and spread of OXA-48 producers. Most recently, the emergence of class D carbapenemases has become evident. (47) For instance, OXA-181 together with NDM-5 is on the rise in America and together they have been called the evil twins. (48)

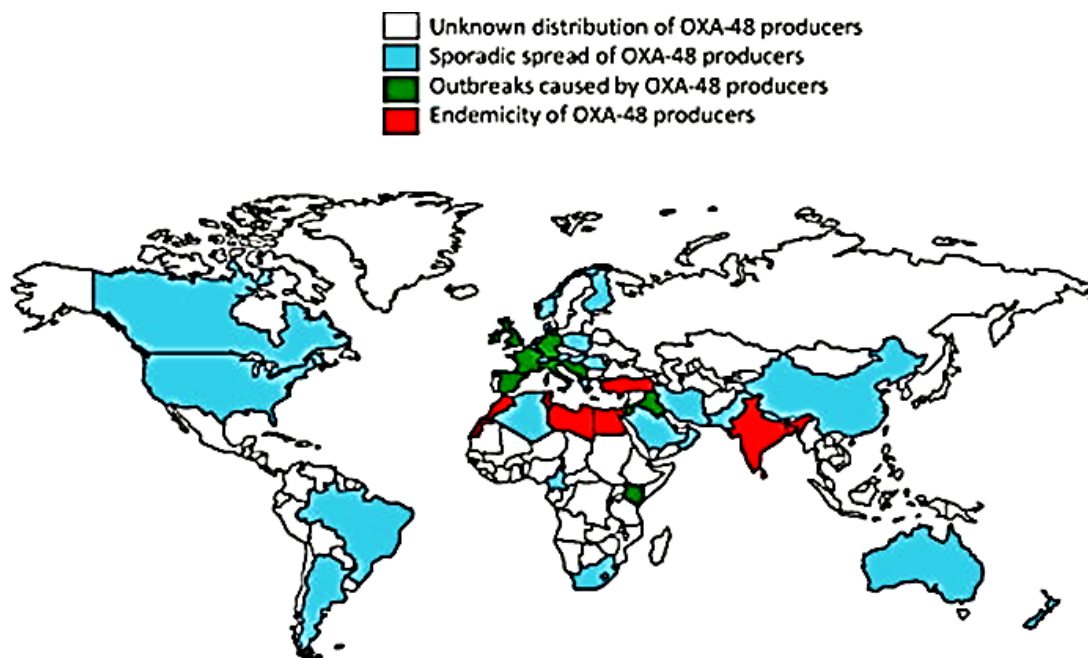
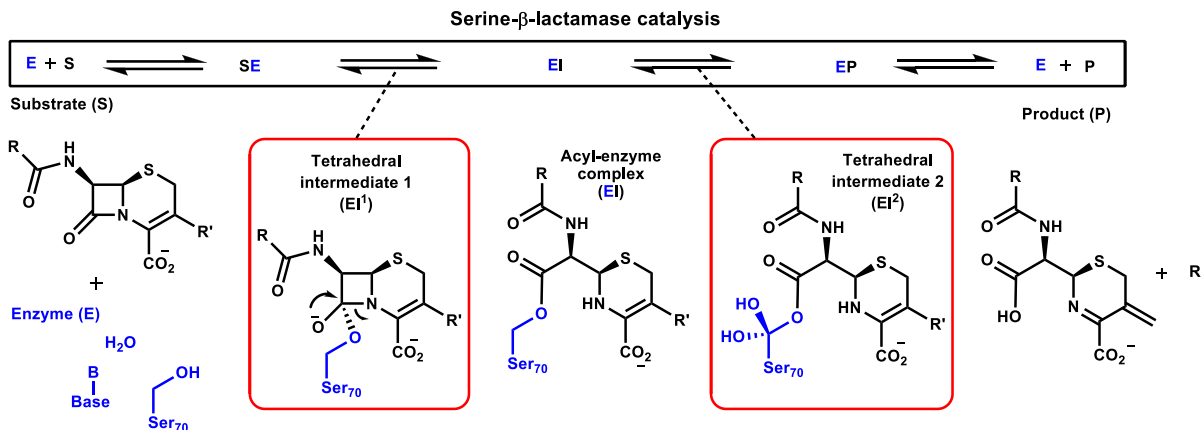


Figure 2.8. Dissemination of OXA-48 like producers in different parts of the world. Figure reprinted with permission from Nordmann et al. (2)

2.4.1.2.1 Mechanism of action of SBLs

The OXA enzymes act via the same mechanism of action as other SBLs (Figure 2.9). The serine 70 residue present in the active site plays an important role in the formation of a covalent acyl intermediate (EI^1) that forms the acyl-enzyme complex (EI) (Figure 2.9). The formation of this complex leads, through a tetrahedral intermediate (EI^2) to deacylation leading to the inactivated antibiotic. (49-52) Moreover carbon dioxide is believed to play an important role in the hydrolysis of the C-N bond of the β -lactam ring. The carboxylation of

lysine 73 residue carbamate is responsible for the activation of the catalytic serine residue. (53-55)



2.5 β -Lactamase inhibitors

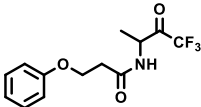
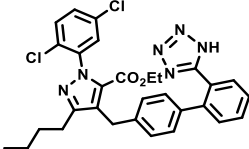
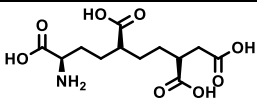
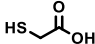
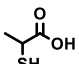
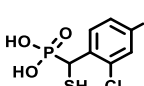
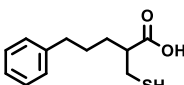
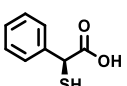
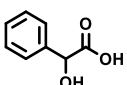
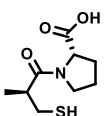
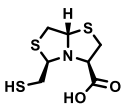
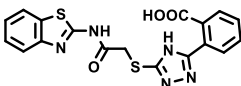
The focus of our studies was to comprehend and develop inhibitors targeting various MBLs (Paper 1 and 2) and the SBL OXA-48 (Paper 3) included in this thesis.

A successful approach against BLs is combination therapy, where BLs inhibitors can be used along with β -lactams. Although there are some SBL inhibitors available for clinical use such as clavulanic acid, avibactam, sulbactam, vaborbactam and tazobactam, but they are inactive towards MBLs. The following discussion describes some of the most prominent inhibitors studied in the literature.

2.5.1 Metallo- β -lactamase inhibitors

Although various compounds with natural or synthetic origins have shown inhibitory potential against MBLs (see Table 2.1) there is still no MBL inhibitor available for clinical use up till now. Some of the inhibitor classes are described in this section.

Table 2.1. Reported MBL inhibitors studies.

Entry	Inhibitor type	Compounds	Enzyme tested	References
1	Trifluoromethyl alcohols and ketones		BcII, L1	(56)
2	Biphenyl tetrazole		IMP-1, CcrA	(57,58)
3	Metal chelators		NDM-1, NDM-4, VIM-1, IMP-1, IMP-8, VIM-2, IMP-7	(59)
4	Thiol		IMP-1	(60)
4.1			IMP-1	(61)
4.2			VIM-4, CphA	(62)
4.3			IMP-1, VIM-2	(63,64)
4.4			IMP-1, CcrA	(65)
4.5			BcII	(66)
4.6			BcII, CphA, VIM-2, IMP-1, NDM-1	(67-69)
4.7			NDM-1, IMP-1, BcII, L1, Sfh-I	(6)
4.8			VIM-2, CcrA, ImiS	(70)

The first synthetic MBL inhibitors (Entry 1, Table 2.1) were reported by Walter et al. in 1996. They tested α -amido trifluoromethyl alcohols and ketones against B1, B2 and B3 MBLs. (56) The inhibitors were found to be potent against CphA and LI but inactive towards B1 MBLs. In 1998, Toney and colleagues identified a series of biphenyl tetrazoles (Entry 2, Table 2.1) as potent inhibitors of CcrA from a screening campaign of the Merck chemical collection and molecular docking study. (71) Toney et al. later expanded the work by assaying a series of synthetic biphenyl tetrazoles on CcrA and IMP-1, B1 MBLs. Synthetic biphenyl tetrazoles were found to exhibit moderate inhibitory potency against both of the B1 MBLs tested. (72)

Since MBLs employ Zn^{+2} in their active site MBLs can easily be inhibited by metal chelators as EDTA (Entry 3, Table 2.1) and dipicolinic acid. (73,74) Metal chelators are found to be active towards VIM-1, VIM-2, NDM-1, NDM-4, IMP-1, IMP-7, IMP-8 etc. (75-77)

The high potency and broad-spectrum inhibitory activity demonstrated by some thiol-based mercaptocarboxylates against MBLs have made this class of inhibitors the most studied of all MBL inhibitors (Entry 4, Table 2.1). Racemic thiomandelic acid was the first reported mercaptocarboxylate type broad-spectrum MBL inhibitor in 2001. (66) In a recent study Tehrani et al. reported the ability of thiomandelic acid and 2-mercapto-3-phenylpropionic acid to enhance the activity of meropenem particularly against IMP producing *Klebsiella pneumoniae*. (78)

Both D- and L-captopril (Entry 4.6, Table 2.1) have been studied as broad-spectrum inhibitors of MBLs with the D-isomer exhibiting more potent inhibitory activity than the L-isomer against the MBLs such as NDM-1, VIM-2 and IMP-1. Captopril is also used as a standard for comparison of inhibitory potency when screening for new inhibitors. (67,79,80) MBL inhibitors containing bithiazolidines (BTZs), (Entry 4.7, Table 2.1) as the basic core are found effective against enzymes from class B1, B2, and B3. (81) In addition, BTZs with a free thiol group, a carboxylate group and a tetrahedral nitrogen are considered cross class MBL inhibitors that are able to inhibit enzymes from class B1, B2, and B3, simultaneously. (6,37) Another thiol-based inhibitor is triazolylthioacetamide (Entry 4.8, Table 2.1) that is found to inhibit VIM-2 along with other MBLs such as ImiS and CcrA. (70) Thus, the thiol-

based inhibitors have a strong potential and optimization of thiol-based inhibitors may lead to potent inhibitors with a broad-spectrum of activity against MBLs. (82)

2.5.2 Serine- β -lactamase inhibitors

Several combinations of inhibitors along with β -lactam antibiotics have proven to work efficiently against SBLs while being inactive towards MBLs. Combinations like ceftolozan with tazobactam and ceftazidime with avibactam are used against SBLs (Figure 2.10). (83)

Meropenem/vaborbactam, ceftazidime/avibactam and ceftolozane/tazobactam are some of the latest cephalosporin/ β -lactamase inhibitor combinations approved for clinical use by FDA (Food and Drug Administration) in August 2017, February 2015 and December 2014, respectively. (84,85) These are marketed as Vabomere, Aycaz and Zerbaxa (Figure 2.10). (16,86)

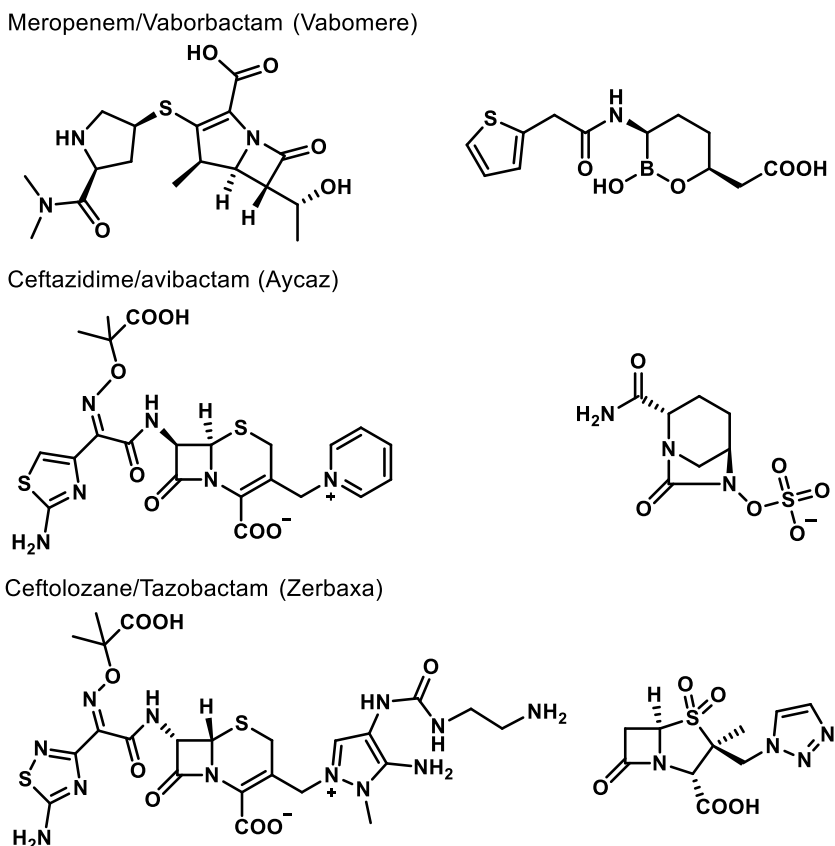


Figure 2.10. Structures of approved β -lactam/ β -lactamase inhibitor combinations by FDA.

Avibactam is a new β -lactamase inhibitor, as it possesses a broad-spectrum of inhibition against SBLs. It has the potential to treat infection caused by Gram-negative pathogens producing class A and C enzymes including extended spectrum β -lactamases (ESBL) and carbapenemases (*Klebsiella pneumoniae* carbapenemase (KPC) type are currently the most clinically relevant carbapenemases). Although avibactam does not inhibit the class B MBLs, it does have the potential to inhibit class D carbapenemase such as OXA-48 which is only inhibited by avibactam. However, resistance towards ceftazidime/avibactam has been observed recently in clinical, multiresistant, OXA-48 by Anna Both et al. (87) The mechanism of inhibition of avibactam with OXA-48 is described later in this section.

Avibactam has been studied and found to be effective for use in combination with aztreonam, fosamil, and ceftaroline. (88,89) Recently Lahiri et al. described the mechanism of inhibition of OXA-24 and OXA-48 by avibactam (Figure 2.11a and b). (90) The X-ray crystal structures of OXA-48 and OXA-24 are shown in Figure 2.11c. Studies on OXA-48 suggests that the acylation of avibactam most likely proceeds by the attack of carboxamate group of Lys73, acting as the general base that abstract a proton from the catalytic Ser70. The acylation also requires a general acid to donate a proton to the aminosulfate nitrogen. The binding modes of avibactam with the two enzymes suggest that Ser118 assisted by Lys208 in OXA-48, helps in this role, as depicted in Figure 2.11. (91,92)

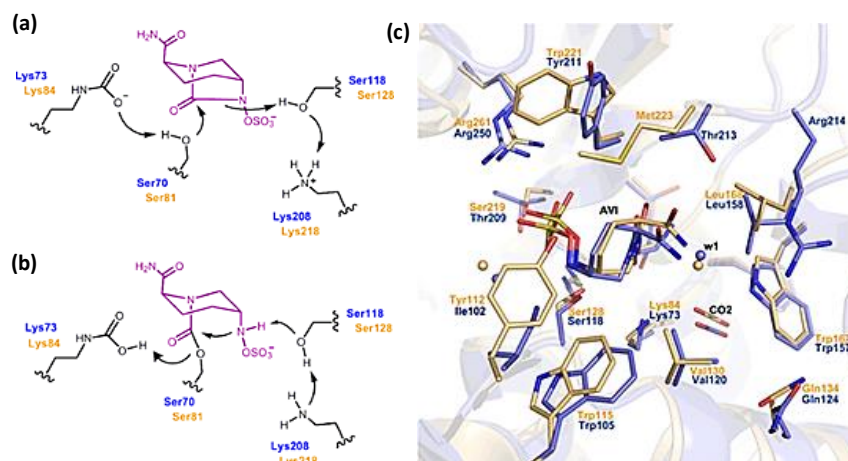
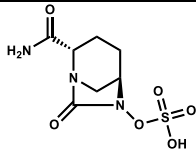
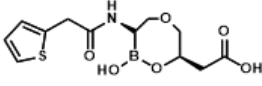
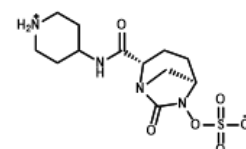
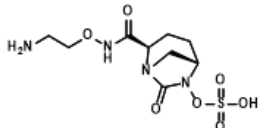


Figure 2.11. Mechanism of inhibition of avibactam on class D SBLs (in light brown stick and labels of residues for OXA-24 and blue sticks and labels of residues for OXA-48), (a) acylation and (b) deacylation of the lactam ring. (c) Comparison of the avibactam binding in OXA-24 and OXA-48. Modified figure used with permission from Lahiri et al. (90)

Currently, there are only 40 new antibiotics in the development phase with only nine in phase I, twenty-one in phase II and eight in the phase of the clinical trials. (93) In addition, not all of these drugs are able to target the drug-resistant bacterial pathogens. From these numbers, we can clearly estimate that the drugs in the pipeline are not enough and not all of them will be approved and marketed. (94) The lack of new antibiotics points towards the reuse of the drugs that were forgotten or abandoned because of their side effects. For example, colistin is one such drug that is known for causing severe kidney damage but is found to be useful as a drug of last resort. (85,94) The combination of the inhibitor with antibiotics is a promising approach, which can lead to restoring the activity of the antibiotic against BLs. (28) Some of the prominent resistance-breaking β -lactam/BLs inhibitor combinations are already in early clinical developmental stages. For example, avibactam, relebactam, and a novel BLs inhibitor named OP0595 (Table 2.2). (94) Whereas, vaborbactam in combination with meropenem, is recently approved by FDA to treat urinary tract infections.

Table 2.2. Inhibitor name, target enzymes and molecular structures of inhibitors approved or in clinical trials as combination with an antibiotic partner. (95,96)

Inhibitor name	Target enzymes	Structure	Antibiotic partner	Development stage
Avibactam (NXL104)	OXA-48, OXA-24		Ceftazidine Aztreonam Ceftaroline	Approved in 2015 Phase II Phase II
Vaborbactam (R PX7009) (97)	KPC-2, KPC-3, KPC-4		Meropenem	Approved in August 2017
Relebactam (MK-7655)	AmpC, KPC-2		Imipenem	Phase III
OP0595 (RG6080) (98)	AmpC		Cefepime	Phase I

2.6 Drug development

This section will give a short introduction to the main strategies for drug development applied within this work.

2.6.1 Structure- and ligand-based drug design

Drug design can be categorized as structure-based drug design (SBDD) or ligand-based drug design (LBDD). Indirect drug design or LBDD employs the ligands known to show binding to the target enzyme. LBDD is useful when 3D information about the receptor molecule is missing. (99) Direct drug design or SBDD is an approach where information about the structure of the drug target is available and therefore utilized for the development of the inhibitor for the target enzyme. (100) To determine the structure of the target proteins experimental techniques like Nuclear magnetic resonance (NMR) or X-ray crystallography are utilized. (101) In LBDD and SBDD various strategies are utilized to develop drug molecules including lead identification, design, development and optimization. (102,103)

2.6.2 Hit generation strategies

The search for hit compounds towards a predefined drug target can be divided into high-throughput screening (HTS) and fragment based drug design (FBDD). HTS is a process used in drug discovery, where a large collection of compounds is screened and evaluated against the biological macromolecule of interest. It employs techniques like robotics, sensitive detectors, and data processing software that allow rapid identification of active compounds. HTS has consistently failed to yield meaningful lead compounds for SBLs. In contrast, HTS has successfully identified novel inhibitors against MBLs. For example, HTS at Meiji Seika Kaisha Ltd (104), Merck (71) and academic group, (105) were successful in the identification of novel compounds. The reason for the success might be the presence of functional groups as tetrazole, carboxylate, thiol etc. as these functional groups can make interactions with the zinc ions present in the active site of MBLs. The results promote the use of focused libraries containing some of these chemotypes.

2.6.2.1 Fragment-based drug design (FBDD)

This thesis describes the initial steps of fragment-based development of OXA-48 inhibitors.

We used fragment merging technique to elaborate the initial fragment hits (Paper 3).

In contrast to HTS, FBDD identifies small molecules with molecular masses less than 300 Dalton and low affinity in the range of milli-molar to micro-molar. FBDD is a very promising approach for screening compounds against both SBLs and MBLs and has been proven to be successful in identifying inhibitors against class A, B and C enzymes. SBLs have multiple binding sites making them attractive targets for fragment-based approaches. (106-110) In addition to lead identification, FBDD has also been used for lead optimization to probe additional binding hot spots for inhibitors. FBDD is based on the close collaboration of the synthetic chemistry and structural biology also referred to as “Fragment elaboration cycles”. Elaboration of such weak binding fragments with rapid and easy derivatization, determining structure-activity relationships studies, followed by further optimization into potent inhibitors by merging, linking or growing the fragment that can result in potent compounds. Moreover, fragments can be optimized to acquire drug-like properties. Structural information on inhibitor-enzyme complex plays the fundamental role in the optimization of the hit fragments. FBDD approach was first utilized for drugs targeting cancer cell and resulted in the discovery of Zelboraf (PLX4032) in 2011. Since 2011, several success stories can be found in the literature (82,111-114)

Some fragment-sized molecules have been identified by Nicholas et al. particularly polycarboxylic acids (Figure 2.12, panels a and b), that may serve as starting points for the future development of novel inhibitors able to target both Class A and D enzymes. (Figure 2.12, panel b) (115)

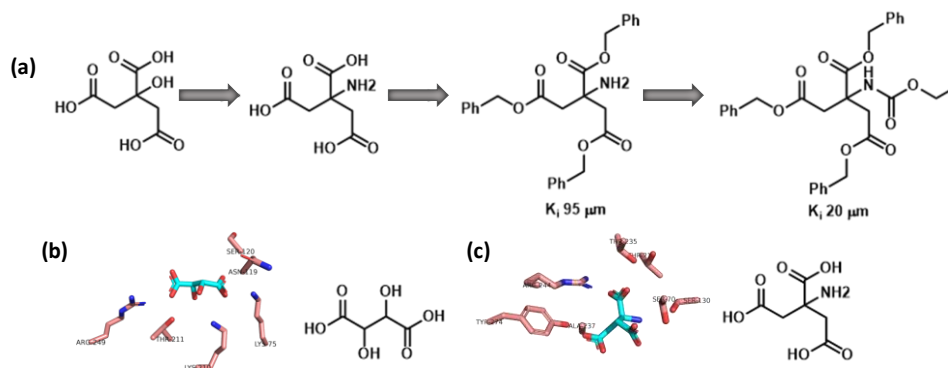


Figure 2.12. Polycarboxylic acid molecules have shown ability to act against both class A and D BLs (a) FBDD approach to develop inhibitors against OXA-10. Active site view showing (b) tartaric acid (cyan sticks) in complex with OXA-46 (PDB ID 3IF6), and (c) aminocitrate (cyan sticks) in complex with BS3 (PDB ID 3B3X). the active site residues of the enzymes are depicted in pink sticks; figures are made using PyMOL.

Due to the small size, and specific interactions, fragments are able to show high ligand binding efficiency (L.E) defined as the binding energy per heavy atom present in the fragment and is used as an important measuring tool for the potency of a ligand in drug discovery. (116) Certain tools (Figure 2.13) can be used to identify and characterize interactions between the fragment and the target protein such as computer-based in-silico drug design, surface plasmon resonance (SPR), NMR fragment-based screening that identifies binders to the protein target (117,118) and X-ray crystallography. The X-ray crystallographic technique is quite advantageous as it can give an insight to the interaction of the ligand to the target protein, which can be very useful to design and optimize the potent fragments in to lead like molecules. (119)

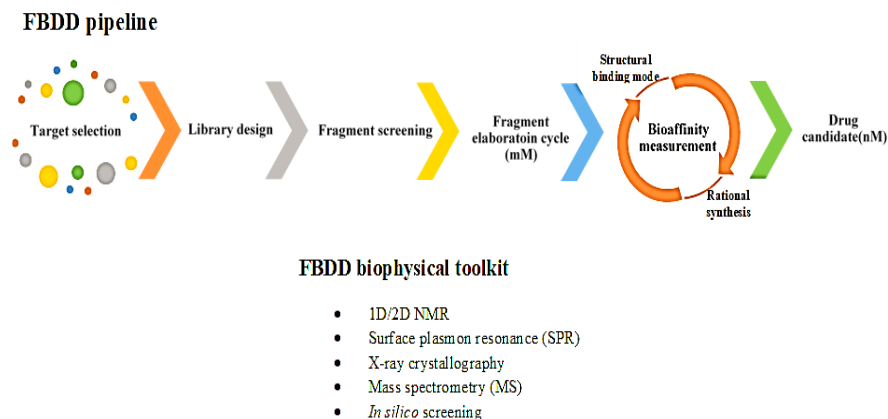


Figure 2.13. A schematic illustration of FBDD Pipeline. Figure modified from (112)

2.6.3 Bioisosteric replacement

Bioisosteric replacement is a valuable tool for medicinal chemists that is used for lead optimization and structure activity relationship studies. The basic concept is the selection and replacement of an atom or groups to rationally improve the biological activity or physicochemical properties of the lead compound. (120,121) The bioisoster should maintain some of the properties of the parent structure, for e.g. inhibitor binding to the biological target, while other properties may change, e.g. lipophilicity or steric size.

For the compounds described in Chapter 3, we utilized bioisosteric approach to modify activity of mercaptocarboxylic acids, where we replaced the carboxylic acid group with its bioisosters to find potential inhibitors for MBLs. Typical bioisosteres of carboxylic acids include phosphonates, *NH*-tetrazoles and sulphonamides. (122)

3. Metallo- β -lactamase inhibitors by bioisosteric replacement

3.1 Rationale for design of bioisosters

As mentioned previously, several MBL inhibitors have been identified and studied, however none has been developed to a clinically useful inhibitor for MBLs. The thiophilic nature of zinc makes thiol containing compounds an interesting starting point for the search for an inhibitor that can target a wide variety of MBLs. In addition, thiol-based compounds have already shown some inhibitory activities against MBLs (Section 2.5.1).

The inhibitory activity and high potency of mercaptocarboxylates against MBLs inspired us to modify these scaffolds to obtain more potent inhibitors. In our studies, we replaced the carboxylate group in the mercaptocarboxylic acid scaffold; (P1-1, Figure 3.1, reported by Jin et al.), (123) with bioisosters to elucidate the effect on the biological activity and inhibitor binding. Thus, bioisosteric replacement of the carboxylate group of P1-1 with typical bioisosters like phosphonate esters, phosphonic acids or *NH*-tetrazoles (122) lead to the target structures P1-2 to P1-4 (Figure 3.1). The concept of bioisosteric replacement is described in Section 2.6.3, Chapter 2.

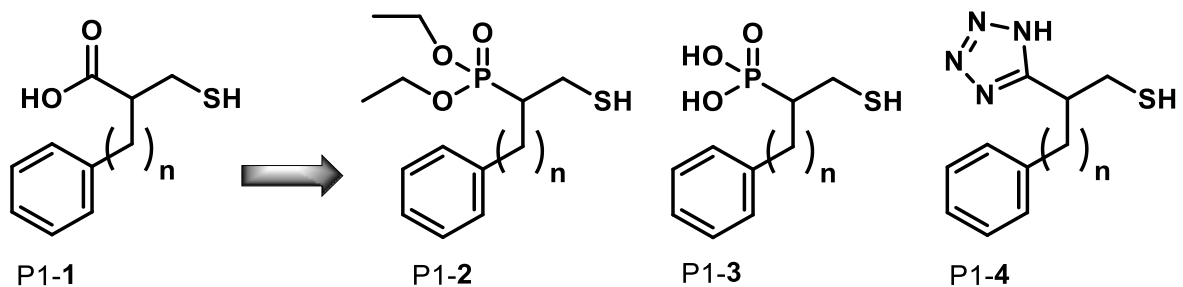
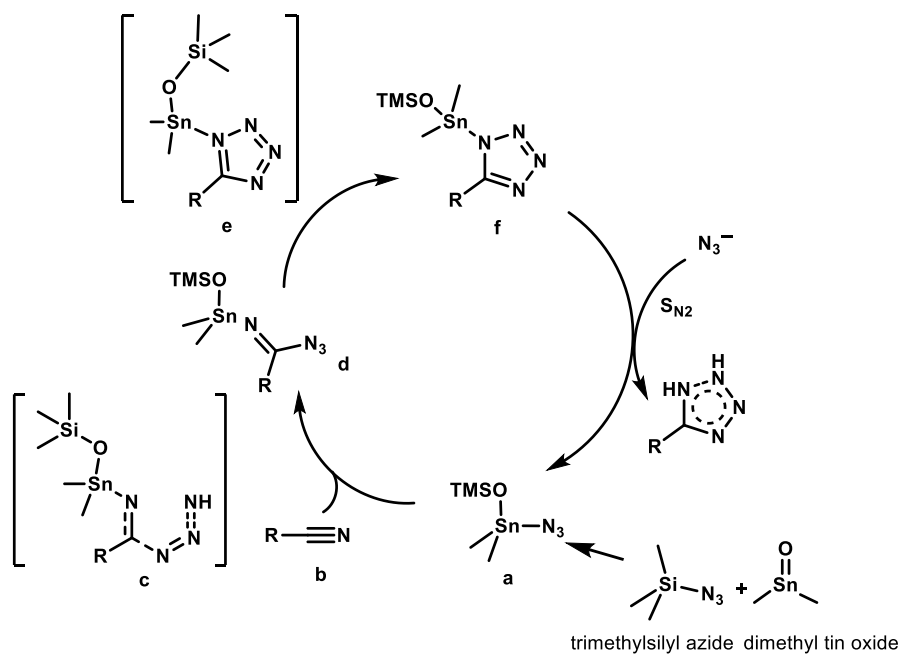


Figure 3.1. Bioisosteric substitution of the carboxylate group.

3.2 Reactions utilized in the synthesis

To create the targeted compounds P1-2 and P1-3, a series of reactions such as alkylation, reduction, mesylation followed by thioacetylation and deprotection of phosphonic ester and thioacetate group were carried out.

The tetrazole moiety is also known to be an excellent replacement for the carboxylic acid (124) and is almost 10 times more lipophilic while having similar acidity as a carboxylic acid group, (pKa 4.9 and 4.2-4.4 respectively). (121) For the synthesis of tetrazole containing compounds P1-4, alkylation was followed by dialkyltin oxide promoted azide-nitrile cycloaddition reaction. Further thioacetylation and deprotection of the thioacetate group gave the desired compound P1-4. The mechanism of the tetrazole formation reaction is described below (Scheme 3.1). In the first step of the mechanism, dimethyl tin oxide and trimethyl silyl azide (TMSN₃) react irreversibly to form the complex **a**. Next the nitrile group reacts with the tin in complex **a**, whilst the azide binds to the nitrile carbon forming complex **d** through the transition structure **c**. Complex **d**, undergoes a cyclization reaction to give the complex **f** through intermediate **e**. The attack by azide nucleophile in an S_N2 reaction on complex **f** gives the free tetrazole containing product. (125)



Scheme 3.1. The catalytic cycle of tetrazole formation. (125)

3.3 Results and discussion

3.3.1 Synthesis

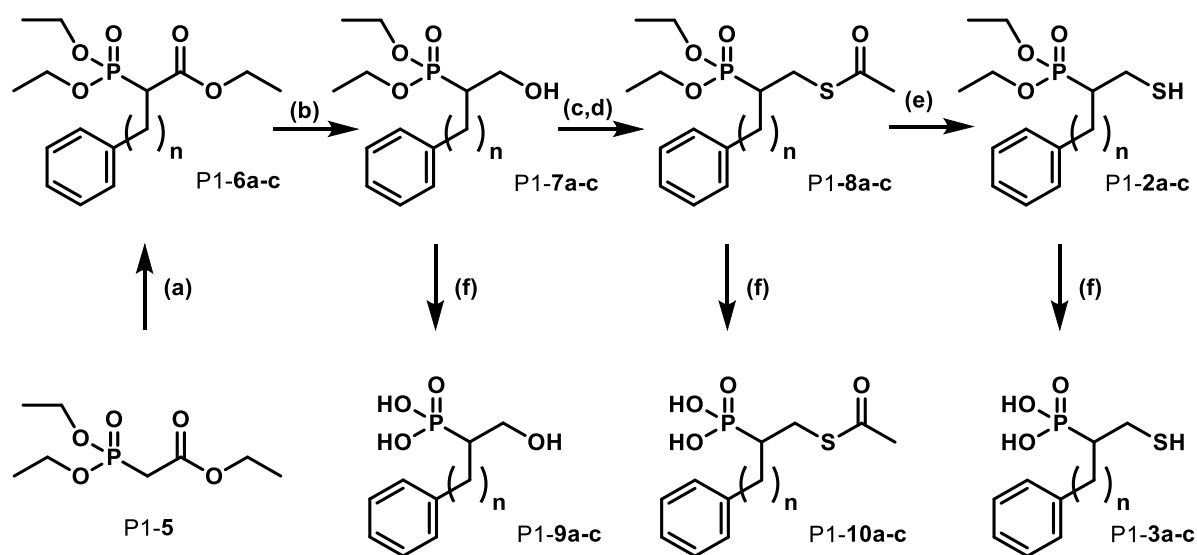
The mercaptophosphonate esters P1-2a-c and mercaptophosphonic acids P1-3a-c were prepared according to the synthetic strategy shown in Scheme 3.2. We observed that alkylation of triethyl phosphonoacetate P1-5 was prone to dialkylation in the presence of a strong base and reactive alkylating agents. Thus alkylation was carried out using strong but sterically hindered base, potassium *tert*-butoxide (KO*t*Bu), along with the corresponding alkyl halide to avoid dialkylation. We also observed that the ratio of triethyl phosphonoacetate P1-5 to alkyl halide was crucial in limiting the unwanted dialkylation reaction. When the ratio was kept at 1:0.5 a low yield (45%), was observed for the monoalkylated product. On the contrary, when a 1:1 ratio was used, the undesirable dialkylated product was formed, whereas if the ratio was kept at 1:0.7 the desirable monoalkylated product was obtained in 65-73% yield for the compound P1-6b. Thus, a ratio of P1-5:alkyl of 1:0.7 was considered to be the best ratio. Another major impurity found in the reaction mixtures was unreacted phosphonoacetate.

With the alkylated product P1-6a-c in hand, we proceeded to the chemoselective reduction of the ester in presence of the phosphonate group. This reaction was carried out using lithium borohydride under microwave irradiation at 80°C for 10 min, which yielded alcohols P1-7a-c (56-95% yield). Attempts to increase the yield were made by increasing the microwave irradiation time from 10 to 15 minutes which resulted in the decomposition of the reactants.

Alcohols P1-7a-c were treated with mesyl chloride to form the mesylated alcohol, which serves as a good leaving group under nucleophilic substitution reaction conditions. Subsequent substitution with potassium thioacetate as a nucleophile gave thioacetates P1-8a-c in 34-71% yield. We also attempted to improve the yield of this reaction by using cesium thioacetate as cesium ions are known to exhibit superior solubility in polar aprotic solvents and higher solvation of cesium ions can provide more nucleophilic thioacetate counter ion in comparison to potassium thioacetate. (126) But the reaction in presence cesium thioacetate gave a very similar result with 72% yield for P1-8c over two steps. For deprotection of the thioacetates, several methods were evaluated utilizing sodium methoxide, methoxyethylamine, and sodium methylthiolate (NaSMe). (127-129) NaSMe was found to be

the best reagent providing the free thiols P1-2a–c with good yields (74-77%) and purity (>95% by High-performance liquid chromatography (HPLC)).

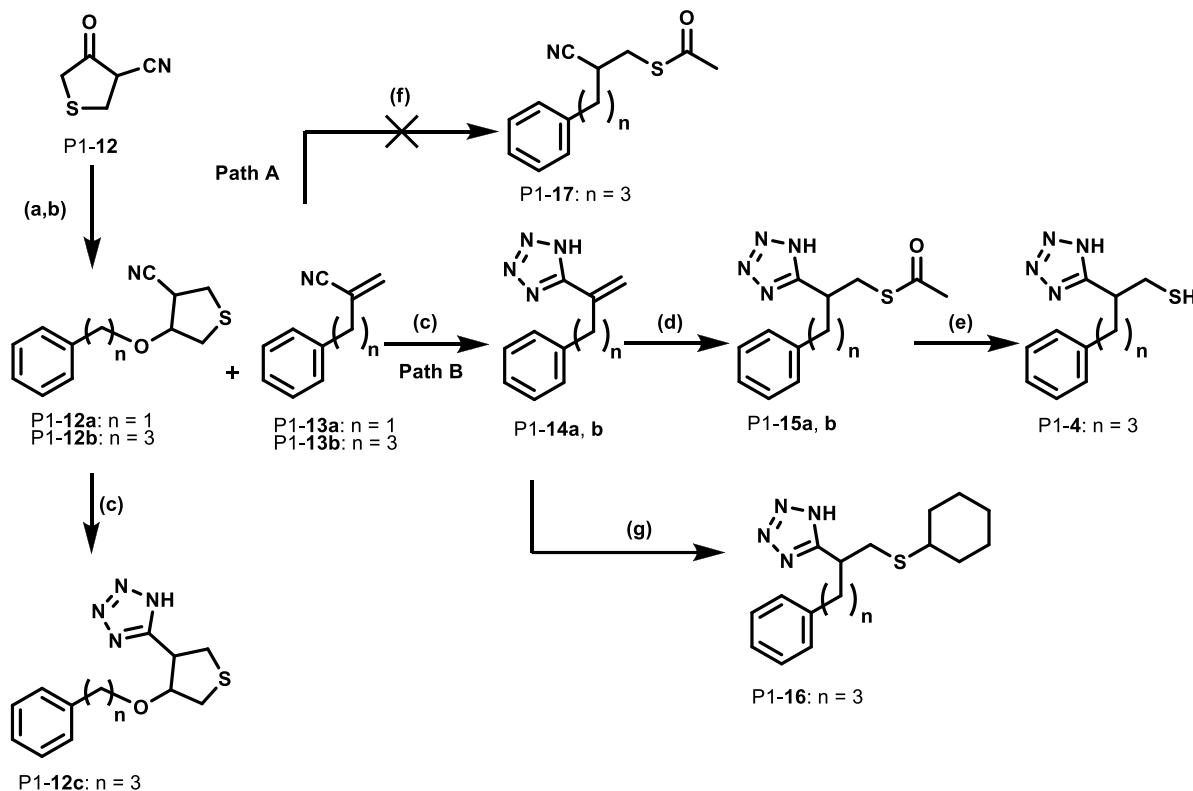
The analogues P1-2, P1-7 and P1-8 containing phosphonate esters were purified by flash column chromatography and converted to the corresponding phosphonic acid derivatives P1-3, P1-9 and P1-10 by treatment with trimethylsilyl bromide (TMSBr) followed by a MeOH quench. Purification of the phosphonic acid analogues P1-3, P1-9 and P1-10 was achieved by washing with EtOAc-pentane to provide the target compounds with moderate to good yields (55-98%) and purity (>95% as determined by HPLC analysis).



Scheme 3.2. Synthesis of thiol-based inhibitors. **a:** $n = 2$; **b:** $n = 3$; **c:** $n = 4$. Reagents and conditions: (a) R—Br, KO^tBu, DMF, 0 °C, P1-6a: 62%, P1-6b: 73%, P1-6c: 45%; (b) LiBH₄, THF, MW 80 °C for 10 min, P1-7a: 60%, P1-7b: 95%, P1-7c: 56%; (c) MsCl, Et₃N, DMAP, CH₂Cl₂, rt; (d) KSAc, DMF, rt.; P1-8a: 54%, P1-8b: 34%, P1-8c: 71% over two steps; (e) NaSMe, MeOH, -20 °C, P1-2a: 30%, P1-2b: 74%, P1-2c: 77%; (f) TMSBr, CH₂Cl₂, then MeOH, rt., P1-3a: 96%, P1-3b: 90%, P1-3c: 98%, P1-9a: 76%, P1-9b: 61%, P1-9c: 55%, P1-10a: 91%, P1-10b: 71%, P1-10c: 65%.

For the synthesis of NH-tetrazole analogues P1-4, P1-15 and P1-16 (Scheme 3.3), we started with 4-cyano-3-oxotetrahydrothiophene P1-12. Alkylation was carried out using potassium carbonate and corresponding alkyl halide, followed by treatment with 5% NaOH to yield α -substituted acrylonitriles P1-13a and P1-13b (51% and 21% respectively) with varying chain lengths ($n = 1, 3$) (130). The other major product was found to be the *O*-

alkylated compounds P1-12a and P1-12b (49% and 79% yield, respectively). Although the yields of our desired C-alkylated product P1-13a and P1-13b were low, they were sufficient to continue for the next step of the synthesis.



Scheme 3.3. Synthesis of NH-tetrazole containing thiol-based inhibitors. Reagents and conditions: (a) R-Br, K_2CO_3 , acetone, reflux; (b) 5% aq. NaOH, P1-13a: 51%, P1-13b: 21%; (c) $TMSN_3$, $n-Bu_2SnO$ (20 mol%), 1,4-dioxane, MW 150 °C for 50 min, P1-12c: 71%, P1-14a: 78%, P1-14b: 74%; (d) HSAc, DMF, 60 °C, P1-15a: 95%, P1-15b: 98%; (e) NaSMe, MeOH, -20 °C, P1-4: 74%; (f) HSAc, DMF, 60 °C, P1-17: no product observed (g) cyclohexylthiol, DMF, 60 °C, P1-16: 93%.

Our first approach was to obtain the thioacetate based compound P1-17 through path A (Scheme 3.3). Several attempts were made for the addition to acrylonitrile P1-13 using thioacetic acid or potassium thioacetate as a nucleophile with different solvents such as DMF, CH_2Cl_2 , and several other solvents such as toluene, tetrabutylammonium, dioxane and water were used resulting in no success (Scheme 3.3). (130) We then decided to change our synthetic route to path B, where the nitrile group is first converted to NH-tetrazole, which is an electron deficient aromatic system and a stronger electron-withdrawing group than nitrile. For this conversion, a microwave promoted reaction of the acrylonitriles with $TMSN_3$ and

dibutyltin oxide as catalyst (20 mol%) was used, (131) which gave the corresponding NH-tetrazoles P1-14a and P1-14b in 74% and 78% yield.

The compounds P1-14a and P1-14b with NH-tetrazoles substituent turned out to be excellent Michael acceptors facilitating the addition of thioacetic acid to the olefin to give the desired tetrazolyl thioacetates P1-15a and P1-15b in good yields (>95% after purification).

The final deprotection of the thioacetates was achieved by treatment with NaSMe to yield free thiol P1-4 in 74% yield and purity >96% (after purification). In addition to these compounds, the undesired major *O*-alkylated product, P1-12c was also treated with TMSN₃ and dibutyltin oxide as catalyst (20 mol%) to yield the corresponding NH-tetrazoles, P1-12c in 71% yield.

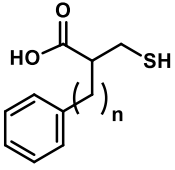
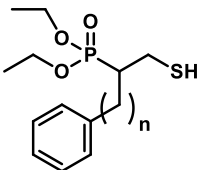
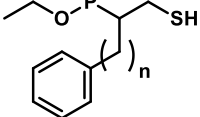
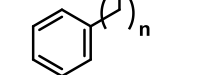
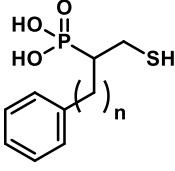
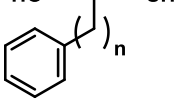
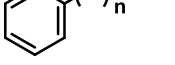
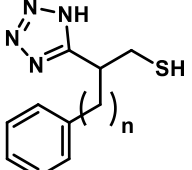
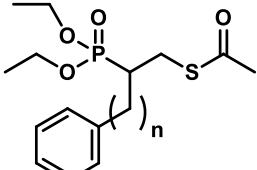
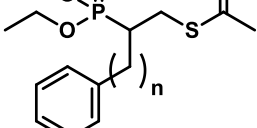
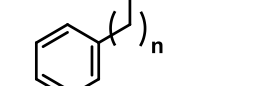
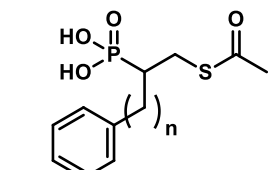
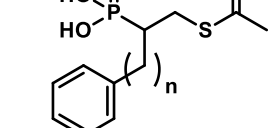
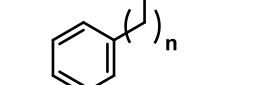
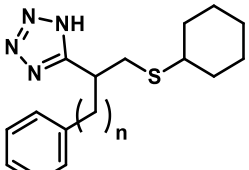
The mercaptophosphonate esters P1-2a-c, mercaptophosphonic acids P1-3a-c and mercapto-NH-tetrazole P1-4, were synthesized (Scheme 3.2; Scheme 3.3) as racemic mixtures. The previously reported racemic mercaptocarboxylic acid inhibitor P1-1c was synthesized as a reference compound in our lab. (127)

3.3.2 Evaluation of inhibitors against VIM-2, GIM-1, and NDM-1

The target molecules P1-2-4 (Figure 3.1) and the intermediates P1-8 and P1-10 from the synthetic pathway were assessed against the three MBLs VIM-2, NDM-1, and GIM-1. The IC₅₀ values were determined through enzyme inhibition assays and the effect of the inhibitors in the whole cell *E. coli* assays containing VIM-2, GIM-1 or NDM-1 were evaluated. Some inhibitors were also tested in a synergy assay with a few clinical isolates of MBL producing *Pseudomonas aeruginosa*, *K. pneumoniae* and *E. coli*. The enzyme-inhibitor complexes of the best inhibitors were further evaluated by X-ray analysis.

All the compounds displayed generally lower IC₅₀ values when tested against VIM-2 as compared to GIM-1 and NDM-1 (Table 3.1). The replacement of the carboxylic acid in P1-1c with NH-tetrazole P1-4, gave a reduced inhibitory effect, while the phosphonate acids and esters, gave almost similar activity (for P1-10, P1-2 inhibitor series) or increased activity (for P1-3 series).

Table 3.1 Evaluation of compound 1 and its bioisosters as inhibitors of VIM-2, GIM-1 and NDM-1. Inhibition concentrations (IC₅₀) against purified enzyme and percent inhibition of MBLs expressed in *E. coli* SNO3 bacterial whole cell experiments.

Compound	ID	VIM-2 ^a		GIM-1 ^a		NDM-1 ^b	
		IC ₅₀ (μM)	% inhib	IC ₅₀ (μM)	% inhib	IC ₅₀ (μM)	% inhib
	P1-1c (n = 4)	2.9 (1.1) ^c	-	-	56	-	
	P1-2a (n = 2)	0.89	78	0.18	64	2.2	33
	P1-2b (n = 3)	0.38	79	0.31	48	1.8	62
	P1-2c (n = 4)	p	p	p	p	p	p
	P1-3a (n = 2)	7.8	92	23	37	5.9	42
	P1-3b (n = 3)	33.2	95	28	46	7.1	45
	P1-3c (n = 4)	8.6	94	16	31	8.5	42
	P1-4 (n = 3)	28	67	68	25	12	16
	P1-8a (n = 2)	133	17	18	25	nh	i
	P1-8b (n = 3)	34	14	26	21	nh	i
	P1-8c (n = 4)	20	12	13	25	nh	i
	P1-10a (n = 2)	2.3	94	12	40	2.9	39
	P1-10b (n = 3)	4.7	95	26	37	6.6	38
	P1-10c (n = 4)	1.8	97	20	50	2.5	37
	P1-16 (n = 3)	5	73	36	8	10	i

^a Reporter substrate was nitrocefin (NCF); ^b Reporter substrate was imipenem (IPM); ^c Values in parentheses as reported by Jin et al. (123);

p = precipitated in the buffer and was not tested; nh = no hydrolysis; i = inactive.

The alcohol inhibitors (P1-7, P1-9), lack the activity exhibited by corresponding thiols and thioacetates (P1-2, P1-3, P1-10), supporting the importance of the presence of sulfur atom in the inhibitor scaffold. The inhibitor P1-3, shows the highest activity having the combination of phosphonate ester and a thiol group. However, when thiol group is replaced with thioacetate group, as in inhibitor P1-8, the combination gives the lowest IC₅₀ value among the inhibitors P1-2, P1-3, P1-8 and P1-10.

The phosphoric acid derivatives containing thiol (P1-2) and thioacetate (P1-10) substituents, on the other hand, were on a similar level of inhibitory activity. This observation may indicate that in the series P1-2 and P1-10 the phosphoric acid group is responsible for the activity observed.

The length of the carbon chain between the chiral carbon and phenyl ring was best when n = 2 or 3. When n = 4 for P1-2c, the inhibitor precipitated and hence was not further used for testing. In short, the most active inhibitors are the mercaptophosphonate esters (inhibitor P1-3a-c) and mercaptophosphonate acids (inhibitor P1-2a and P1-2b). For the most active inhibitors, we observed IC₅₀s in the range of low micromolar to high nano-molar. Despite the promising results obtained during this study, a large deviation in the activities of the three B1 MBLs was observed that indicates the unsuitability of these inhibitors as a broad-spectrum MBL inhibitor.

The best inhibitor with the lowest IC₅₀ and highest percent inhibition in the cell-based screening assay for NDM-1 was P1-2b (IC₅₀= 1.8 μM, percentage inhibition= 62%). The inhibitors were also tested for activity against MBLs in bacterial cells. For several inhibitors, high inhibition (>70%) was observed (Table 3.1) confirming the permeability of inhibitors across the cell membrane of the bacteria. The best inhibitors in terms of percentage inhibition were P1-3a-c and P1-10a-c with inhibition values ranging in between 92-97% against *E. coli* with VIM-2, (where P1-10a-c being slightly more active than P1-3a-c). The percentage inhibition values are also in accord with the IC₅₀ values against VIM-2 for these inhibitors.

Inhibitors P1-2, P1-3 and P1-10 were further tested in a synergy assay with clinical isolates from *E. coli* containing VIM-29 and meropenem, where the MIC values were reduced from 8-32 mg/L with meropenem only to 1 mg/L, 1 mg/L, 2 mg/L with the combination of meropenem and inhibitors P1-3b, P1-10b and P1-10c respectively. (The sequence identity between VIM-29 and VIM-2 is 91%, thus the inhibitors are most likely

active for both VIMs). Crystal structure complexes of VIM-2 with P1-**2b**, P1-**10b** and P1-**10c** were also evaluated during this project. The main observations are described here for a detailed description see Paper 1. (132)

The VIM-2:P1-**2b** complex was used to investigate the two different enantiomers. Herein, only the (*R*)-form (see Figure 1, Paper 1) of the inhibitor P1-**2b** fitted into the observed Fo-Fc omit electron density map indicating that VIM-2 selectively binds to the (*R*)-enantiomer of P1-**2b**. This is also the case for the reported complex of VIM-2-P1-**1c**, where the (*S*)-enantiomer of P1-**1c** binds selectively to VIM-2. (133) The sulfur atom of P1-**2b** interacted with the Zn⁺² ions of VIM-2. Similar interactions are also observed for VIM-2:P1-**1c** (133) and several thiol-B1 MBL complex structures. (133-140) The phosphonate group of P1-**2b** forms hydrogen bonds with Asn233.

In both the VIM-2:P1-**10b** and P1-**10c** structures, the thioacetate interacts with Zn⁺² and Asn233 through the sulfur atom, with His263, and through a water molecule to the guanidinium group of Arg228, (Figure 3, Paper 1).

3.4 Conclusion

The bioisosteric approach was found to be successful in searching for new MBL inhibitors and this study is a step further towards developing potent MBL inhibitors. Inhibitor P1-**2a** and P1-**2b** exhibited lowest IC₅₀ values towards all three enzymes, VIM-2, GIM-1, and NDM-1. The inhibitors from series P1-**3** and P1-**10** were found to give the highest inhibition level of MBLs expressed in the β-lactamase-negative *E. coli* SNO3 cells. Although a broad inhibitor for VIM-2, GIM-1 and NDM-1 were not found, however P1-**10b**, targeting both VIM-2 and NDM-1, is a promising candidate and provides a valuable starting point for a structure-guided design of an inhibitor targeting both VIM-2 and NDM-1.

4. Triazole inhibitors against metallo- β -lactamases

4.1 Rationale for the choice and design of triazole based inhibitors

1,2,3-Triazole is an aromatic nitrogen containing heterocycle, which can form hydrogen bonding and dipole-dipole interactions with various receptors and enzymes in biological systems. (141) Triazoles are also a part of several pharmaceutical drugs like the β -lactam antibiotic cefatrizine, the β -lactamase inhibitor tazobactam, and other antifungal drugs like fluconazole and itraconazole. (142) Moreover, a recent study utilized click alkyne-azide reaction to synthesize a series of homo and hetero vancomycin derived antibiotics with potent activity against vancomycin-resistant bacteria. (143)

In 2005, Loren et al. reported a small library of triazoles that exhibited sub-micromole activity (for e.g. compound P2-1, ($K_i = 0.41 \pm 0.03 \mu\text{M}$), Figure 4.1), as promising VIM-2 inhibitors. (144) With this study in mind, we decided to synthesize a small focused library of new and reported analogues of 1,2,3-NH-triazoles and evaluate their inhibitory activity against VIM-2, GIM-1, and NDM-1. Moreover, we were interested to investigate the binding mode of our inhibitors with VIM-2, through the enzyme inhibitor complex crystal structures.

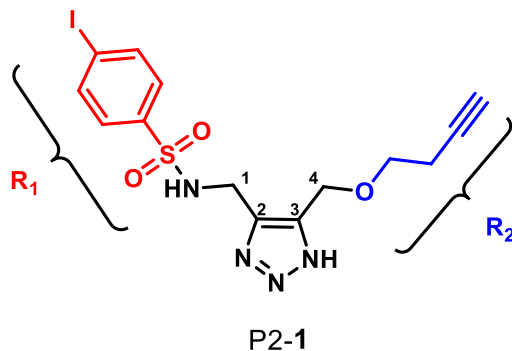
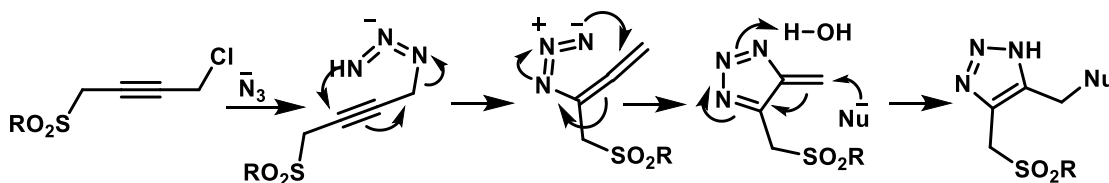


Figure 4.1. N-((4-((but-3-ynoxy)methyl)-1H-1,2,3-triazol-5-yl)methyl)-4-iodo-benzenesulfonamide, P2-1.

According to these previous studies a hydrogen bond acceptor at C-4 such as O or N, contributes positively to the activity of inhibitor (145) we therefore utilized side chains (R_2) such as cyclohexylamine, adamantyl amine, trityl amine, methoxy and acetoxy, for the improvement of inhibitor binding. We also selected some sulfur containing R_2 side chains in order to take advantage of the thiophilic nature of zinc.

4.2 Banert cascade (BC) reaction

The Banert cascade (BC) reaction (Scheme 4.1) was utilized for the synthesis of the target triazole based inhibitors as the main reaction. (146) BC is an organic reaction, in which *NH*-1,2,3-triazoles are prepared from a propargyl halide and sodium azide in a dioxane-water mixture at elevated temperatures. In the first step, nucleophilic displacement of chloride by the azide ion creates an azido compound *in situ*. In the second step, a 3,3-sigmatropic rearrangement takes place, where allenyl azide is formed. This allene rearranges to the triazafulvene. A nucleophilic attack of a second azide ion ($Nu = N_3^-$ in Scheme 4.1) on the exocyclic double bond of the triazafulvene followed by proton abstraction from a proton source concludes the triazole formation reaction. However, in our studies, we isolated the azide containing compounds after the nucleophilic displacement of chloride, so that other nucleophiles than azide could be introduced in the second nucleophilic attack.



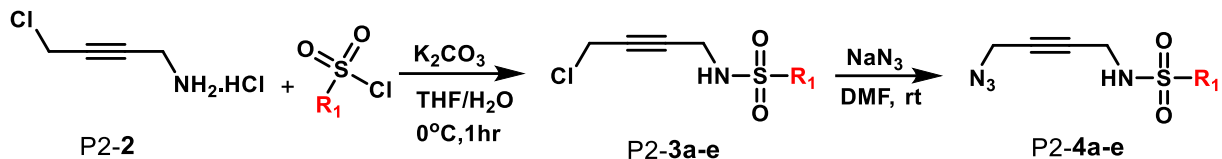
Scheme 4.1. Mechanism of Banert cascade reaction

4.3 Results and discussion

4.3.1 Synthesis

The synthetic strategy for the triazoles is described in Schemes 4.2 and 4.3. Starting from 4-chlorobutylamine hydrochloride P2-2, various chlorosulfonamides were synthesized by treatment with respective sulfonyl chloride in THF/ H_2O mixture in the presence of K_2CO_3 as base. The reaction was completed in 1 hour. Purification was carried out by crystallization

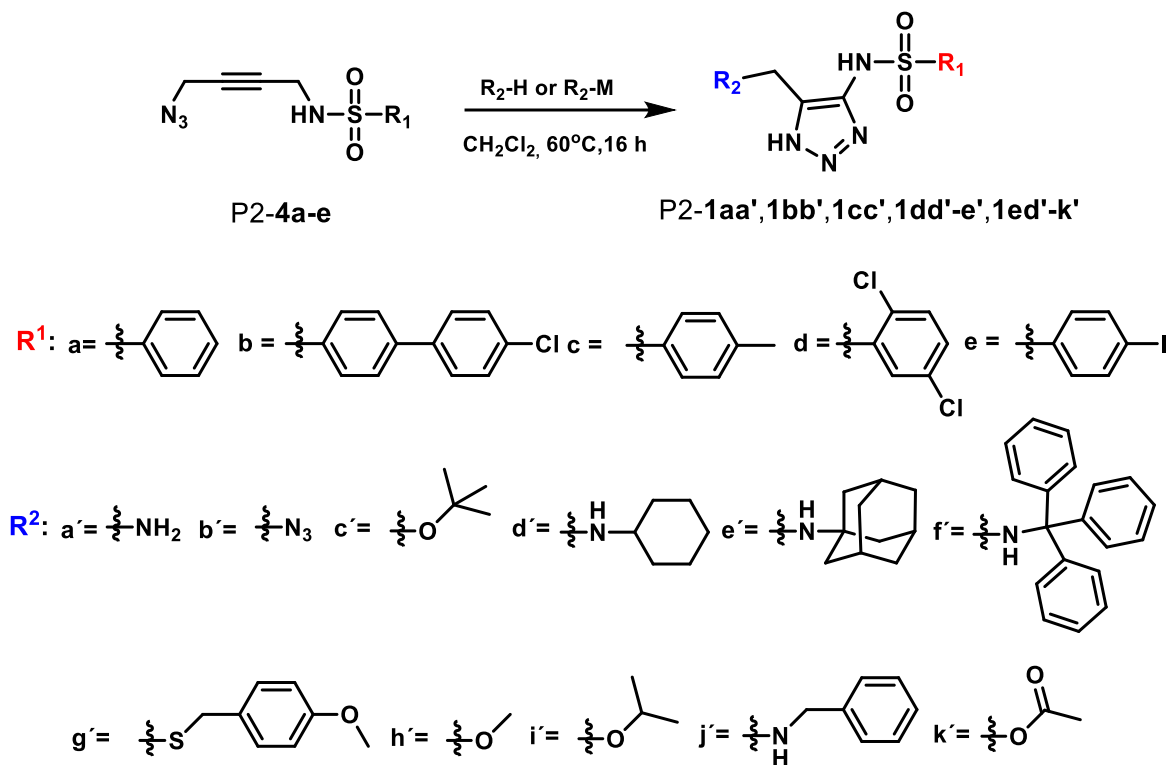
from hexane/EtOAc to yield the corresponding sulfonamides P2-3a to P2-3e in almost quantitative yield.



Scheme 4.2. Synthesis of sulfonamide P2-4a-e.

The chloride substituent of compound P2-3a-e was substituted with azide by using sodium azide in DMF to provide azido sulfonamides P2-4a-e. In the beginning, we experienced difficulty in the purification with flash column chromatography of azido sulfonamides due to the presence of DMF. However, when the reaction mixture was sonicated in water, the product crystallized out and was easily separated by filtration to give pure azido sulfonamides in good yields.

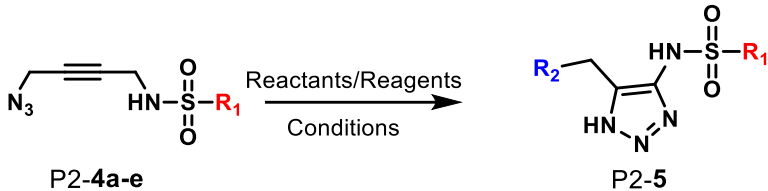
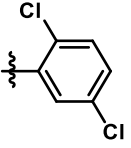
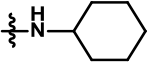
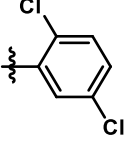
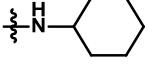

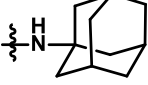
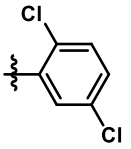
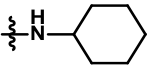
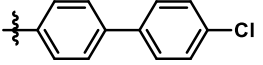
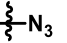
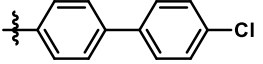
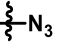

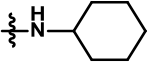

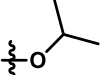
For the synthesis of triazoles from azido sulfonamides various conditions were tested, see Table 4.1. We started with the reaction of azido sulfonamides with different nucleophiles using conventional heating, the reactions gave conversion (Entry 1, Table 4.1). Increasing or decreasing the temperature, varying the equivalency of the nucleophile (cyclohexylamine or adamantylamine) or changing the solvent (dioxane, dioxane: water (3:1) or THF) had no effect (Entry 2-4, Table 4.1). We then reacted chlorosulfonamide P2-3 in the presence of NaN₃ and NH₄Cl in a Banert-cascade reaction to yield the corresponding triazole in 35% yield (Entry 5, Table 4.1). The reaction failed to give conversion with other nucleophiles.



Scheme 4.3. Conversion of azides to triazoles

Therefore, we changed the solvent and utilized dry CH_2Cl_2 and an excess of the nucleophile to react with the azido sulfonamides P2-4a-e at 60 °C for 16 h, to afford the desired triazoles in good yields (Entry 6-7, Table 4.1). In the cases where the nucleophile itself can act as solvent, e.g. isopropanol, methanol and cyclohexylamine no additional solvent was used, (Entry 8, Table 4.1).

Table 4.1. Investigation of reaction conditions for triazole formation.

						
Entry	Substituents		Reagents	Temp. [°C]	Time [h]	Conv [%]
	R ¹	R ²				
1			Cyclohexylamine, 1.5 equiv Dioxane	75	12	0
2			Cyclohexylamine, 3 equiv Dioxane	100	72	0
3			NH-adamantylamine, 3 equiv Dioxane: Water (3:1)	150	24	0
4			Cyclohexylamine, 3 equiv THF	60	24	0
5*			NaN ₃ , 1.5 equiv NH ₄ Cl, 2 equiv Dioxane: Water (3:1)	75	8	35
6			NaN ₃ , 3 equiv, CH ₂ Cl ₂	60	16	70
7			Cyclohexylamine, 4 equiv, CH ₂ Cl ₂	60	16	86
8			Isopropanol, 2 mL	60	16	86

* Reaction performed using chlorosulfonamide instead of azido sulfonamide as the starting material

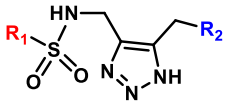


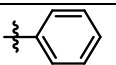
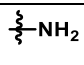
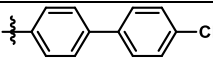
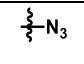
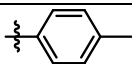
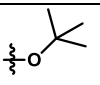
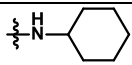
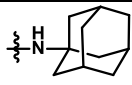
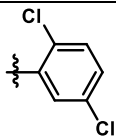
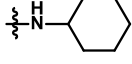
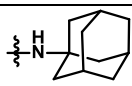

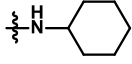
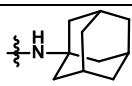
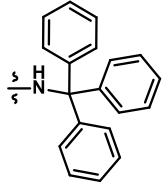
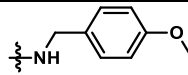
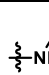
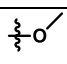
4.3.2 Evaluation of inhibitors against VIM-2, GIM-1, and NDM-1

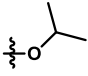
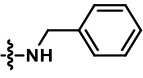
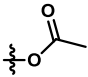
The inhibitors were tested for their potential to inactivate NDM-1, VIM-2, and GIM-1 (see Table 4.2). In addition, we also obtained crystal structures of 4 inhibitors (P2-**1ei'**, P2-**1ej'**, P2-**1ek'** and P2-**1dd'**) in complex with VIM-2. This helped us in understanding the observed inhibition patterns and their relation to structure using the crystal structures of the studied enzymes.

First, the compounds ability to inhibit VIM-2, GIM-1, and NDM-1 in a biochemical assay and a whole-cell assay with MBLs expressed in *E. coli* SNO3 was evaluated. IC₅₀ values were determined with nitrocefin for VIM-2 and GIM-1 whereas, for NDM-1 imipenem was used as reporter substrate.

Generally, the inhibitors showed more activity towards VIM-2 than GIM-1 and NDM-1. The triazoles P2-**1dd'**, P2-**1de'**, P2-**1ed'**, P2-**1ee'** and P2-**1ei'** gave high nano-molar activity (IC₅₀ = 0.067-0.533 μM and 85% to 96% inhibition in the whole cell assays) thus proved to be the best inhibitors in this study against VIM-2. The inhibitors P2-**1ce'**, P2-**1ed'**, P2-**1ee'** and P2-**1ek'** gave the best inhibition values in the range of IC₅₀ = 18.4-128.3 μM against GIM-1, but low levels of percent inhibition (3-25%) were observed for all the inhibitors tested. For NDM-1 the inhibitor P2-**1ef'** with a bulky R₂ substituent gave the best result (IC₅₀ of 80.7 μM), while the level of inhibition in the whole cell assay was rather low (for e.g., P2-**1ee'** and P2-**1eg** showed 17% and 34% respectively) (see Paper 2).

Table 4.2. The molecular structures of the synthesized inhibitors with measured inhibition concentrations (IC₅₀) against pure VIM-2, GIM-1, and NDM-1 enzymes; followed by % inhibition in *E. coli* SNO3 bacterial whole cell experiments.

Entry	ID/ yield			VIM-2 ^a		GIM-1 ^a		NDM-1 ^b	
				IC ₅₀	%	IC ₅₀	%	IC ₅₀	%
				(μM) a	inhib a	(μM) a	inhib a	(μM) a	inhib a
1	P2-1aa [✓] / 65%			23.17	28.6	NI	NI	NI	NI
2	P2-1bb [✓] /70 %			NI	NI	NI	24.9 5	117. 8	14.4
3	P2-1cc [✓] / 65%			7.16	60.3	128.3	4.45	142. 2	NI
4	P2-1cd [✓] / 71%			1.54	82.1	NI	2.3	143. 8	NI
5	P2-1ce [✓] / 83%			2.31	83.7	82.6	NI	ND	NI
6	P2-1dd ^{✓*} / 72%			0.228	94	NI	7	98.1	NI
7	P2-1de [✓] / 73%			0.115	NI	P	21	ND	NI
8	P2-1ed [✓] / 86%			0.067	94.7	69.35	3.2	148	NI
9	P2-1ee [✓] / 96%			0.163	95.8	18.4	21.6	ND	17
10	P2-1ef [✓] / 93%			>250	18.7	353	3%	80.7	NI
11	P2-1eg [✓] / 93%			21.02	44.7	227.2	33.1	ND	34.3
12	P2-1eh [✓] / 88%			14.87	51.1	168.9	10.7	NI	NI

13	P2- 1ei ^{~*} / 86%		0.533	85.3	193	11.1	NI	NI
14	P2- 1ej ^{~*} / 72%		P	ND	ND	ND	ND	ND
15	P2- 1ek ^{~*}		23	ND	48	ND	231	ND

^a the reported substrate was nitrocefin; ^b the reported substrate was imipenem; NI, No observable inhibition; ND, Not determined; P, precipitated. *, a VIM-2 complex structure is present.

Most interestingly, the synergy assay found P2-**1ek**[~] to effect two clinical isolates. In one *P. aeruginosa* isolate producing VIM-2 the MIC was reduced from 64 mg/L (with only meropenem) to 1 mg/L for the combination of meropenem and P2-**1ek**[~]; and for an *E. coli* isolate producing VIM-29 the MIC was reduced from 16 mg/L (with only meropenem) to 1 mg/L when combining meropenem and P2-**1ek**[~] (see Paper 3).

Analysis of the crystal structures obtained for inhibitors P2-**1ei**[~], P2-**1dd**[~], P2-**1ej**[~] and P2-**1ek**[~] in complex with VIM-2 revealed that triazole ring interacts with one of the zinc ions and a bridging hydroxide ion in the active site, as a common binding feature. As was proposed in the initial report on triazole inhibition of VIM-2, (144) sulfonamide group did not participate in Zn²⁺ binding.

4.4 Conclusion

We synthesized several NH-1,2,3-triazole derivatives and our new P2-**1ed**[~] inhibitor gave nano-molar affinity with IC₅₀ of 0.067 μM. Interestingly P2-**1ed**[~] also gave some low level inhibition for GIM-1 (IC₅₀=69 μM) and NDM-1 (IC₅₀=148 μM). Our most promising inhibitor is our new P2-**1ek**[~] with moderate IC₅₀ values of 23 μM (VIM-2), 48 μM (GIM-1) and 231 μM (NDM-1), but it is affecting all the three enzymes studied. Most remarkably, the synergy assay found P2-**1ek**[~] to reduce the meropenem MIC in two MBL-producing clinical isolates. Our new complex structure of VIM-2 P2-**1ek**[~] is, therefore, a valuable starting point for further structure-guided inhibitor design.

5. Focused fragment library targeting OXA-48

5.1 Rationale for the design of fragments

In this project we continued with the development of the fragment P3-1 with IC_{50} of 250 μM , previously reported by our group, using structure-based inhibitor design (Figure 5.1). (114) The hit fragment P3-1 became the starting point for this project and a synthesis of a focused fragment library was initiated. In addition, we aimed to find and merge fragments with different binding conformations to improve inhibitory activity. The merging of the fragments was based on the observation of two different binding poses in the enzyme-fragment complex of OXA-48:P3-1, leading to the design of the merged compound P3-2 that gave 10 fold increased binding affinity. (114)

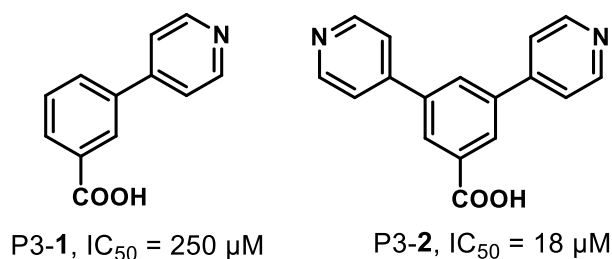


Figure 5.1. (a) 3-(pyridin-4-yl)benzoic acid P3-1 hit from our previous study (b) merged fragment 3,5-di(pyridin-4-yl)benzoic acid P3-2 with an improved binding affinity towards OXA-48. (114)

The benzoic acid moiety is kept unaltered since it provides an essential part for binding and activity of the fragments. To be specific the carboxylic acid group on ring A (Figure 5.2), showed ionic interactions with the side chain of Arg250. (114) This interaction is in accordance with the role of Arg250 in substrate binding, where the side chain of arginine can change its position and interact with the carboxylic acid group of the β -lactam

substrates. (147) Ring B and its substituents were coupled with different heterocycles and polar groups to spatially explore the active site of OXA-48. Among these were tetrazole, amines, amides, sulphonamides, sulphides and esters as ortho, meta or para substituents on the ring B (Figure 5.2). In addition, 33 fragment-enzyme complexes were analysed by X-ray crystallography. A continuous feedback from enzyme inhibition assays, together with crystal structures obtained, helped us to explore the binding site of OXA-48 and determine potential fragments with improved binding affinity.

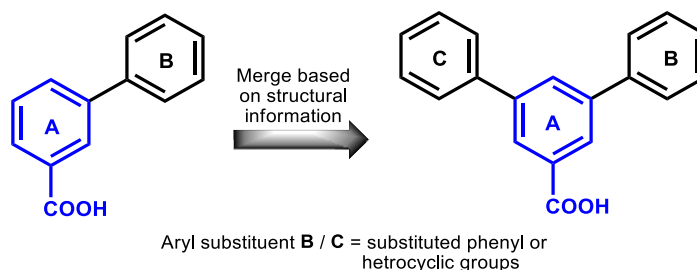


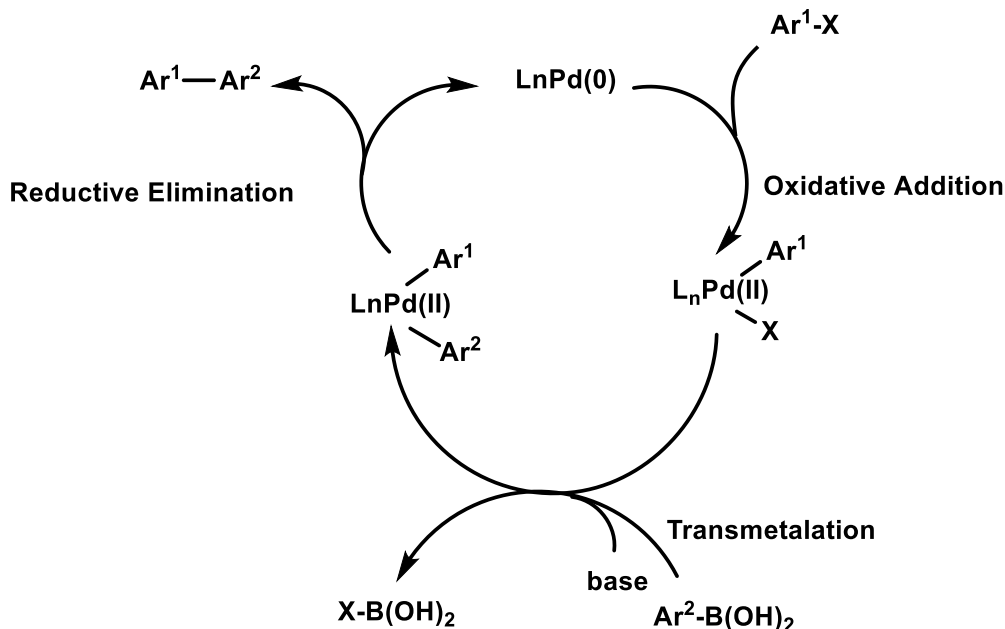
Figure 5.2. Fragment merging approach

5.2 Suzuki-Miyaura coupling reaction (SMC)

For the synthesis, a versatile and efficient Suzuki-Miyaura coupling (SMC) reaction was applied to generate substituted and/or heteroatom containing biaryl moieties. Heck, Stille and Suzuki-Miyaura reactions are the most common reactions utilized for coupling and C–C bond formation between aryl groups. The syntheses of our target fragments were facilitated by the mild and versatile SMC reaction. SMCs join two sp^2 -hybridized carbons to form biaryl or diene/polyene compounds. This method has proven to be a useful tool for making carbon frameworks because of its functional group tolerance, easy availability of boron compounds, wide substrate scope, and high turnover rates with modern catalysts (148) and is the method of choice for the synthesis of polyene and biaryl moieties in the pharmaceutical and material industries. (149) During the last decade efforts have been directed towards greener version of SMC reaction (150) e.g. the development of heterogeneous palladium catalysts using green solvents like water, 2-methyl-tetrahydrofuran, and *tert*-amyl alcohol or the use of microwave irradiation provide greener alternatives for SMC. (151)

The mechanism (Scheme 5.1) of the catalytic cycle of SMC follows a sequence of oxidative addition, transmetalation, and reductive elimination to give the biaryl compound

while regenerating the Pd(0) species. In the first step, oxidative addition of the alkyl halide occurs to form the arylpalladium(II) halide intermediate. Reactivity of the Ar¹-X group decreases in the order I > OTf > Br > Cl. Then transmetalation with an organoboron species occurs in the presence of a base, where an alkyl or aryl is transferred from the organoborane to the palladium. The final reductive elimination step forms the corresponding coupling product while Pd(0) is regenerated. (152-154)



Scheme 5.1. Mechanism of Suzuki Miyaura coupling (SMC) reaction

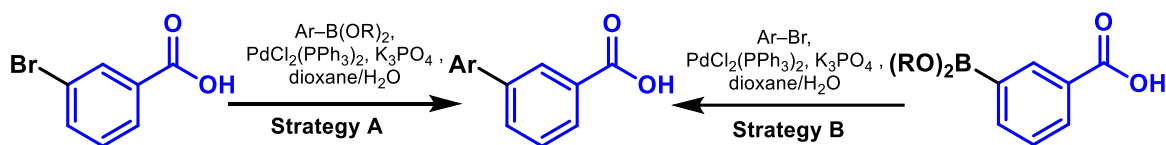
5.3 Results and discussion

5.3.1 Synthesis

5.3.1.1 3-Substituted benzoic acid derivatives

All the fragments fulfil the criteria for fragment-based ligand design (MW < 300 Da, clogP < 3, hydrogen bond acceptor/donors < 3). (155) A focused library of 49 3-substituted benzoic acid fragments (P3-3 to P3-35) were prepared (Scheme 5.2, Table 5.3). The synthesis of the fragments involved the construction of the aryl-aryl or aryl-heteroaryl core by SMC reaction. Various substitutions on the aryl ring B (Figure 5.2) were explored in order to determine whether the position or different substituents the activity of the inhibitors against the OXA-48 enzyme.

For most of the couplings, reactions were carried out in 1:1 dioxane/water with $\text{PdCl}_2(\text{PPh}_3)_2$ (1, 5, or 10 mol%, for details see SI for Paper 3) and potassium phosphate as a base, at 95 °C for 16-20 hours. (114) Two alternate couplings strategies were found successful using either 3-bromobenzoic acid (Strategy A, Scheme 5.2) or 3-carboxyphenylboronic acid pinacol ester (Strategy B, Scheme 5.2) as the starting materials. This allowed us to use a wide range of aryl boronic acids or aryl bromides to introduce versatility in the library. The former being slightly more feasible in terms of yields of the reaction. While some reactions were also carried out in organic solvents such as THF, due to the insolubility or sensitivity of the starting material towards hydrolysis in an aqueous medium (See SI of Paper 3).



Scheme 5.2. Synthetic strategy 3-substituted benzoic acids analogues against OXA-48

Inspired by the results of fragment P3-21a (see Table 5.3), we envisioned a small series containing sulfonamides and amide substituents and a longer chain length which could give more flexibility in the fragment structures, thus, allowing the fragments to be close enough to neighbor residues and increase the potential of H-bonding or other interactions. Furthermore, the sulfonamides have two hydrogen bonding acceptors, which might be an advantage over the amides. Thus, fragments P3-13-20 and P3-22-23 were synthesized.

Some fragments (P3-17-20 and P3-22-23) did not show coupling under normal reaction conditions. This may be due to the presence of an electron donating group (NH_2 or NHR group as a substituent) which is known to slow the oxidative addition step (156,157) resulting in the deactivation of C-X bond. (158,159) However, there are examples of Suzuki couplings in the literature performed in the presence of free NH_2 groups, but the yields are generally lower. (160-164) This problem was solved by the use of the second generation (Pd-G2) pre-catalysts, which in contrast to the previous generation can easily create the active Pd species even at room temperature and in the presence of weak phosphate or carbonate bases. Moreover, these pre-catalysts are soluble in various organic solvents as well as being air, and

moisture stable. Additionally, Buchwald and coworkers reported Xphos-Pd to accelerate oxidative addition step. (154) Thus more efficient catalysts (XPhos-Pd G2) and water-free conditions (anhydrous THF instead of dioxane/ water) were successfully employed to solve reactivity and solubility problems.

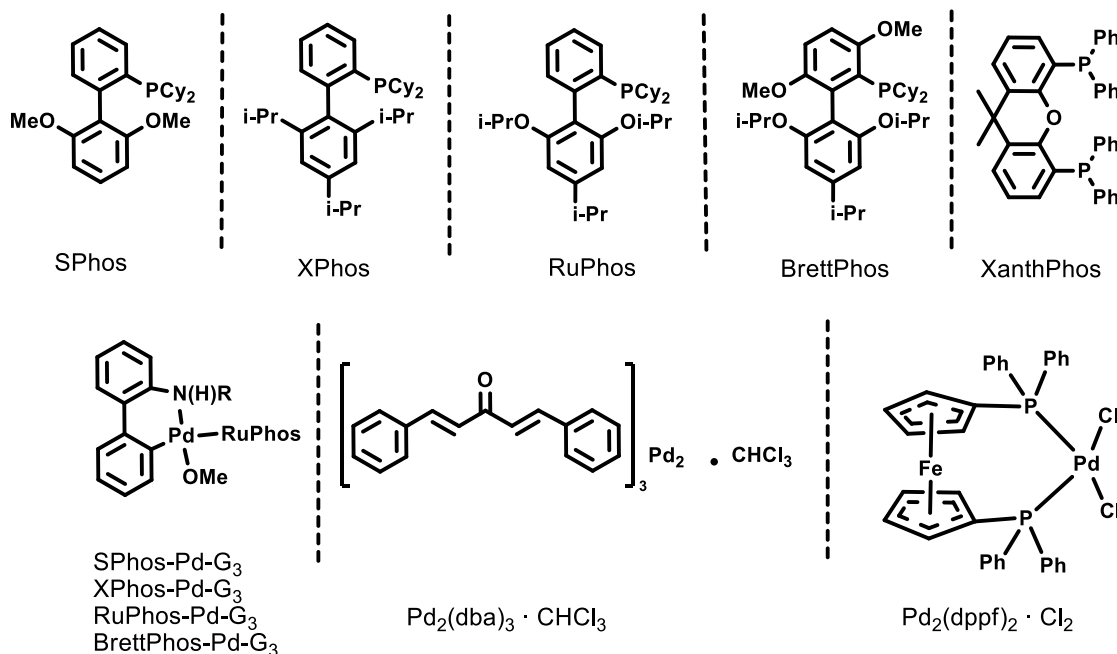
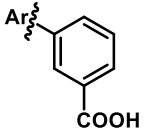
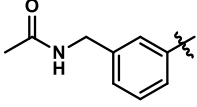
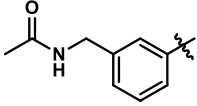
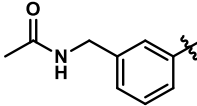
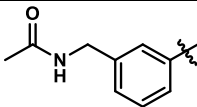
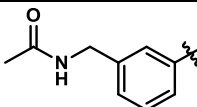
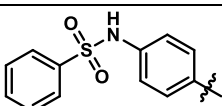
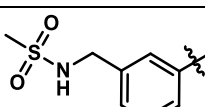
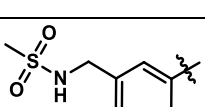
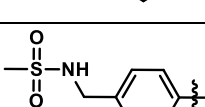
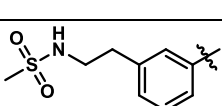
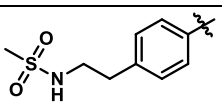


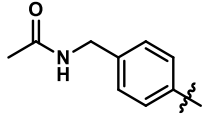
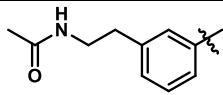
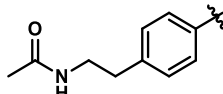
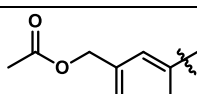
Figure 5.3. Catalyst utilized in the course of this study

For compound, P3-22 (Entry 1-4, Table 5.1) different Buchwald catalysts (Figure 5.3) were screened to optimize reaction conditions. We found out that the best yields (87% for P3-22, Entry 3, Table 5.1) were obtained when we used commercially available XPhosPd G2 catalyst for the coupling reactions. Although PdCl₂(dppf) can also be used with similar reaction conditions for some fragments (P3-7–10 and P3-13–14, Table 5.1).

The purification of NH₂ or NHR group containing fragments using automated reverse phase C18 flash column chromatography led only to around 60% purity according to HPLC. For further purification, a normal phase silica flash column was used with an acidic eluent (1:9 mixture of acetic acid/water/methanol/ethyl acetate (3:2:3:3) and ethylacetate). As a result, the respective fragments were obtained in a purity of 95% or higher.

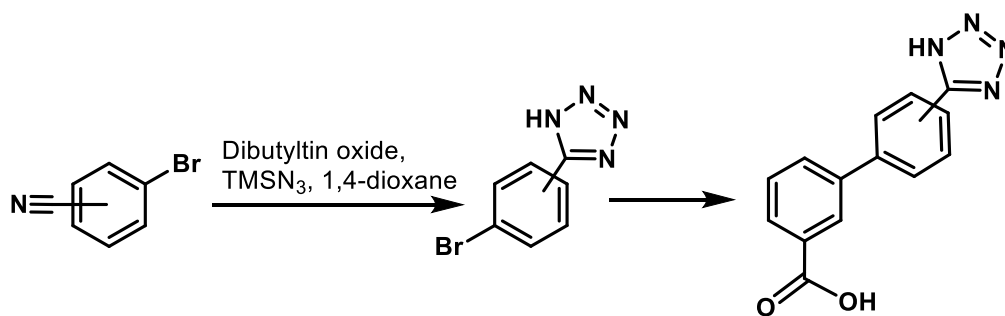
Table 5.1. Catalyst screening for substituents with NH and NHR substituents.

Entry	Catalyst	Conversion %	 Ar
			Ar
1	BrettPhos Pd G3	34%	
2	XPhos Pd G2	74%	
3	XPhos Pd G2	87%	
4	Pd ₂ (dba) ₃ + SPhos1 ^a	40%	
5	Pd ₂ (dba) ₃ + RuPhos ^a	14%	
6	XPhos Pd G2 ₂	65%	
7	PdCl ₂ (dppf)	41%	
8	PdCl ₂ (dppf)	26%	
9	PdCl ₂ (dppf)	10%	
10	PdCl ₂ (dppf)	11%	
11	XPhos Pd G2	89%	

12	XPhos Pd G2 ^a	11%	
13	PdCl ₂ (dppf)	46%	
14	PdCl ₂ (dppf)	34%	
15	XPhos Pd G2	34%	

^a Pd₂(dba)₃ (1 mol%) and SPhos or RuPhos (2 mol%) in anhydrous THF.

For the synthesis of compound P3-26a and P3-26b, [3+2] intermolecular cycloaddition between 3-bromobenzonitrile or 4-bromobenzonitrile and trimethyl silyl azide was carried out in the presence of dibutyltin oxide in anhydrous 1,4-dioxane. The reaction mixture was subjected to microwave irradiation in a tightly sealed microwave vessel for 50 min at 150 °C to afford 3- or 4-bromobenzotetrazole respectively, which were then subjected to SMC reaction (Scheme 5.3). (131)

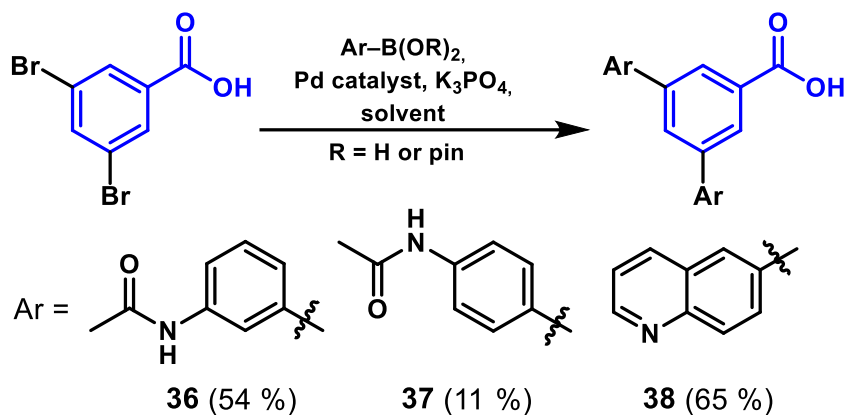


Scheme 5.3. Synthetic strategy for compound P3-26a and P3-26b.

5.3.1.2 Synthesis of 3,5-disubstituted benzoic acid derivatives

A small series of 5 symmetrical and unsymmetrical, 3,5-disubstituted derivatives (P3-36-40) was also prepared to investigate the inhibitory activity of merged fragments. For the synthesis of symmetrical 3,5-disubstituted compounds P3-36 and P3-38 (Scheme 5.4), the conditions established for mono-substituted fragments with Pd₂(dba)₃/XPhos or XPhos-Pd G2 as the catalyst, 3,5-dibromobenzoic acid as starting material and an increased amount of

the boronic acid derivative (2 equiv.) were used. The compounds P3-36 and P3-38 were obtained in 54% and 65% yields, respectively (Scheme 5.4) (165). Compound P3-37 was isolated in 11% yield as a by-product, in an attempt to prepare the mono-substituted analogue (Scheme 5.4).



Scheme 5.4. Preparation of symmetrical 3,5-disubstituted benzoic acids. Reagents and conditions: P3-36: 3-acetamidophenylboronic acid (1.5 equiv.), Pd₂(dba)₃•CHCl₃ (5 mol%), XPhos (5 mol%), dioxane:water (1:1), 60 °C, 54%; P3-37: 4-acetamidophenylboronic acid (0.75 equiv.), PdCl₂(PPh₃)₂ (10 mol%), dioxane:water (1:1), 95 °C, 11%; P3-38: quinolin-6-ylboronic acid pinacol ester (2.0 equiv.), XPhos-Pd G2 (5 mol%), tert-butanol, 60 °C, 65%.

For unsymmetrical 3,5-disubstituted benzoic acids P3-39, our strategy with the step by step addition of two different aryl boronic acids with the previously established conditions was not very successful, with only 15% isolated yield (Scheme 5.5). Moreover, the product was not found to be pure enough and required HPLC purifications due to the presence of symmetrical by-products with similar properties. Thus, an improved strategy was required. For this, we replaced 3,5-dibromobenzoic acid with 3-iodo-5-bromobenzoic acid in order to steer the reaction to the iodide during the first coupling and thereby prevent the formation of symmetrical disubstituted by-products (Scheme 5.5). Quinolin-6-ylboronic acid pinacol ester was allowed to react with 3-iodo-5-bromobenzoic acid to form mono-substituted P3-int-40, the chemo-selectivity of the starting material alone was not found sufficient to prevent unwanted coupling therefore a careful screen of catalysts (RuPhos-Pd G3, XantPhos-Pd G3, Sphos / Pd₂(dba)₃, Xphos / Pd₂(dba)₃, SPhos-Pd G3, XPhos-Pd G2, Pd₂(dppf)Cl₂), solvent (toluene / water, anhydrous THF, dioxane /water, tert-butanol), reaction temperature (40-80 °C) and time (10-48 h) was initiated (see Table 5.2).

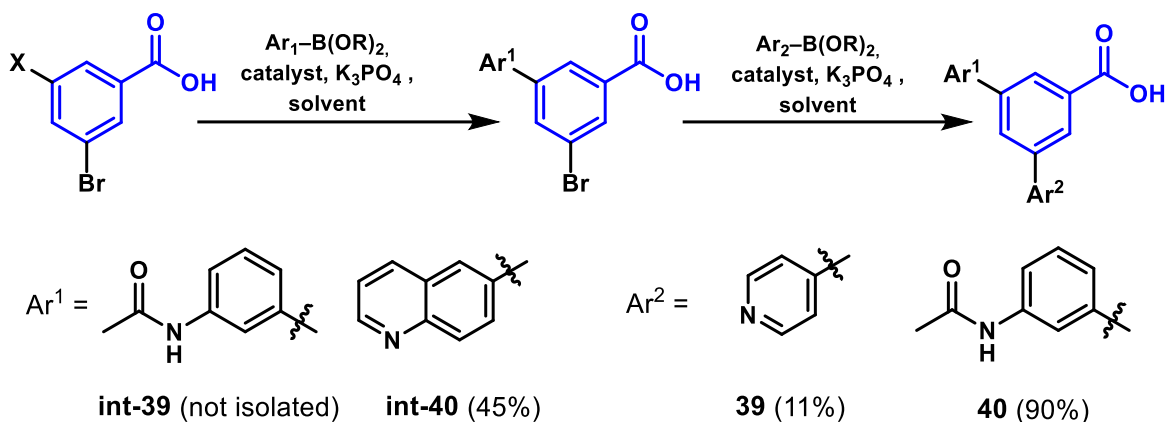
Table 5.2. Screening of reaction conditions for the coupling of 3-bromo-5-iodobenzoic acid

Entry	Catalyst [mol% in Pd]	Base	Temp [°C] / Time [h]	Solvent	Ratio (int-39:38:sm)	Isol. yield [%]
1	RuPhos-Pd G3 (10)	K ₃ PO ₄	60 / 24	dioxane/water (1:1)	8 : 10 : 10	nd
2	RuPhos-Pd G3 (5)	K ₃ PO ₄	60 / 24	toluene/water (1:1)	10 : 6 : 0.3	nd
3	XantPhos-Pd G3 (5)	K ₃ PO ₄	60 / 48	dioxane/water (1:1)	10 : 1 : 0	nd
4	XantPhos-Pd G3 (5)	K ₃ PO ₄	40 / 24	toluene/water (1:1)	10 : 1 : 3	70
5	Pd(dppf)Cl ₂ (5)	K ₃ PO ₄	60 / 24	dioxane/water (1:1)	10 : 1 : 3	80
6	XPhos-Pd G2 (1)	K ₃ PO ₄	60 / 24	dioxane/water (1:1)	10 : 7 : 1	nd
7	SPhos-Pd G3 (5)	K ₃ PO ₄	60 / 24	dioxane/water (1:1)	10 : 2 : 0	40
8	Pd ₂ (dba) ₃ •CHCl ₃ / SPhos 1:1 (10)	K ₃ PO ₄	60 / 24	dioxane/water (1:1)	10 : 1 : 0.4	55
9	Pd ₂ (dba) ₃ •CHCl ₃ / SPhos 1:1 (10)	K ₃ PO ₄	80 / 24	dioxane/water (1:1)	10 : 1 : 0.3	55
8	Pd ₂ (dba) ₃ •CHCl ₃ / SPhos 1:1 (10)	K ₃ PO ₄	40 / 24	<i>t</i> BuOH	10 : 4 : 4	nd
9	Pd ₂ (dba) ₃ •CHCl ₃ / SPhos 1:1 (10)	K ₃ PO ₄	40 / 20	toluene/water (1:1)	10 : 1 : 3	65
10	Pd ₂ (dba) ₃ •CHCl ₃ / SPhos 1:1 (10)	K ₃ PO ₄	60 / 10	dioxane:water (1:1)	5 : 4 : 10	nd
11	Pd ₂ (dba) ₃ •CHCl ₃ / SPhos 1:1 (10)	K ₃ PO ₄	60 / 48	dioxane:water (1:1)	10 : 4 : 1	nd
12	Pd ₂ (dba) ₃ •CHCl ₃ / SPhos 1:2 (5)	K ₃ PO ₄	60 / 24	dioxane/water (1:1)	10 : 0.7 : 0	40

nd not determined

The ratios of the monosubstituted and disubstituted products together with unreacted starting material were monitored by mass spectrometry (MS). XantPhos-Pd G3, Pd₂(dppf)Cl₂ and SPhos/Pd₂(dba)₃ were found to be the most chemoselective catalysts for the aryl iodide

when the reaction was performed with K_3PO_4 as a base in dioxane/water at 60 °C for 24 hours (Entries 3,5 and 12, Table 5.2). With these conditions and SPhos/ $Pd_2(dba)_3$ as a catalyst, P3-**int-40** was the main product along with 8-10% disubstituted product as the by-product. Careful purification provided P3-**int-40** in moderate yield (45%). The mono-substituted P3-**int-40** was further subjected to a second coupling with XPhos-Pd G2 (5 mol%) as a catalyst to provide P3-**40** in good yields (90%).



Scheme 5.5. Preparation of unsymmetrical 3,5-disubstituted benzoic acids. Reagents and conditions: P3-**39**: i. X = Br, 3-acetamidophenylboronic acid (0.75 equiv.), $PdCl_2(PPh_3)_2$ (10 mol%), dioxane: water (1:1), 60 °C; ii. pyridin-4-ylboronic acid (1.2 equiv.), $PdCl_2(PPh_3)_2$ (10 mol%), dioxane: water (1:1), 60 °C; P3-**int-40**: X = I, quinolin-6-ylboronic acid pinacol ester (2.0 equiv.), $Pd_2(dba)_3 \cdot CHCl_3$ (5 mol%), SPhos (5 mol%), dioxane:water (1:1), 60 °C; P3-**40**: 3-acetamidophenylboronic acid (1.5 equiv.), XPhos-Pd G2 (5 mol%), *t*BuOH, 60 °C.

5.3.2 Evaluation of the fragments against OXA-48

All the fragments were subjected to biochemical, enzymatic assay. Fragments P3-**4a** (IC_{50} 50 μ M), P3-**18** (IC_{50} 60 μ M), P3-**21a** (IC_{50} 35 μ M), P3-**26a** (IC_{50} 60 μ M), P3-**26b** (IC_{50} 36 μ M) and P3-**35** (IC_{50} 35 μ M) were found to have stronger inhibitory activity while generally most of the other fragments showed inhibition at similar level (IC_{50} > 200 μ M) to the original hit fragment P3-**1**. We also obtained crystal structures of 33 of the fragment-enzyme complexes, which gave us insight into the binding mode and further design of the improved disubstituted compounds, (Scheme 5.5).

By analyzing the individual crystal structures carefully two different binding sites were identified for the fragments, called the **R₁** and **R₂** binding sites (binding sites were named with respect to binding interactions of 6 α -hydroxyethyl (**R₁**) and amidine group (**R₂**)).

group of imipenem with residues (Trp105, Val120, Leu158) and (Ile102, Tyr211, Leu247, Thr213) respectively), (see Figure 2 in Paper 3).

The most common interactions were between the carboxylate group of the fragments and the guanidine group of Arg250 π - π stacking interaction of the 3-aryl ring system attached to benzoic acid with Tyr211 (except for fragment P3-**21a** and P3-**26b**). Fragment P3-**21a** and P3-**26b** both showed enhanced activity (10-fold increased inhibition, IC₅₀: 35 and 36 μ M respectively), where acetamide group of P3-**21a** formed a hydrogen bond to the guanidine group of Arg214 and T-shaped π - π -stacking interaction with Trp105, while the *para*-tetrazolyl substituent on ring B of the fragment P3-**26b** formed a hydrogen bond with the guanidine group of Arg214. Both these fragments occupy the **R**₁ site, whereas most of the fragments were binding to the **R**₂ site. In addition, pyridin-2-yl substituted fragment P3-**35** with IC₅₀ 35 μ M also showed 10-fold increased activity, which could be explained by two alternative conformations one with occupying **R**₂ site as for most of the fragments and other showing hydrogen bond to Tyr117 in the **R**₁ binding site.

With these results, we initiated the synthesis of disubstituted compounds P3-**36** to P3-**40** (merged fragments showing **R**₁ and **R**₂ binding) and as expected we found the improved inhibitory activity of two of the merged fragments P3-**36** and P3-**40** to be as low as 2.9 μ M. Where P3-**36** is the merged symmetrically disubstituted fragment based on P3-**21a**/ **21a** and P3-**40** is the merged unsymmetrically disubstituted fragment based on P3-**21a**/ P3-**28** combination, (see Figure 9, Paper 3).

Table 5.3. Inhibitor activities of a library of 3-substituted benzoic acids analogues against OXA-48 (IC₅₀ and K_D).

ID Strategy / yield	Ar =	IC ₅₀ (μM)	K _D (μM)	ID Strategy/ Yield	Ar =	IC ₅₀ (μM)	K _D (μM)
P3-3a* B/ 78%		90	170	P3-16b B/ 67%		1000	970
P3-3b* B/ 67%		170	300	P3-17* ^{a, c} B/ 41%		370	100
P3-4a* A/ 94%		50	175	P3-18 ^{a, c} B/ 65%		60	210
P3-4b* A/ 98%		110	110	P3-19a ^{a, c} B/ 26%		110	110
P3-4c* A/ 39%		470	170	P3-19b ^{a, c} B/ 10%		450	240
P3-5* A/ 84%		900	230	P3-20 ^{a, c} B/ 11%		370	200
P3-6a* A/ 98%		250	123	P3-21a* A/ 98%		35	100
P3-6b* A/ 98%		360	226	P3-21b* A/ 98%		450	290
P3-6c* A/ 86%		150	250	P3-22 ^{a, b} A/ 87%		130	130
P3-7 A/ 91%		400	1000	P3-23a ^{a, c} B/ 46%		230	170
P3-8a* A/ 68%		130	170	P3-23b ^{a, c} B/ 34%		520	190
P3-8b* A/ 98%		130	240	P3-24* ^{a, b} A/ 34%		250	140
P3-8c* A/ 78%		360	312	P3-25 B/ 15%		1300	>1000

P3-9a ^{a, c} A/ 57%		210	200	P3-26a* B/ 98%		60	70
P3-9b* A/ 54%		260	144	P3-26b* B/ 98%		36	70
P3-10 A/ 98%		380	280	P3-27* B/ 67%		110	400
P3-11a A/ 98%		260	220	P3-28* B/ 87%		240	160
P3-11b* A/ 97%		180	350	P3-29 B/ 36%		170	130
P3-12a* A/ 82%		120	150	P3-30 B/ 45%		800	900
P3-12b A/ 90%		380	361	P3-31 B/ 67%		350	113
P3-13* B/ 35 %		330	330	P3-32 A/ 6%		500	590
P3-14* A/ 95%		390	220	P3-33 B/ 24%		800	900
P3-15a B/ 36 %		600	800	P3-34 B/ 20%		310	400
P3-15b B/ --%		1400	550	P3-35* A/ 98%		35	159
P3-16a B/ 15%		110	300				

* X-ray structure of fragment-enzyme complex available. ^a Reaction in anhydrous THF instead of dioxane:water as a solvent; ^b XPhos-Pd G2 as a catalyst instead of PdCl₂(PPh₃)₂; ^c PdCl₂(dppf) as a catalyst instead of PdCl₂(PPh₃)₂.

5.4 Conclusion

By rationally changing the substituent-groups of the benzoic acid derivatives we have been able to use structural information to design an improved inhibitor of the OXA-48 enzyme. We identified inhibitory fragments with $IC_{50} < 40 \mu\text{M}$ (P3-**21a**, P3-**26b** and P3-**35**). Moreover, the most interesting fragments were selected from crystal structures of 33 fragment enzyme complexes, to design five merged fragments. The inhibitors P3-**36** and P3-**40** showed IC_{50} values as low as $2.9 \mu\text{M}$, had improved inhibitory potential and were the best inhibitors of this study. The complex crystal structures of P3-**36** and P3-**40** revealed that the interactions of the individual fragments were mainly retained in the merged structures.

6. Inhibitor design and future perspective

During the course of our studies, we explored and analysed various crystal structures of the target enzymes bound to our inhibitors to gain the structural insight necessary to improve our synthesized inhibitors and design new inhibitors. The first half of this chapter describes synthesis of 2nd generation of inhibitors for the thiophosphonate- (Paper 1) and triazole-based inhibitors (Paper 2), that is supported by the knowledge gained from the crystal structures of the target enzymes bound to our inhibitors described in Chapters 3 and 4. The second half of this chapter focusses on comparative studies, where we explored and compared some recently reported inhibitors in the literature with our inhibitors bound to the enzymes.

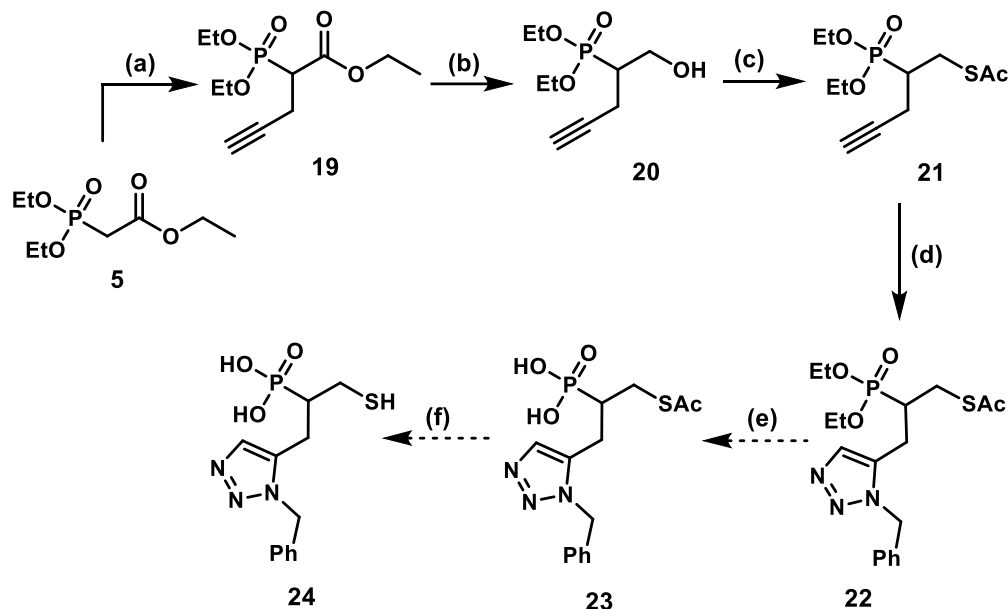
6.1 Towards 2nd generation of thiophosphonate- and triazole-based inhibitors

6.1.1 2nd Generation of mercaptophosphonate compounds

In Paper 1, analogues of mercaptocarboxylic acids were prepared by replacing the carboxylate group with bioisosteric groups such as phosphonate esters, phosphonic acids and *NH*-tetrazoles. The inhibition potentials of the resulting compounds were measured against VIM-2 and NDM-1 and GIM-1 MBLs.

The new MBL inhibitors showed IC₅₀ values in the low micro- and high nano-molar range for the three MBLs studied. Encouraged by these results another series was planned (not included and published in Paper 1) with the aim to enable the modular synthesis of inhibitors with various side chains. At this stage, however, we had not yet obtained crystal structures. A series of mercaptophosphonate-based compounds having an *N*-substituted triazole moiety incorporated in the side chain was envisioned (Scheme 6.1). A key

intermediate in the synthesis was alkyne **21**, which was envisioned to allow for introduction of side chains late in the synthesis via formation of the triazole in an azide-alkyne click reaction.



Scheme 6.1. Synthesis of phosphonate and phosphonic acid containing thiol-based inhibitors. Reagents and conditions: (a) R-Br (3-bromoprop-1-yne), K_2CO_3 , DMF, $0\text{ }^\circ\text{C}$ - rt- $60\text{ }^\circ\text{C}$ (28 h), **19**: 57%; (b) LiBH_4 , THF, MW $80\text{ }^\circ\text{C}$, 10 min, **20**: 38%; (c) MsCl , NEt_3 , DMAP, CH_2Cl_2 , rt; then KSAc , DMF, rt.; **21**: 36% over two steps; (d) CuSO_4 , Na-(+)-ascorbate, H_2O : *t*BuOH (1:1), Benzoic acid, NaOH, **22**: 10%. (e) NaSMe , MeOH, $-20\text{ }^\circ\text{C}$, (not performed); (f) TMSBr , CH_2Cl_2 , then MeOH, rt., (not performed).

For the synthesis of this library, the alkylation of triethylphosphonate P1-5 was carried out using potassium carbonate and propargyl bromide with a ratio of 1: 0.7 (P1-5: propargyl bromide) in DMF at $0\text{ }^\circ\text{C}$. The reaction mixture was brought to room temperature before heating up to $60\text{ }^\circ\text{C}$. The alkylation of compound P1-5 to yield compound **19**, that was found to be more efficient in terms of the yields when the reaction was performed at $60\text{ }^\circ\text{C}$. Purification was carried out with column chromatography using ethyl acetate and hexane (60:40), but it was found impossible to separate the mono- and dialkylated products completely even after repeated column chromatography. At this stage, we did not focus on the purification of the monoalkylated product.

The ester **19** was converted to alcohol **20** using LiBH_4 by the same strategy as described for compound P1-7 (Chapter 3). The yield for alcohol **20** was low (38%) but

conventional heating at 50 °C for 18 hours gave no improvement in the yield. Mesylation of the alcohol **20** was carried out using mesyl chloride followed by substitution with potassium thioacetate as a nucleophile, which gave thioacetate **21** in 36% yield.

The synthesis of triazole **22** from alkyne **21** (Table 6.1) was attempted with conventional heating in DMF and then in the presence of CuSO₄ as catalyst without success. In other attempts CuSO₄ in the presence of sodium ascorbate as a reducing agent (166) was used Entry 4-7, Table 6.1 but did not yield the target compound unless stoichiometric amounts of CuSO₄ and sodium ascorbate were used (Table 6.1, Entry 7) to yield the target triazole in only 10% yield.

The yield of the reaction was low and we speculated that chelation of the copper catalyst by the product may lead to loss of product during purification with column chromatography. However, at this point the continuation of this project was put aside, due to the unavailability of the crystal structures of P1-inhibitors (described in Chapter 3) at that time, and for the benefit of other projects.

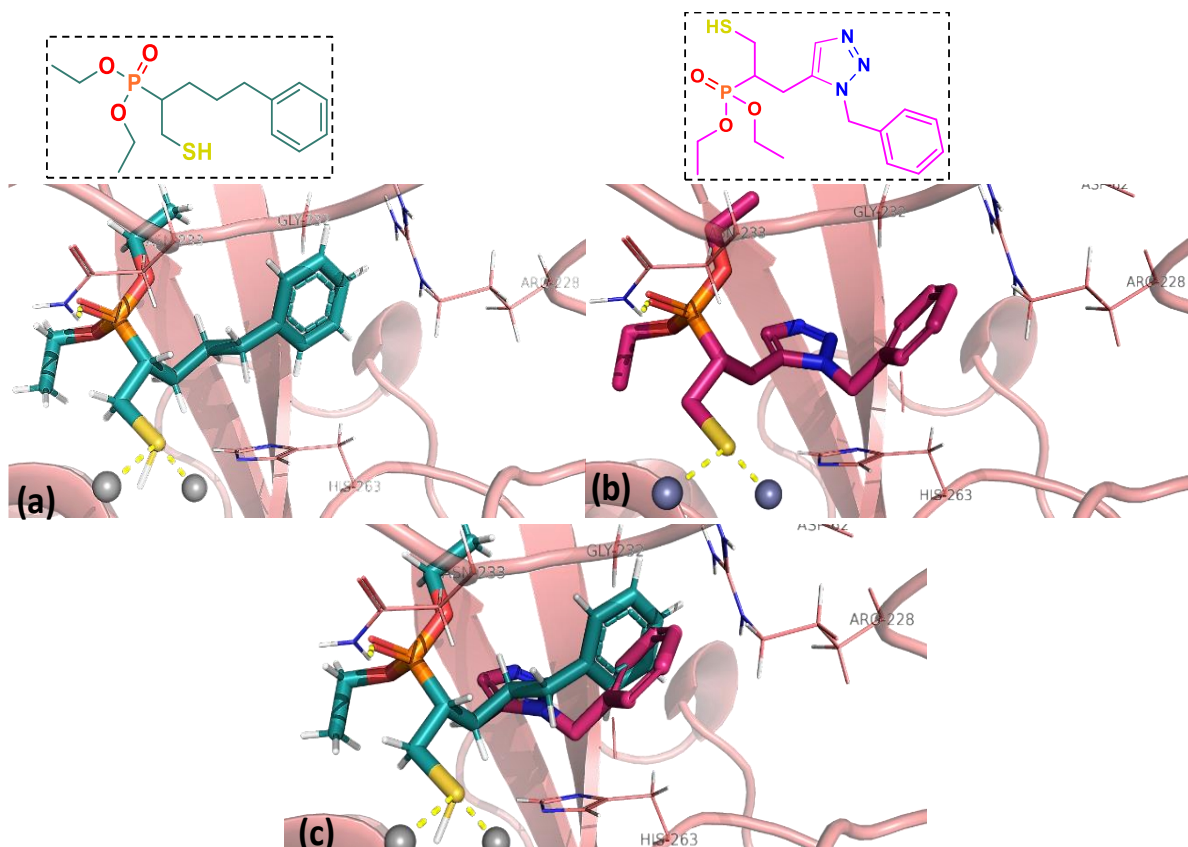
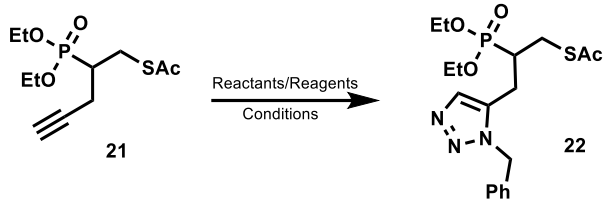


Figure 6.1. The crystal structures of VIM-2 with inhibitors: (a) P1-**2b**, shown as cyan sticks, (b) compound **23**, based on the crystal structure of VIM-2:P1-**2b**, PDB ID: 5MM9, (magenta sticks). The compound is built in the active site of VIM-2 using PyMOL. (c) Overlay of inhibitor P1-**2b** and the built compound **23**. The overlay points out the possibility of exploring different aryl groups that can be easily introduced by using click chemistry. VIM-2 is shown in a pink cartoon representation with important binding site residues shown as pink lines and Zn²⁺ ions are shown as grey spheres.

Later, the crystal structure of VIM-2:P1-**2b** was used as starting point to model inhibitor **23**. The modeled inhibitor **23**, (Figure 6.1 panel b), indicates that the introduction of an *N*-substituted triazoles moiety alone would not give significant interactions that can enhance binding affinity, although it has similar pose to that of inhibitor P1-**2b**. However, the introduction of other substituents as side chains seems feasible from a structural point of view, leading to the conclusion that compounds **22-24** could provide an interesting series of inhibitors.

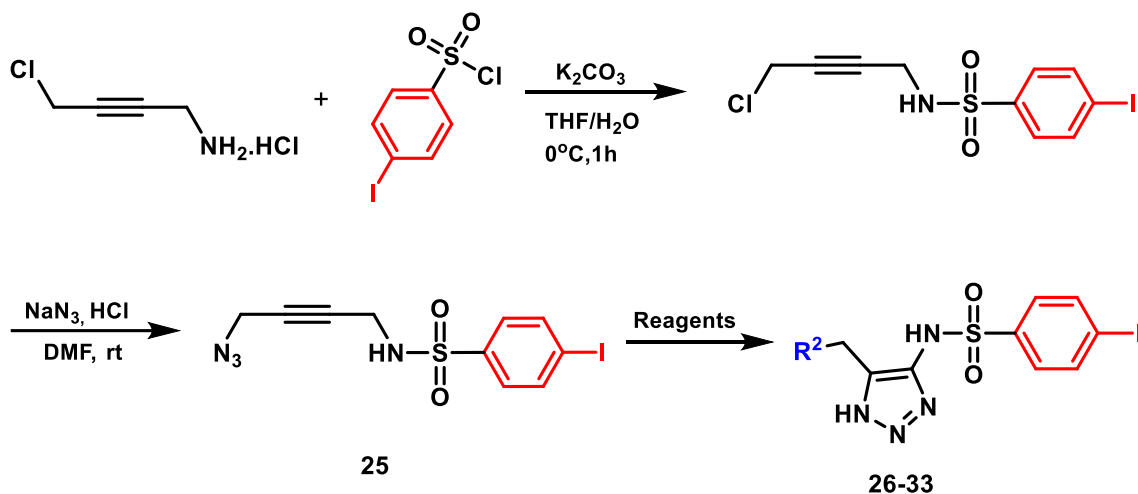
Table 6.1. Screening of reaction conditions for the synthesis of triazole **22**


Entry	Reactants	Solvent/Reagents	Temp. [°C]	Time [h]	Conv [%]
1	PhCH ₂ N ₃	DMF	80	18	0
2	PhCH ₂ N ₃	CuBr (2 mol %), TEA, DMF	60	24	0
3	PhCH ₂ N ₃	CuI (2 mol %), TEA, CH ₂ Cl ₂	40	22	0
4	PhCH ₂ N ₃	1) CuSO ₄ , 1.5 equiv Na-(+)-ascorbate, 2.5 equiv H ₂ O: <i>t</i> BuOH (2:1), 2) EDTA, 3) NaOH	rt	48	0
5	PhCH ₂ N ₃	1) CuSO ₄ , 0.04 equiv, Na-(+)-ascorbate, 1 equiv, H ₂ O: <i>t</i> BuOH (2:1) 2) EDTA, 3) NaOH	rt	48	0
6	PhCH ₂ N ₃	1) CuSO ₄ , 0.2 equiv Na-(+)-ascorbate, 1 equiv H ₂ O: <i>t</i> BuOH (1:2), 2) Formic acid, 3) NaOH	rt	48	0
7	PhCH ₂ N ₃	1) CuSO ₄ , 1 equiv, Na-(+)-ascorbate, 1.5 equiv H ₂ O: <i>t</i> BuOH (1:1), 2) Benzoic acid, 3) NaOH	rt	48	10

6.1.2 2nd Generation of triazole inhibitors

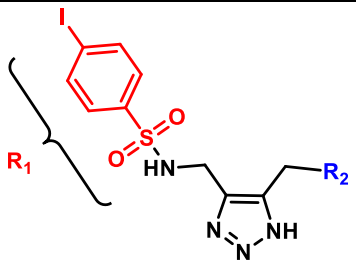
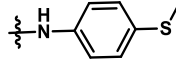
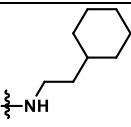
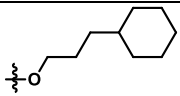
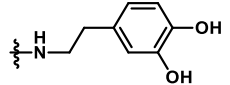
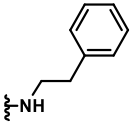
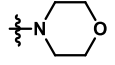
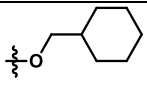
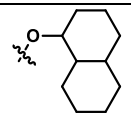
The crystal structures of inhibitors P2-**1ei'** and P2-**1dd'** described earlier (Chapter 4), gives insight into the binding mode of these inhibitors. The main interactions included, the interaction of the triazole ring with one of the Zn²⁺ ions and H-bonding between of one of the triazole nitrogen and Arg228, in addition to the interaction of the sulfonamide moiety with Ala231 and/or Asn233. Close inspection of the crystal structures shows available space around the R2 group of the inhibitor (Figure 6.2 panels b and d). This space motivated us to modify the inhibitors described in Chapter 4. Thus, we designed a small series of compounds in which the R2 group would be extended by 0-3 carbon spacer, with the expectation that the compounds with more than one methylene spacer may give a tighter fit in the binding pocket.

For the synthesis of these targets, compound **25** was prepared using the same strategy as described in Scheme 4.2 (Chapter 4). **25** underwent the Banert-cascade rearrangement to give *NH*-triazole sulphonamides **26-33**, in the presence of selected nucleophiles under the conditions described in Table 6.2. The compounds **26-28** were obtained with low purity even after repeated column chromatography (Entries 1-3, Table 6.2). Moreover, when testing the impure compounds, precipitation from the buffer solution was observed and thus no tests were performed. The reason for this is not obvious. Attempts to synthesize **29-33** (Entries 4-8, Table 6.2) resulted in complex reaction mixtures, which after repeated column chromatography did not yield the purified desired compounds. Other attempts for Entries 5 and 8, in which the solvent was changed to DMF, were also unsuccessful.



Scheme 6.2. Synthesis of intermediate **25** and inhibitors **26-33**.

Table 6.2. 2nd Generation of triazoles based inhibitors

Entry	ID		Solvent/Reagents *	Yield
		R ²		
1	26		Methylthioaniline 3 equiv, CH ₂ Cl ₂	86%
2	27		2-phenylethylamine, 3 equiv	61%
3	28		3-cyclohexylpropanol, 5 equiv	65%
4	29		2-aminoethylbenzene-1,2-diol, 5 equiv, 1:4 H ₂ O:DMF	ND
5	30		2-phenylethylamine, 5 equiv, dioxane	ND
6	31		Morpholine, 10 equiv, CH ₂ Cl ₂	ND
7	32		Cyclohexylmethanol, 5 equiv, dioxane	ND
8	33		Decahydronaphthalenol, 5 equiv, dioxane	ND

*all the reactions were carried out at 60 °C for 16h, ND not determined

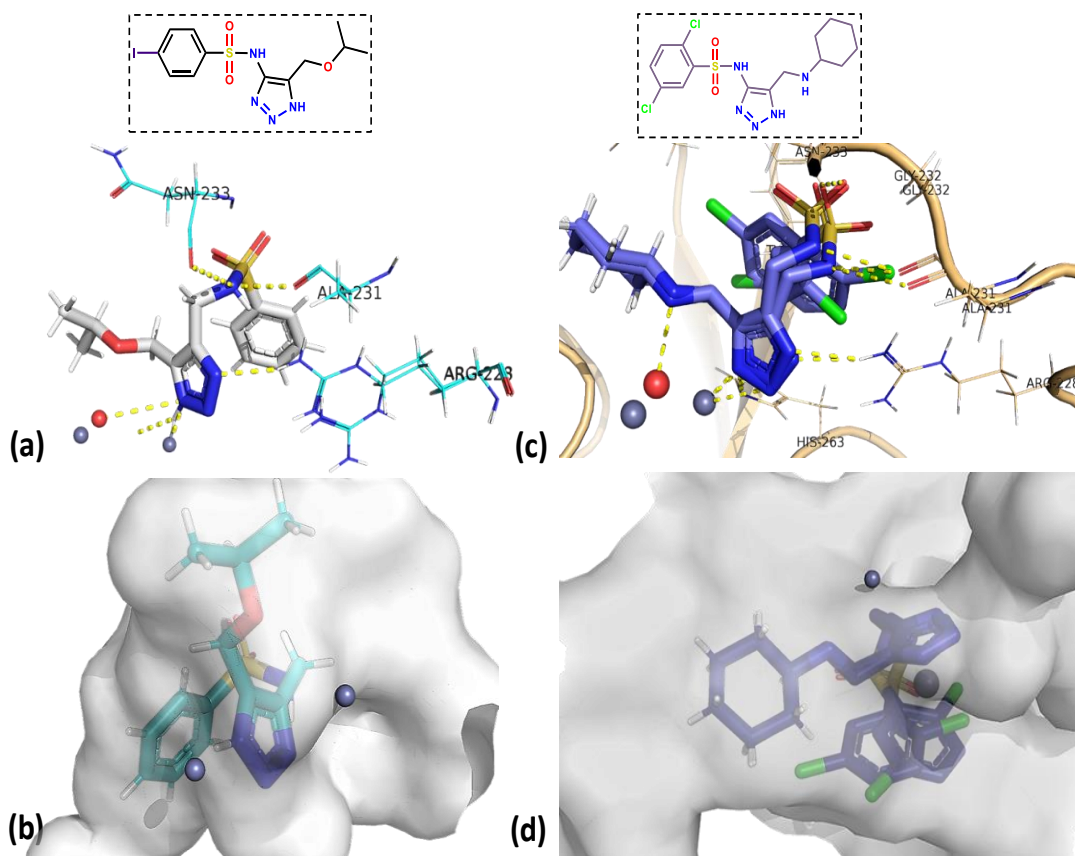


Figure 6.2. The crystal structures of inhibitors P2-1ei' and P2-1dd' in complex with VIM-2: (a) interactions shown in the active site with inhibitor P2-1ei', shown as white sticks; (b) interactions shown in the active site with inhibitor P2-1dd', shown as purple sticks; (c) Surface view of the active site with inhibitor P2-1ei', shown as cyan sticks; (d) Surface view of active site with inhibitor P2-1dd', shown as purple sticks. Zn²⁺ ions are shown as grey spheres.

6.2 Literature based search for scaffolds directed towards inhibitor development

The following section covers interesting findings and future directions based on the overlay of crystal structures of our inhibitors with some of the inhibitors from literature.

6.2.1 Inhibitors active across different subclasses in MBLs

6.2.1.1 Bisthiazolidines (BTZs)

Bisthiazolidines (BTZs) are described in the literature as cross-class inhibitor and is known to show multiple binding modes, (Figure 6.3 panels a, b and c). These binding modes enable them to be effective across different MBL sub-classes. BTZs can bind the di-zinc centers of B1 (NDM-1, IMP-1 and BcII) and B3 (L1) MBLs via their free thiol. While in NDM-1, the thiol group interacts with the Zn^{2+} ions, in addition to an interaction of the hydrogen of the thiol group with His189. An overlay of the poses of bisthiazolidine observed in the B chain of VIM-2 (Figure 6.3 panel b) shows a similar thiol interaction with Zn^{2+} as observed with the metal-chelating moieties in our inhibitors P2-**1dd'**, P1-**10c** and P2-**1ei'** (Figure 6.3, panels d, e and f, respectively). Surprisingly, in another pose, bisthiazolidine observed in the chain A of VIM-2 binds between Asn146 and the carboxylate group, whereas no interaction is observed between thiol group and the metal ions. For the mono-zinc B2 MBL, Sfh-I, the carboxylate group interacts with the Zn^{2+} ion, while the thiol is buried deep into the hydrophobic cavity adjacent to the active site ($\alpha 3$ helix), thus making the thiol group incapable of binding to the Zn^{2+} ion. (167,168)

The different poses of BTZs, as can be observed in the active site of NDM-1 and in VIM-2 chain A and B (Figure 6.3, panels a, b and c), suggest that the presence of different groups in a single molecule can give rise to different interactions across different classes of MBLs. In our inhibitors, we also have different functional groups, e.g., in our mercaptophosphonate inhibitors, the presence of both the thiol and phosphonate can make them versatile.

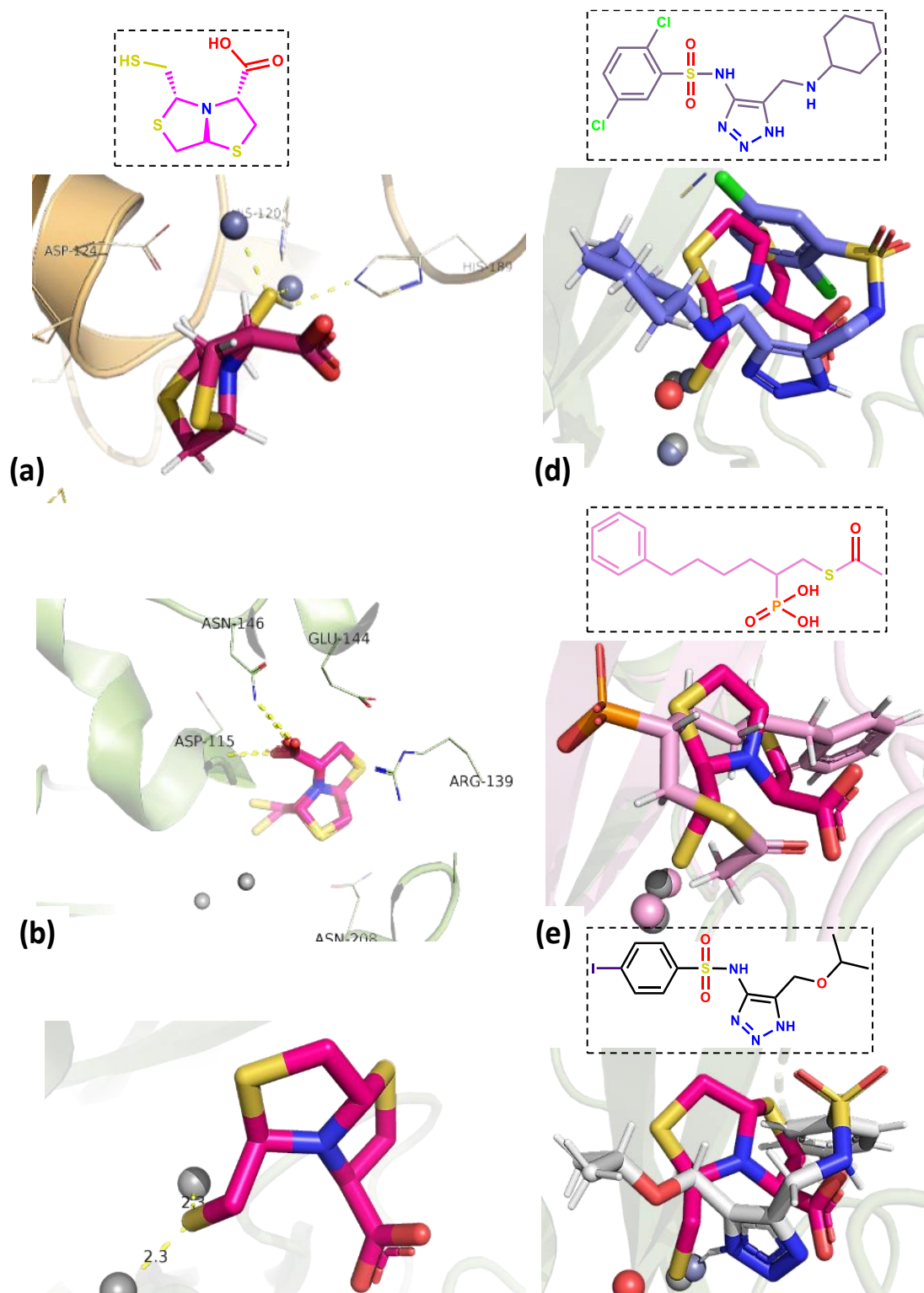
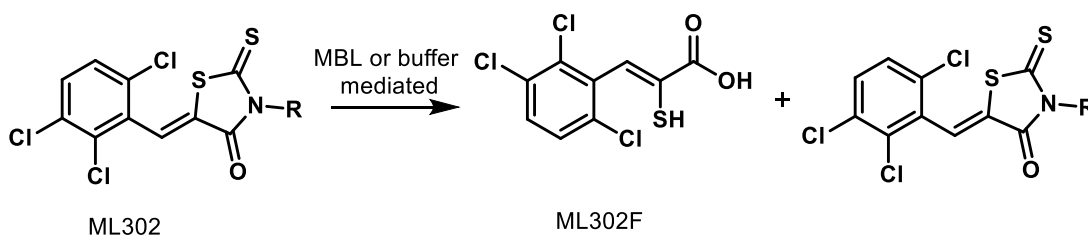


Figure 6.3. Different binding poses of BTZs across subclasses of MBLs and overlays with inhibitor P2-**1dd'**, P2-**1ei'** and P1-**10c**. (a) NDM-1 with BTZ, (b) BTZ in chain A of VIM-2. There seems to be more than 1 poses and the SH group does not interact with the Zn²⁺ ions as observed in the chain A of VIM-2, (c) BTZ in chain B of VIM-2, (d) overlay of BTZ with P2-**1dd'**, (e) overlay of BTZ with P1-**10c**, (f) overlay of BTZ with P2-**1ei'**.

6.2.2 Inhibitors with dual action targeting both SBLs and MBLs

6.2.2.1 Rhodanine-based inhibitors

An increase in the number of organisms containing both SBLs and MBLs is being observed, (169,170) which accentuates the need for compounds able to target all BLs. Only a few compounds are reported to target both SBLs and MBLs. Rhodanine-based compounds are class of compounds that show inhibitory potential towards penicillin binding protein (PBP), (171,172) SBLs (173) and more recently reported towards MBLs as well. (170,174) The 5-membered heterocycle containing thiazolidine, is considered to be a privileged scaffold, despite being promiscuous binder. (175,176) It can inhibit PBP and SBLs by non-competitive binding (mechanism not clear). (171) ML302 is one such inhibitor that shows nano-molar inhibition towards MBLs such as VIM-2 and IMP-1 ($K_i = 183 \pm 24$ and 930 ± 97 nM, respectively). Jürgen et.al. performed crystallization studies to determine the mechanism for MBL inhibition by rhodanines, which reveal that ML302 (a rhodanine-based inhibitor of VIM-2 and IMP-1), undergoes hydrolysis to yield thioenolate fragment (ML302F) that can bind to the active site zinc ions of the MBL enzymes. The enzyme complex VIM-2:ML302 shows the presence of both ML302 and ML302F in chain A and ML302 only in chain B. Further studies suggested, that both ML302F ($IC_{50} = 307 \pm 15$ nM) or ML302 ($IC_{50} = 498 \pm 18$ nM) alone have lower inhibition activity than a 1:1 mixture of ML302 and ML302F ($IC_{50} = 16 \pm 4$ nM). (170)



Scheme 6.3. Hydrolysis of Rhodanine

When compared to our inhibitors P1-**10c** and P2-**1ei'**, we can see in the overlay structure (Figure 6.4, panels c and d) that our inhibitors occupy very similar areas in the binding pocket to ML302+ML302F. In addition, the aryl group of our inhibitors overlaps with the aryl group of ML302. Furthermore, SAR-studies carried out on rhodanine derivatives, demonstrated the importance of an *ortho* di-substitution pattern (as on the

aromatic moiety of ML302 and ML302F, (170,174) see Figure 6.4) for activity against VIM-2 and IMP-1. This thus suggests that the incorporation of an *ortho*-dichloro-phenyl (as the aryl group) may enhance the activity of our inhibitors (Papers 1 and 2) for MBLs, VIM-2 and IMP-1. One can also see that the ethylidene-thioxothiazolidinone moiety occupies an area in the active site which is not yet explored by our inhibitors (Figure 6.4, panels c and d). It would therefore be interesting to introduce either thioxothiazolidinone or other heterocycles with one or two-carbon spacers at the *ortho* position of the aryl group. The resulting inhibitors might show good fits in the active site.

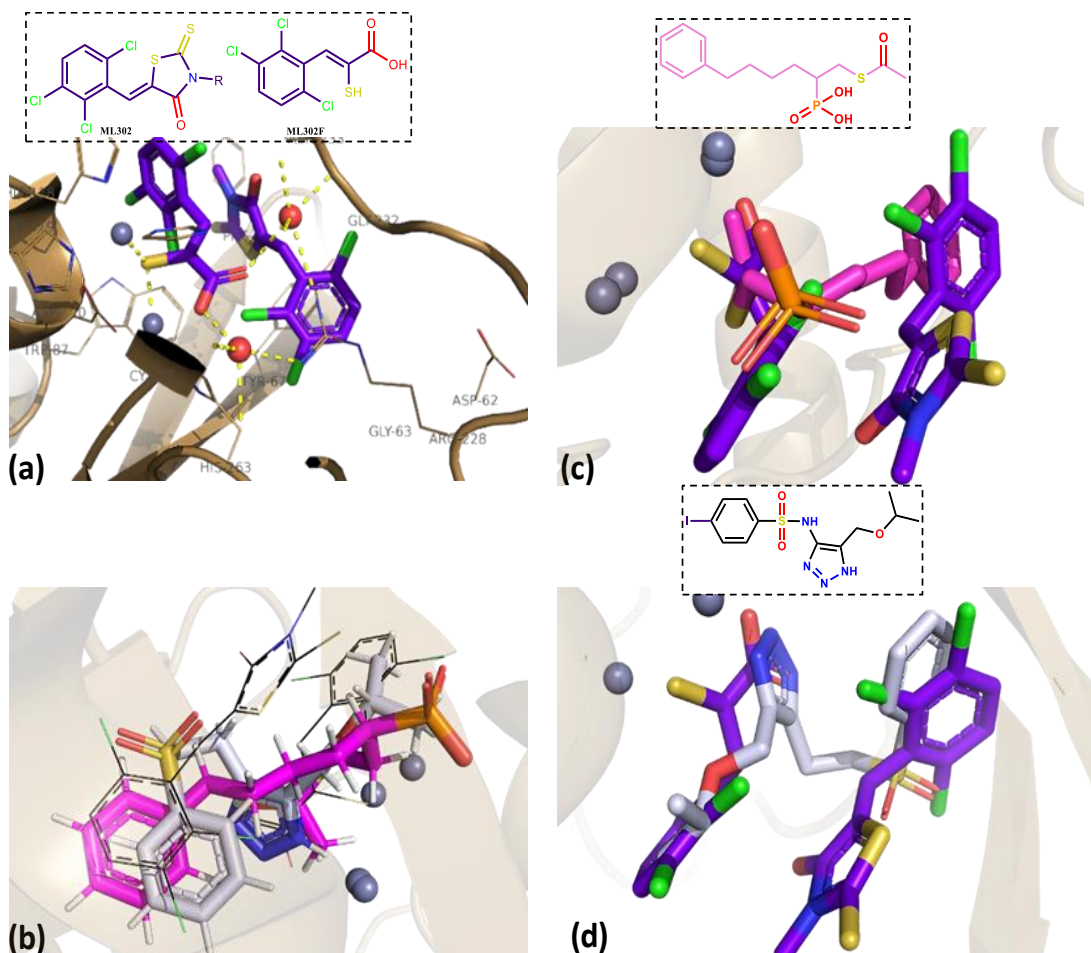


Figure 6.4. The crystal structures of VIM-2 showing active site view, (a) In complex with ML302 and ML302F. The inhibitors are shown in purple sticks; (b) overlay of P1-10c and P2-1ei' shown in magenta and white sticks respectively, with ML302 and ML302F. ML302 and ML302F are represented in black lines for clarity; (c) overlay of P1-10c with ML302 and ML302F shown in magenta and purple sticks respectively; (d) overlay of P1-1ei' with ML302 and ML302F, (shown in white and purple sticks respectively). The enzyme VIM-2 is shown in a light brown cartoon representation and Zn²⁺ ions are shown as grey spheres.

6.2.2.2 Cyclic boronates

Another such class of inhibitors are cyclic boronates, which have recently been shown to inhibit both SBLs and MBLs, (Figure 6.5, panels a and b). (177) The mechanism of action of the cyclic boronates targeting the MBLs BcII and VIM-2 was studied by Jürgen et.al. (52) and Cahill et al. (38) with the help of crystal structures of the cyclic boronate, CB2 in complex with these enzymes, (Figure 6.5 panel a). The study revealed that the two hydroxy groups of the boronic acid co-ordinate with one of the Zn^{2+} ions, thus mimicking the tetrahedral oxyanion intermediate from the β -lactam hydrolysis, (see Figure 6.5, panel c as well as Section 2.5.2, Chapter 2 for more detail). The binding mode of CB2 particularly shows a close resemblance to the hydrolyzed form of cephalosporin. (52,177)

Moreover, cyclic boronates CB1 and CB2 are also able to exhibit inhibition against some class C SBLs and class D SBLs such as OXA-24, OXA-48. (52) Mechanistic studies with the help of the crystal structure of the cyclic boronate CB1 in complex with OXA-10 (Figure 6.5, panel b), reveal a covalent interaction between the nucleophilic hydroxyl group of Ser-67 and the tetrahedral boron atom, (Figure 6.5, panel d). This binding mode shows a strong resemblance to the tetrahedral Intermediate **1** that leads to the formation of acyl-enzyme complex (see Section 2.5.3, Chapter 2 for more details).

Although the overall sequence of the enzymes OXA-48 and OXA-10 is not very similar, the active site residues are quite conserved and consequently the two can be compared. It would be interesting to incorporate a cyclic boronate group together with R2 binders for OXA-48 (described in Chapter 5), where they may provide similar covalent interactions with OXA-48 as seen between the nucleophilic hydroxyl group of Ser67 in OXA-10 and tetrahedral boron atom of the CB1 cyclic boronate. (52) This may enhance the potency of our inhibitors by mimicking the tetrahedral oxyanion intermediate from the β -lactam hydrolysis. The overlay of the CB1 with inhibitor P3-**26b** strengthens our hypothesis of achieving a potent inhibitor.

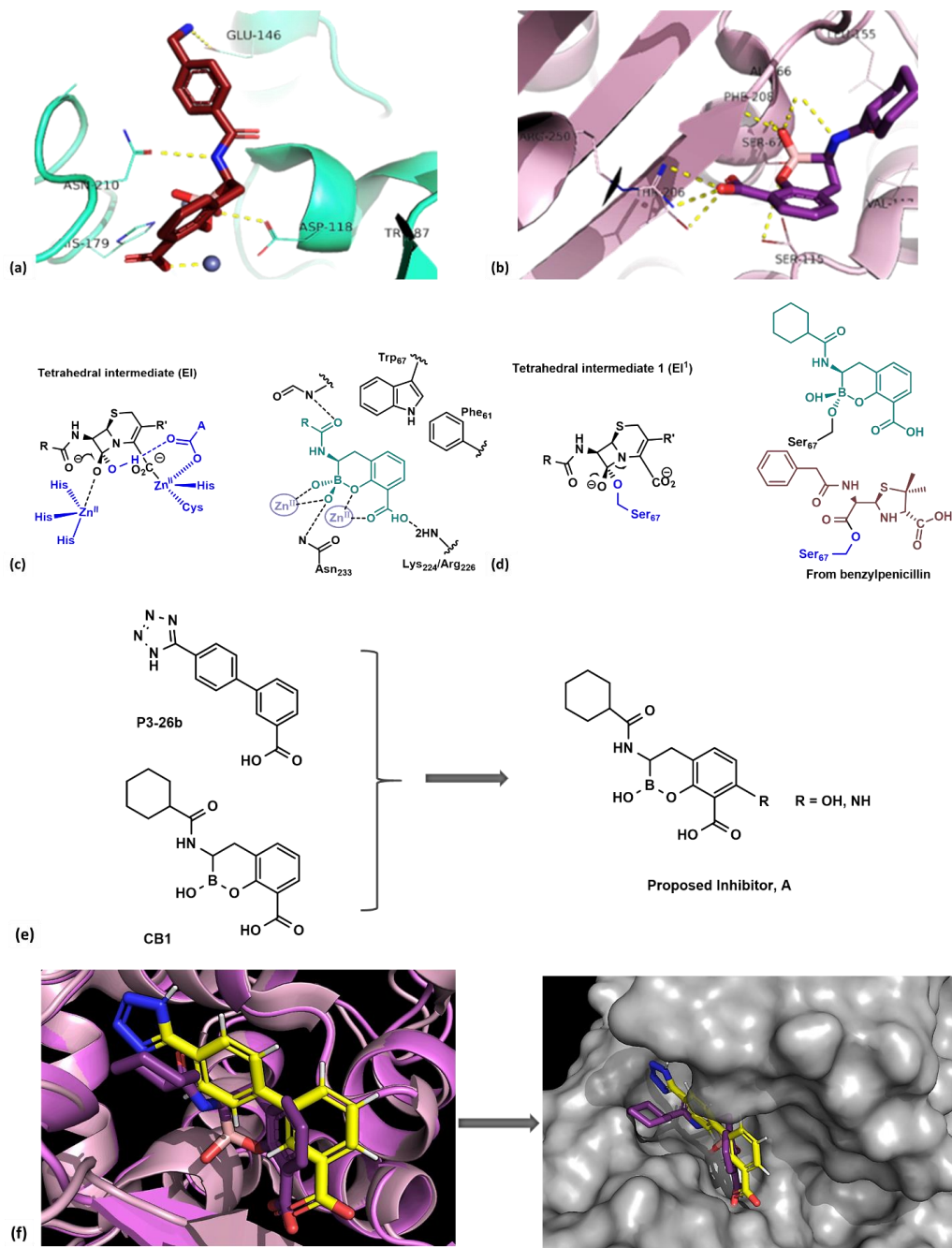


Figure 6.5. The crystal structures of (a) VIM-2 with inhibitor CB2, shown as red sticks; (b) OXA-10 with CB1, shown as purple sticks (52); (c) Resemblance of oxyanionic intermediate, (EI) in MBL hydrolysis, with cyclicboronate bound to VIM-2; (d) Resemblance of Intermediate 1, (EI¹) in SBL hydrolysis with cyclicboronate bound to OXA-10; (e) Molecular structures of our inhibitor P3-**26b** and the cyclic boronate-based inhibitor, CB1 that allowed us to propose inhibitor A; (f) Overlay of inhibitor P3-**26b** and the cyclic boronate based inhibitor, CB1 (depicted in yellow and purple sticks, respectively) bound to the enzymes OXA-48 and OXA-10, leading to the proposed inhibitors shown on a surface representation of the active site of OXA-

6.2.3 Inhibitors targeting class D SBLs

6.2.3.1 Penicillanic acid sulfone-based inhibitors; a possibility to achieve additional interactions

The inhibitors described in the Paper 3, were found to occupy mostly the R2 binding pocket in the active site while some occupied R1 binding site, (the amino acids that defines R1 and R2 binding pockets are described in the Paper 3). LN-1-255, is a penicillanic acid sulfone-based inhibitor able to inhibit the class D carbapenemase OXA-48, with an IC_{50} of 3nM with nitrocefin as the reporter substrate as compared to IC_{50} 1.5 μ M for tazobactam. (178) Docking studies on LN-1-255, done by Vallejo et.al (178) points out that the catechol moiety in the side chain occupies another region than the R1 and R2 binding pockets. In addition, docking studies suggest that the catechol moiety can provide an additional hydrogen bonding interaction between the phenol groups of the catechol moiety and the amino group of Lys208 present in the large pocket close to the active site (which is not the same as R1 or R2 binding pocket). (178) In addition, a catechol moiety may introduce other beneficial properties to the compound, such as facilitating the entry of the molecule through the bacterial cell membrane. (178,179)

A side chain containing catechol group with 3-4 carbon spacer, when merged with one of our R1 binders, e.g. P3-**26b**, can give the same hydrogen bonding interaction. To confirm this possibility, a hypothetical molecule has been constructed in the active site of OXA-48, (Figure 6.6, panels d-g). The new molecule is more flexible and shows the hydrogen bonding interaction of the phenolic group of the catechol moiety, with the amino group of Lys-208, as expected, (Figure 6.6, panels d and f).

Another possibility is to start with 4-amino-4'-(1H-tetrazol-5-yl)-[1,1'-biphenyl]-3-carboxylic acid, compound **X**, that will permit us to introduce side chains with ease, thus allowing us to explore the corresponding binding pocket. In addition, various amides, sulphonamides and esters could be made. Another hypothetical structure was built by using the crystal structure of the fragment OXA-48 in complex with P3-**26b**, which shows the possibility of hydrogen bonding between the C=O group of the amide and the hydroxyl group of Ser118, (Figure 6.6, panels c, f and g).

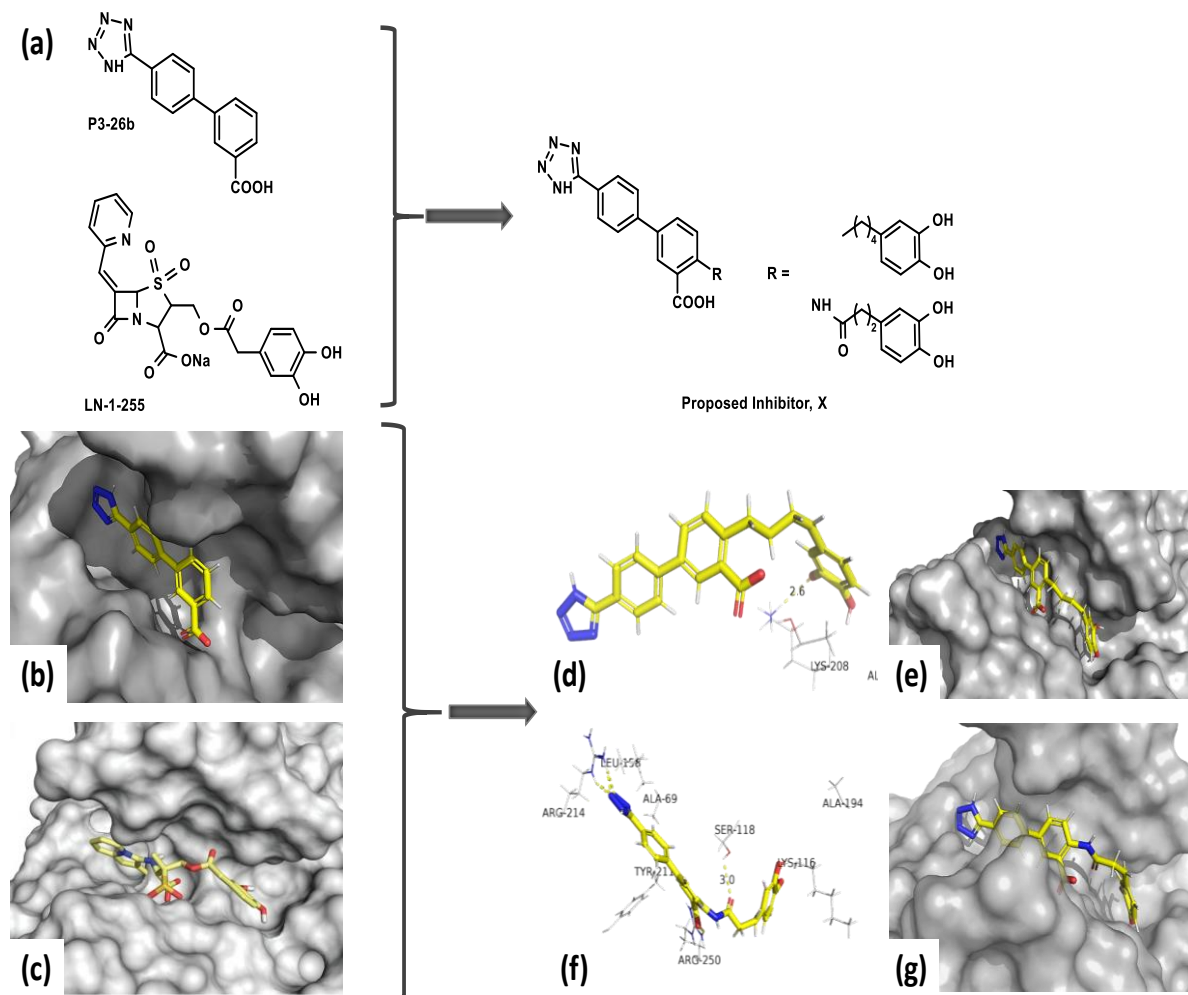


Figure 6.6. (a) Molecular structures of our inhibitor P3-26b and penicillanic acid-based inhibitor LN-1-255 that allowed us to propose inhibitor X; (b) Surface view of active site of OXA-48 in complex with inhibitor P3-26b; (c) molecular docking of LN-1-255 in to the active site of OXA-48, (figure reproduced with permission from (178)). Analysis of (b and c) allowed us to design the hypothetical *inhibitors* as shown in panel (d and f) built in the active site of OXA-48, (as yellow sticks). The figure shows important interactions with the side chains of active site residues (white lines); (e, g) The surface representations of the hypothesized inhibitors in the active site of OXA-48.

6.3 Conclusion

With the enzyme inhibitor complexes obtained during the studies in hand, we have explored and compared some recently reported inhibitors in the literature with our enzyme-inhibitor complexes. The comparative studies turned out to be valuable and paved our way for future directions and design of improved inhibitors.

7. Concluding remarks

This thesis describes the synthesis and evaluation of inhibitors targeting carbapenemases.

To search for inhibitors targeting a range of class B MBLs, namely VIM-2, NDM-1, and GIM-1, we modified the known mercaptocarboxylic acid with a bioisosteric approach. The search revealed new MBL inhibitors with IC_{50} values in micro- to nano-molar range, described in Chapter 3. Among the synthesized inhibitors, the most potent inhibitors contain a thioacetate and a phosphonic acid group.

In Chapter 4 the synthesis of another series based on the *NH*-triazoles motif was synthesized and evaluated against VIM-2, NDM-1, and GIM-1. Generally, inhibitors displayed good inhibition against VIM-2. Some inhibitors were also active but to a lesser extent against NDM-1 and GIM-1.

In Chapter 5, we explored the active site of OXA-48, a class D, serine β -lactamase with the help of a hit from our fragment library search utilizing surface plasmon resonance and enzyme inhibition assays. Several interesting fragments were found and modified to give improved inhibitors.

In all the studies crystal structures were obtained and assessed to give further insight in inhibitor-enzyme binding with the aim to guide future inhibitor design. The crystal structures revealed relevant information for further development of the inhibitors. In addition, comparison with some reported inhibitor-enzyme complex structures with our inhibitors-enzyme complex structure yielded interesting starting points for the future design of broad-spectrum inhibitors presented in Chapter 6 of the thesis.

8. References

1. Patel, G., and Bonomo, R. A. (2013) “Stormy waters ahead”: global emergence of carbapenemases. *Frontiers in Microbiology* **4**, 48
2. Nordmann, P., and Poirel, L. (2014) The difficult-to-control spread of carbapenemase producers among Enterobacteriaceae worldwide. *Clinical Microbiology and Infection* **20**, 821-830
3. Nordmann, P., Gniadkowski, M., Giske, C. G., Poirel, L., Woodford, N., and Miriagou, V. (2012) Identification and screening of carbapenemase-producing Enterobacteriaceae. *Clinical Microbiology and Infection* **18**, 432-438
4. World Health Organization, (2018). Fact sheet for antimicrobial resistance. Available at: <http://www.who.int/mediacentre/factsheets/fs194/en/> [Accessed 6 Mar. 2018].
5. Tipper, D. J., and Strominger, J. L. (1965) Mechanism of action of penicillins: a proposal based on their structural similarity to acyl-D-alanyl-D-alanine. *Proceedings of the National Academy of Sciences of the United States of America* **54**, 1133-1141
6. González, M. M., Kosmopoulou, M., Mojica, M. F., Castillo, V., Hinchliffe, P., Pettinati, I., Brem, J., Schofield, C. J., Mahler, G., Bonomo, R. A., Llarrull, L. I., Spencer, J., and Vila, A. J. (2015) Bisthiazolidines: A substrate-mimicking scaffold as an inhibitor of the NDM-1 carbapenemase. *ACS Infectious Diseases* **1**, 544-554
7. Palzkill, T. (2013) Metallo- β -lactamase structure and function. *Annals of the New York Academy of Sciences* **1277**, 91-104
8. Santajit, S., and Indrawattana, N. (2016) Mechanisms of antimicrobial resistance in ESKAPE pathogens. *BioMed Research International* **2016**, 2475067
9. Frimodt-Moller, N. (2004) Microbial threat-The Copenhagen recommendations initiative of the EU. *Journal of veterinary medicine. B, Infectious diseases and veterinary public health* **51**, 400-402
10. Medina, E., and Pieper, D. H. (2016) Tackling threats and future problems of multidrug-resistant bacteria. in *How to Overcome the Antibiotic Crisis : Facts, Challenges, Technologies and Future Perspectives* (Stadler, M., and Dersch, P. eds.), Springer International Publishing, Cham. pp 3-33
11. Tan, S. Y., and Tatsumura, Y. (2015) Alexander Fleming (1881–1955): Discoverer of penicillin. *Singapore Medical Journal* **56**, 366-367
12. Duemling, W. W. (1946) Clinical experiences with penicillin in the navy. *Annals of the New York Academy of Sciences* **48**, 201-220
13. Armstrong, G. L., Conn, L. A., and Pinner, R. W. (1999) Trends in infectious disease mortality in the united states during the 20th century. *JAMA* **281**, 61-66
14. Finberg, R. W., Moellering, R. C., Tally, F. P., Craig, W. A., Pankey, G. A., Dellinger, E. P., West, M. A., Joshi, M., Linden, P. K., Rolston, K. V., Rotschafer, J. C., and Rybak, M. J. (2004) The importance of bactericidal drugs: future directions in infectious disease. *Clinical Infectious Diseases* **39**, 1314-1320

15. Pankey, G. A., and Sabath, L. D. (2004) Clinical relevance of bacteriostatic versus bactericidal mechanisms of action in the treatment of Gram-positive bacterial infections. *Clinical Infectious Diseases* **38**, 864-870
16. Bush, K., and Bradford, P. A. (2016) β -Lactams and β -lactamase inhibitors: an overview. *Perspectives In Medicine* **6**, 1-22
17. Tamma, P. D., Girdwood, S. C., Gopaul, R., Tekle, T., Roberts, A. A., Harris, A. D., Cosgrove, S. E., and Carroll, K. C. (2013) The use of cefepime for treating AmpC β -lactamase-producing Enterobacteriaceae. *Clinical Infectious Diseases* **57**, 781-788
18. Siedner, M. J., Galar, A., Guzman-Suarez, B. B., Kubiak, D. W., Baghdady, N., Ferraro, M. J., Hooper, D. C., O'Brien, T. F., and Marty, F. M. (2014) Cefepime vs other antibacterial agents for the treatment of Enterobacter species bacteremia. *Clinical Infectious Diseases* **58**, 1554-1563
19. Pacifici, G. M. (2010) Clinical pharmacokinetics of penicillins, cephalosporins and aminoglycosides in the neonate: a review. *Pharmaceuticals* **3**, 2568-2591
20. Walsh, C. T., and Wencewicz, T. A. (2014) Prospects for new antibiotics: a molecule-centered perspective. *The Journal of antibiotics* **67**, 7-22
21. Nukaga, M., Bethel, C. R., Thomson, J. M., Hujer, A. M., Distler, A., Anderson, V. E., Knox, J. R., and Bonomo, R. A. (2008) Inhibition of Class A β -lactamases by carbapenems: crystallographic observation of two conformations of meropenem in SHV-1. *Journal of the American Chemical Society* **130**, 12656-12662
22. El-Gamal, M. I., Brahim, I., Hisham, N., Aladdin, R., Mohammed, H., and Bahaaeldin, A. (2017) Recent updates of carbapenem antibiotics. *European Journal of Medicinal Chemistry* **131**, 185-195
23. Duran, M., Faljoni-Alario, A., and Duran, N. (2010) *Chromobacterium violaceum* and its important metabolites. *Folia microbiologica* **55**, 535-547
24. Schäberle, T. F., and Hack, I. M. (2014) Overcoming the current deadlock in antibiotic research. *Trends in Microbiology* **22**, 165-167
25. Brogan, D. M., and Mossialos, E. (2016) A critical analysis of the review on antimicrobial resistance report and the infectious disease financing facility. *Globalization and Health* **12**, 8-16
26. Nordmann, P., Dortet, L., and Poirel, L. Carbapenem resistance in Enterobacteriaceae: here is the storm! *Trends in Molecular Medicine* **18**, 263-272
27. Davies, J., and Davies, D. (2010) Origins and evolution of antibiotic resistance. *Microbiology and Molecular Biology Reviews* **74**, 417-433
28. Silverman, R. B., and Holladay, M. W. (2014) Chapter 7 - Drug resistance and drug synergism. in *The Organic Chemistry of Drug Design and Drug Action (Third Edition)*, Academic Press, Boston. pp 333-356
29. Webber, M. A., and Piddock, L. J. V. (2003) The importance of efflux pumps in bacterial antibiotic resistance. *Journal of Antimicrobial Chemotherapy* **51**, 9-11
30. Poole, K. (2004) Efflux-mediated multiresistance in Gram-negative bacteria. *Clinical microbiology and infection* **10**, 12-26
31. Jeon, J. H., Lee, J. H., Lee, J. J., Park, K. S., Karim, A. M., Lee, C.-R., Jeong, B. C., and Lee, S. H. (2015) Structural basis for carbapenem-hydrolyzing mechanisms of carbapenemases- Conferring antibiotic resistance. *International Journal of Molecular Sciences* **16**, 9654-9692

32. Llarrull, L. I., Testero, S. A., Fisher, J. F., and Mobashery, S. (2010) The future of the β -lactams. *Current Opinion in Microbiology* **13**, 551-557
33. Khan, A. U., Maryam, L., and Zarrilli, R. (2017) Structure, genetics and worldwide spread of New Delhi Metallo- β -lactamase (NDM): a threat to public health. *BMC Microbiology* **17**, 101
34. Drawz, S. M., and Bonomo, R. A. (2010) Three decades of β -lactamase inhibitors. *Clinical Microbiology Reviews* **23**, 160-201
35. Bush, K., and Jacoby, G. A. (2010) Updated functional classification of β -lactamases. *Antimicrobial Agents and Chemotherapy* **54**, 969-976
36. Bush, K. (1989) Characterization of β -lactamases. *Antimicrobial Agents and Chemotherapy* **33**, 259-263
37. Hinchliffe, P., González, M. M., Mojica, M. F., González, J. M., Castillo, V., Saiz, C., Kosmopoulou, M., Tooke, C. L., Llarrull, L. I., Mahler, G., Bonomo, R. A., Vila, A. J., and Spencer, J. (2016) Cross-class metallo- β -lactamase inhibition by bisthiazolidines reveals multiple binding modes. *Proceedings of the National Academy of Sciences of the United States of America* **113**, E3745-E3754
38. Cahill, S. T., Cain, R., Wang, D. Y., Lohans, C. T., Wareham, D. W., Oswin, H. P., Mohammed, J., Spencer, J., Fishwick, C. W. G., McDonough, M. A., Schofield, C. J., and Brem, J. (2017) Cyclic boronates inhibit all classes of β -lactamases. *Antimicrobial Agents and Chemotherapy* **61**, e02260-02216
39. Das, C. K., and Nair, N. N. (2017) Hydrolysis of cephalexin and meropenem by New Delhi metallo- β -lactamase: the substrate protonation mechanism is drug dependent. *Physical Chemistry Chemical Physics*
40. Tripathi, R., and Nair, N. N. (2015) Mechanism of meropenem hydrolysis by New Delhi Metallo β -lactamase. *ACS Catalysis* **5**, 2577-2586
41. King, D. T., Worrall, L. J., Gruninger, R., and Strynadka, N. C. J. (2012) New Delhi Metallo- β -lactamase: Structural insights into β -lactam recognition and inhibition. *Journal of the American Chemical Society* **134**, 11362-11365
42. Spencer, J., Read, J., Sessions, R. B., Howell, S., Blackburn, G. M., and Gamblin, S. J. (2005) Antibiotic recognition by binuclear metallo- β -lactamases revealed by X-ray crystallography. *Journal of the American Chemical Society* **127**, 14439-14444
43. Zhang, H., and Hao, Q. (2011) Crystal structure of NDM-1 reveals a common β -lactam hydrolysis mechanism. *The Federation of American Societies for Experimental Biology* **25**, 2574-2582
44. Hu, Z., Periyannan, G., Bennett, B., and Crowder, M. W. (2008) Role of the Zn1 and Zn2 sites in Metallo- β -lactamase L1. *Journal of the American Chemical Society* **130**, 14207-14216
45. Wu, S., Xu, D., and Guo, H. (2010) QM/MM Studies of monozinc β -lactamase CphA suggest that the crystal structure of an enzyme-intermediate complex represents a minor pathway. *Journal of the American Chemical Society* **132**, 17986-17988
46. Paton, R., Miles, R. S., Hood, J., Amyes, S. G., Miles, R. S., and Amyes, S. G. (1993) ARI 1: β -lactamase-mediated imipenem resistance in *Acinetobacter baumannii*. *International journal of antimicrobial agents* **2**, 81-87
47. Brink, A. J., Coetzee, J., Corcoran, C., Clay, C. G., Hari-Makkan, D., Jacobson, R. K., Richards, G. A., Feldman, C., Nutt, L., van Greune, J., Deetlefs, J. D., Swart, K., Devenish, L., Poirel, L., and Nordmann, P. (2013) Emergence of OXA-48 and OXA-

- 181 Carbapenemases among Enterobacteriaceae in South Africa and evidence of *in vivo* selection of colistin resistance as a consequence of selective decontamination of the gastrointestinal tract. *Journal of Clinical Microbiology* **51**, 369-372
48. Xie, L., Dou, Y., Zhou, K., Chen, Y., Han, L., Guo, X., and Sun, J. (2017) Coexistence of blaOXA-48 and truncated blaNDM-1 on different plasmids in a *Klebsiella pneumoniae* isolate in China. *Frontiers in Microbiology* **8**
49. Maveyraud, L., Golemi-Kotra, D., Ishiwata, A., Meroueh, O., Mobashery, S., and Samama, J. P. (2002) High-resolution X-ray structure of an acyl-enzyme species for the class D OXA-10 β -lactamase. *Journal of the American Chemical Society* **124**, 2461-2465
50. Paetzel, M., Danel, F., de Castro, L., Mosimann, S. C., Page, M. G., and Strynadka, N. C. (2000) Crystal structure of the class D β -lactamase OXA-10. *Nature structural biology* **7**, 918-925
51. Queenan, A. M., and Bush, K. (2007) Carbapenemases: the versatile β -lactamases. *Clinical Microbiology Reviews* **20**, 440-458
52. Brem, J., Cain, R., Cahill, S., McDonough, M. A., Clifton, I. J., Jiménez-Castellanos, J.-C., Avison, M. B., Spencer, J., Fishwick, C. W. G., and Schofield, C. J. (2016) Structural basis of metallo- β -lactamase, serine- β -lactamase and penicillin-binding protein inhibition by cyclic boronates. *Nature Communications* **7**, 12406
53. Girlich, D., Naas, T., and Nordmann, P. (2004) OXA-60, a chromosomal, inducible, and imipenem-hydrolyzing class D β -lactamase from *Ralstonia pickettii*. *Antimicrobial Agents and Chemotherapy* **48**, 4217-4225
54. Heritier, C., Poirel, L., Fournier, P. E., Claverie, J. M., Raoult, D., and Nordmann, P. (2005) Characterization of the naturally occurring oxacillinase of *Acinetobacter baumannii*. *Antimicrobial Agents and Chemotherapy* **49**, 4174-4179
55. Schneider, I., Queenan, A. M., and Bauernfeind, A. (2006) Novel carbapenem-hydrolyzing oxacillinase OXA-62 from *Pandoraea pnomenus*. *Antimicrobial Agents and Chemotherapy* **50**, 1330-1335
56. Walter, M. W., Felici, A., Galleni, M., Soto, R. P., Adlington, R. M., Baldwin, J. E., Frère, J.-M., Gololobov, M., and Schofield, C. J. (1996) Trifluoromethyl alcohol and ketone inhibitors of metallo- β -lactamases. *Bioorganic and Medicinal Chemistry Letters* **6**, 2455-2458
57. Toney, J. H., Fitzgerald, P. M., Grover-Sharma, N., Olson, S. H., May, W. J., Sundelof, J. G., Vanderwall, D. E., Cleary, K. A., Grant, S. K., Wu, J. K., Kozarich, J. W., Pompliano, D. L., and Hammond, G. G. (1998) Antibiotic sensitization using biphenyl tetrazoles as potent inhibitors of *Bacteroides fragilis* metallo- β -lactamase. *Chemistry and Biology* **5**, 185-196
58. Toney, J. H., Cleary, K. A., Hammond, G. G., Yuan, X., May, W. J., Hutchins, S. M., Ashton, W. T., and Vanderwall, D. E. (1999) Structure-activity relationships of biphenyl tetrazoles as metallo- β -lactamase inhibitors. *Bioorganic and Medicinal Chemistry Letters* **9**, 2741-2746
59. King, A. M., Reid-Yu, S. A., Wang, W., King, D. T., De Pascale, G., Strynadka, N. C., Walsh, T. R., Coombes, B. K., and Wright, G. D. (2014) Aspergillomarasmine A overcomes metallo- β -lactamase antibiotic resistance. *Nature* **510**, 503-506
60. Goto, M., Takahashi, T., Yamashita, F., Koreeda, A., Mori, H., Ohta, M., and Arakawa, Y. (1997) Inhibition of the metallo- β -lactamase produced from *Serratia*

- marcescens* by thiol compounds. *Biological and Pharmaceutical Bulletin* **20**, 1136-1140
61. Siemann, S., Clarke, A. J., Viswanatha, T., and Dmitrienko, G. I. (2003) Thiols as classical and slow-binding inhibitors of IMP-1 and other binuclear metallo- β -lactamases. *Biochemistry* **42**, 1673-1683
 62. Lassaux, P., Hamel, M., Gulea, M., Delbrück, H., Mercuri, P. S., Horsfall, L., Dehareng, D., Kupper, M., Frère, J.-M., Hoffmann, K., Galleni, M., and Bebrone, C. (2010) Mercaptophosphonate Compounds as Broad-Spectrum Inhibitors of the Metallo- β -lactamases. *Journal of Medicinal Chemistry* **53**, 4862-4876
 63. Concha, N. O., Janson, C. A., Rowling, P., Pearson, S., Cheever, C. A., Clarke, B. P., Lewis, C., Galleni, M., Frere, J. M., Payne, D. J., Bateson, J. H., and Abdel-Meguid, S. S. (2000) Crystal structure of the IMP-1 metallo- β -lactamase from *Pseudomonas aeruginosa* and its complex with a mercaptocarboxylate inhibitor: binding determinants of a potent, broad-spectrum inhibitor. *Biochemistry* **39**, 4288-4298
 64. Yamaguchi, Y., Jin, W., Matsunaga, K., Ikemizu, S., Yamagata, Y., Wachino, J., Shibata, N., Arakawa, Y., and Kurosaki, H. (2007) Crystallographic investigation of the inhibition mode of a VIM-2 metallo- β -lactamase from *Pseudomonas aeruginosa* by a mercaptocarboxylate inhibitor. *Journal of Medicinal Chemistry* **50**, 6647-6653
 65. Greenlee, M. L., Laub, J. B., Balkovec, J. M., Hammond, M. L., Hammond, G. G., Pompliano, D. L., and Epstein-Toney, J. H. (1999) Synthesis and SAR of thioester and thiol inhibitors of IMP-1 Metallo- β -Lactamase. *Bioorganic and Medicinal Chemistry Letters* **9**, 2549-2554
 66. Mollard, C., Moali, C., Papamicael, C., Damblon, C., Vessilier, S., Amicosante, G., Schofield, C. J., Galleni, M., Frère, J.-M., and Roberts, G. C. K. (2001) Thiomandelic acid, a broad spectrum inhibitor of zinc β -lactamases: kinetic and spectroscopic studies. *Journal of Biological Chemistry* **276**, 45015-45023
 67. Hinchliffe, P., Gonzalez, M. M., Mojica, M. F., Gonzalez, J. M., Castillo, V., Saiz, C., Kosmopoulou, M., Tooke, C. L., Llarrull, L. I., Mahler, G., Bonomo, R. A., Vila, A. J., and Spencer, J. (2016) Cross-class metallo- β -lactamase inhibition by bithiazolidines reveals multiple binding modes. *Proceedings of the National Academy of Sciences of the United States of America* **113**, E3745-3754
 68. Heinz, U., Bauer, R., Wommer, S., Meyer-Klaucke, W., Papamichaels, C., Bateson, J., and Adolph, H. W. (2003) Coordination geometries of metal ions in d- or l-captopril-inhibited metallo- β -lactamases. *Journal of Biological Chemistry* **278**, 20659-20666
 69. Li, N., Xu, Y., Xia, Q., Bai, C., Wang, T., Wang, L., He, D., Xie, N., Li, L., Wang, J., Zhou, H. G., Xu, F., Yang, C., Zhang, Q., Yin, Z., Guo, Y., and Chen, Y. (2014) Simplified captopril analogues as NDM-1 inhibitors. *Bioorganic and Medicinal Chemistry Letters* **24**, 386-389
 70. Christopeit, T., Yang, K. W., Yang, S. K., and Leiros, H. K. (2016) The structure of the metallo- β -lactamase VIM-2 in complex with a triazolylthioacetamide inhibitor. *Acta Crystallographica Section F* **72**, 813-819
 71. Toney, J. H., Fitzgerald, P. M. D., Grover-Sharma, N., Olson, S. H., May, W. J., Sundelof, J. G., Vanderwall, D. E., Cleary, K. A., Grant, S. K., Wu, J. K., Kozarich, J. W., Pompliano, D. L., and Hammond, G. G. Antibiotic sensitization using biphenyl

- tetrazoles as potent inhibitors of *Bacteroides fragilis* metallo- β -lactamase. *Chemistry and Biology* **5**, 185-196
72. Toney, J. H., Cleary, K. A., Hammond, G. G., Yuan, X., May, W. J., Hutchins, S. M., Ashton, W. T., and Vanderwall, D. E. (1999) Structure-activity relationships of biphenyl tetrazoles as metallo- β -lactamase inhibitors. *Bioorganic and Medicinal Chemistry Letters* **9**, 2741-2746
 73. Bebrone, C. (2007) Metallo- β -lactamases (classification, activity, genetic organization, structure, zinc coordination) and their superfamily. *Biochemical pharmacology* **74**, 1686-1701
 74. Bush, K. (2015) A resurgence of β -lactamase inhibitor combinations effective against multidrug-resistant Gram-negative pathogens. *International journal of antimicrobial agents* **46**, 483-493
 75. Somboro, A. M., Tiwari, D., Bester, L. A., Parboosing, R., Chonco, L., Kruger, H. G., Arvidsson, P. I., Govender, T., Naicker, T., and Essack, S. Y. (2015) NOTA: a potent metallo- β -lactamase inhibitor. *Journal of Antimicrobial Chemotherapy* **70**, 1594-1596
 76. King, A. M., Reid-Yu, S. A., Wang, W., King, D. T., De Pascale, G., Strynadka, N. C., Walsh, T. R., Coombes, B. K., and Wright, G. D. (2014) Aspergillomarasmine A overcomes metallo- β -lactamase antibiotic resistance. *Nature* **510**, 503-506
 77. Ishii, Y., Eto, M., Mano, Y., Tateda, K., and Yamaguchi, K. (2010) In Vitro Potentiation of Carbapenems with ME1071, a Novel Metallo- β -Lactamase Inhibitor, against Metallo- β -Lactamase-Producing *Pseudomonas aeruginosa* Clinical Isolates. *Antimicrobial Agents and Chemotherapy* **54**, 3625-3629
 78. Tehrani, K. H. M. E., and Martin, N. I. (2017) Thiol-containing metallo- β -lactamase inhibitors resensitize resistant Gram-negative bacteria to meropenem. *ACS Infectious Diseases*
 79. Jin, W., Arakawa, Y., Yasuzawa, H., Taki, T., Hashiguchi, R., Mitsutani, K., Shoga, A., Yamaguchi, Y., Kurosaki, H., Shibata, N., Ohta, M., and Goto, M. (2004) Comparative study of the inhibition of metallo- β -lactamases (IMP-1 and VIM-2) by thiol compounds that contain a hydrophobic group. *Biological and pharmaceutical bulletin* **27**, 851-856
 80. Brem, J., van Berkel, S. S., Zollman, D., Lee, S. Y., Gileadi, O., McHugh, P. J., Walsh, T. R., McDonough, M. A., and Schofield, C. J. (2016) Structural basis of metallo- β -lactamase inhibition by Captopril stereoisomers. *Antimicrobial Agents and Chemotherapy* **60**, 142-150
 81. Zhang, Y. L., Yang, K. W., Zhou, Y. J., LaCuran, A. E., Oelschlaeger, P., and Crowder, M. W. (2014) Diaryl-substituted azolythioacetamides: Inhibitor discovery of New Delhi metallo- β -lactamase-1 (NDM-1). *Medicinal Chemistry* **9**, 2445-2448
 82. Christopeit, T., Carlsen, T. J., Helland, R., and Leiros, H. K. (2015) Discovery of novel inhibitor scaffolds against the metallo- β -lactamase VIM-2 by Surface Plasmon Resonance (SPR) based fragment screening. *Journal of Medicinal Chemistry* **58**, 8671-8682
 83. Liscio, J. L., Mahoney, M. V., and Hirsch, E. B. (2015) Ceftolozane/tazobactam and ceftazidime/avibactam: two novel β -lactam/ β -lactamase inhibitor combination agents for the treatment of resistant Gram-negative bacterial infections. *International journal of antimicrobial agents* **46**, 266-271

84. Gentile, I., Maraolo, A. E., and Borgia, G. (2016) What is the role of the new β -lactam/ β -lactamase inhibitors ceftolozane/tazobactam and ceftazidime/avibactam? *Expert Review of Anti-infective Therapy* **14**, 875-878
85. Thaden, J. T., Pogue, J. M., and Kaye, K. S. (2017) Role of newer and re-emerging older agents in the treatment of infections caused by carbapenem-resistant Enterobacteriaceae. *Virulence* **8**, 403-416
86. Bush, K., and Bradford, P. A. (2016) β -Lactams and β -Lactamase Inhibitors: An Overview. *Perspectives in Medicine* **6**
87. Both, A., Büttner, H., Huang, J., Perbandt, M., Belmar Campos, C., Christner, M., Maurer, F. P., Kluge, S., König, C., Aepfelbacher, M., Wichmann, D., and Rohde, H. (2017) Emergence of ceftazidime/avibactam non-susceptibility in an MDR *Klebsiella pneumoniae* isolate. *Journal of Antimicrobial Chemotherapy* **72**, 2483-2488
88. Drawz, S. M., Papp-Wallace, K. M., and Bonomo, R. A. (2014) New β -lactamase inhibitors: a therapeutic renaissance in an MDR world. *Antimicrobial Agents and Chemotherapy* **58**, 1835-1846
89. Shlaes, D. M. (2013) New β -lactam- β -lactamase inhibitor combinations in clinical development. *Annals of the New York Academy of Sciences* **1277**, 105-114
90. Lahiri, S. D., Mangani, S., Jahić, H., Benvenuti, M., Durand-Reville, T. F., De Luca, F., Ehmann, D. E., Rossolini, G. M., Alm, R. A., and Docquier, J.-D. (2015) Molecular basis of selective inhibition and slow reversibility of Avibactam against Class D carbapenemases: A structure-guided study of OXA-24 and OXA-48. *ACS Chemical Biology* **10**, 591-600
91. Lahiri, S. D., Mangani, S., Durand-Reville, T., Benvenuti, M., De Luca, F., Sanyal, G., and Docquier, J. D. (2013) Structural insight into potent broad-spectrum inhibition with reversible recyclization mechanism: avibactam in complex with CTX-M-15 and *Pseudomonas aeruginosa* AmpC β -lactamases. *Antimicrobial Agents and Chemotherapy* **57**, 2496-2505
92. Emsley, P., and Cowtan, K. (2004) Coot: model-building tools for molecular graphics. *Acta Crystallographica. Section D* **60**, 2126-2132
93. Fernandes, P., and Martens, E. (2017) Antibiotics in late clinical development. *Biochemical pharmacology* **133**, 152-163
94. Stadler, M., and Dersch, P. (2016) *How to overcome the antibiotic crisis: facts, challenges, technologies and future perspectives*, Cham : Springer International Publishing, Cham
95. Garber, K. (2015) A β -lactamase inhibitor revival provides new hope for old antibiotics. *Nature Reviews and Drug Discovery* **14**, 445-447
96. Blizzard, T. A., Chen, H., Kim, S., Wu, J., Bodner, R., Gude, C., Imbriglio, J., Young, K., Park, Y.-W., Ogawa, A., Raghoobar, S., Hairston, N., Painter, R. E., Wisniewski, D., Scapin, G., Fitzgerald, P., Sharma, N., Lu, J., Ha, S., Hermes, J., and Hammond, M. L. (2014) Discovery of MK-7655, a β -lactamase inhibitor for combination with Primaxin®. *Bioorganic and Medicinal Chemistry Letters* **24**, 780-785
97. Castanheira, M., Rhomberg, P. R., Flamm, R. K., and Jones, R. N. (2016) Effect of the β -Lactamase inhibitor Vaborbactam combined with Meropenem against serine carbapenemase-producing Enterobacteriaceae. *Antimicrobial Agents and Chemotherapy* **60**, 5454-5458

98. Morinaka, A., Tsutsumi, Y., Yamada, K., Takayama, Y., Sakakibara, S., Takata, T., Abe, T., Furuuchi, T., Inamura, S., Sakamaki, Y., Tsujii, N., and Ida, T. (2017) In vitro and in vivo activities of the diazabicyclooctane OP0595 against AmpC-derepressed *Pseudomonas aeruginosa*. *The Journal of antibiotics* **70**, 246-250
99. Acharya, C., Coop, A., Polli, J. E., and Mackerell, A. D., Jr. (2011) Recent advances in ligand-based drug design: relevance and utility of the conformationally sampled pharmacophore approach. *Current computer-aided drug design* **7**, 10-22
100. Kapetanovic, I. M. (2008) Computer-aided drug discovery and development (CADD): in silico-chemico-biological approach. *Chemico-Biological Interactions* **171**, 165-176
101. Angelo, T., Bhattacharyya, R., Kataria, R., Kumar, S., Mathur, G., Mehta, S. K., Mendonça, F. J. B., Nain, S., Paliwal, S., and Patel, S. (2016) *Chemical drug design, Walter de Gruyter GmbH and Co KG*
102. Sun, Q., Law, A., Crowder, M. W., and Geysen, H. M. (2006) Homo-cysteinyll peptide inhibitors of the L1 metallo- β -lactamase, and SAR as determined by combinatorial library synthesis. *Bioorganic and Medicinal Chemistry Letters* **16**, 5169-5175
103. Minond, D., Saldanha, S. A., Subramaniam, P., Spaargaren, M., Spicer, T., Fotsing, J. R., Weide, T., Fokin, V. V., Sharpless, K. B., Galleni, M., Bebrone, C., Lassaux, P., and Hodder, P. (2009) Inhibitors of VIM-2 by screening pharmacologically active and click-chemistry compound libraries. *Bioorganic and Medicinal Chemistry Letters* **17**, 5027-5037
104. Hiraiwa, Y., Morinaka, A., Fukushima, T., and Kudo, T. (2009) Metallo- β -lactamase inhibitory activity of phthalic acid derivatives. *Bioorganic and Medicinal Chemistry Letters* **19**, 5162-5165
105. Minond, D., Saldanha, S. A., Spicer, T., Qin, L., Mercer, B. A., Roush, W. R., and Hodder, P. (2010) HTS assay for discovery of novel metallo- β -lactamase (MBL) inhibitors. in *Probe Reports From the NIH Molecular Libraries Program*, National Center for Biotechnology Information (US), Bethesda (MD). pp
106. Chen, Y., and Shoichet, B. K. (2009) Molecular docking and ligand specificity in fragment-based inhibitor discovery. *Nat Chem Biol* **5**, 358-364
107. Nichols, D. A., Jaishankar, P., Larson, W., Smith, E., Liu, G., Beyrouthy, R., Bonnet, R., Renslo, A. R., and Chen, Y. (2012) Structure-based design of potent and ligand-efficient inhibitors of CTX-M Class A β -lactamase. *Journal of Medicinal Chemistry* **55**, 2163-2172
108. Teotico, D. G., Babaoglu, K., Rocklin, G. J., Ferreira, R. S., Giannetti, A. M., and Shoichet, B. K. (2009) Docking for fragment inhibitors of AmpC β -lactamase. *Proceedings of the National Academy of Sciences of the United States of America* **106**, 7455-7460
109. Vella, P., Hussein, W. M., Leung, E. W. W., Clayton, D., Ollis, D. L., Mitić, N., Schenk, G., and McGeary, R. P. (2011) The identification of new metallo- β -lactamase inhibitor leads from fragment-based screening. *Bioorganic and Medicinal Chemistry Letters* **21**, 3282-3285
110. Faridoun, Hussein, W. M., Vella, P., Islam, N. U., Ollis, D. L., Schenk, G., and McGeary, R. P. (2012) 3-Mercapto-1,2,4-triazoles and N-acylated thiosemicarbazides

- as metallo- β -lactamase inhibitors. *Bioorganic and Medicinal Chemistry Letters* **22**, 380-386
111. Murray, C. W., and Rees, D. C. (2016) Opportunity knocks: Organic chemistry for Fragment-Based Drug Discovery (FBDD). *Angewandte Chemie International Edition* **55**, 488-492
 112. Scott, D. E., Coyne, A. G., Hudson, S. A., and Abell, C. (2012) Fragment-based approaches in drug discovery and chemical biology. *Biochemistry* **51**, 4990-5003
 113. Erlanson, D. A., Fesik, S. W., Hubbard, R. E., Jahnke, W., and Jhoti, H. (2016) Twenty years on: the impact of fragments on drug discovery. *Nature Review Drug Discovery* **15**, 605-619
 114. Lund, B. A., Christopheit, T., Guttormsen, Y., Bayer, A., and Leiros, H.-K. S. (2016) Screening and Design of Inhibitor Scaffolds for the Antibiotic Resistance Oxacillinase-48 (OXA-48) through Surface Plasmon Resonance Screening. *Journal of Medicinal Chemistry* **59**, 5542-5554
 115. Nichols, D. A., Renslo, A. R., and Chen, Y. (2014) Fragment-based inhibitor discovery against β -lactamase. *Future Medicinal Chemistry* **6**, 413-427
 116. Reynolds, C. H., Tounge, B. A., and Bembenek, S. D. (2008) Ligand binding efficiency: Trends, physical basis, and implications. *Journal of Medicinal Chemistry* **51**, 2432-2438
 117. Koskella, B., and Meaden, S. (2013) Understanding bacteriophage specificity in natural microbial communities. *Viruses* **5**, 806-823
 118. Harner, M. J., Frank, A. O., and Fesik, S. W. (2013) Fragment-based drug discovery using NMR spectroscopy. *Journal of biomolecular NMR* **56**, 65-75
 119. Aparoy, P., Kumar Reddy, K., and Reddanna, P. (2012) Structure and ligand based drug design strategies in the development of novel 5-LOX inhibitors. *Current Medicinal Chemistry* **19**, 3763-3778
 120. Patani, G. A., and LaVoie, E. J. (1996) Bioisosterism: A rational approach in drug design. *Chemical Reviews* **96**, 3147-3176
 121. Lima, L. M., and Barreiro, E. J. (2005) Bioisosterism: A useful strategy for molecular modification and drug design. *Current Medicinal Chemistry* **12**, 23-49
 122. Ballatore, C., Huryn, D. M., and Smith, A. B. (2013) Carboxylic acid bioisosteres in drug design. *ChemMedChem* **8**, 385-395
 123. Jin, W. C., Arakawa, Y., Yasuzawa, H., Taki, T., Hashiguchi, R., Mitsutani, K., Shoga, A., Yamaguchi, Y., Kurosaki, H., Shibata, N., Ohta, M., and Goto, M. (2004) Comparative study of the inhibition of metallo- β -lactamases (IMP-1 and VIM-2) by thiol compounds that contain a hydrophobic group. *Biological and Pharmaceutical Bulletin* **27**, 851-856
 124. Allen, F. H., Groom, C. R., Liebeschuetz, J. W., Bardwell, D. A., Olsson, T. S. G., and Wood, P. A. (2012) The hydrogen bond environments of 1H-tetrazole and tetrazolate rings: The structural basis for tetrazole-carboxylic acid bioisosterism. *Journal of Chemical Information and Modeling* **52**, 857-866
 125. Cantillo, D., Gutmann, B., and Kappe, C. O. (2011) Mechanistic insights on azide-nitrile cycloadditions: on the dialkyltin oxide-trimethylsilyl azide route and a new Vilsmeier-Haack-type organocatalyst. *Journal of the American Chemical Society* **133**, 4465-4475

126. Hawryluk, N. A., and Snider, B. B. (2000) Alcohol inversion using cesium carboxylates and DMAP in toluene. *The Journal of Organic Chemistry* **65**, 8379-8380
127. Park, J. D., and Kim, D. H. (2002) Cysteine derivatives as inhibitors for carboxypeptidase A: synthesis and structure–activity relationships. *Journal of Medicinal Chemistry* **45**, 911-918
128. Bikbulatov, R. V., Yan, F., Roth, B. L., and Zjawiony, J. K. (2007) Convenient synthesis and in vitro pharmacological activity of 2-thioanalogs of salvinorins A and B. *Bioorganic and Medicinal Chemistry Letters* **17**, 2229-2232
129. Zervas, L., Photaki, I., and Ghelis, N. (1963) On csteine and cystein peptides. II. S-acylcysteines in peptide synthesis. *Journal of the American Chemical Society* **85**, 1337-1341
130. Baraldi, P. G., Pollini, G. P., Zanirato, V., Barco, A., and Benetti, S. (1985) A new simplesynthesis of α -substituted acrylonitriles. *Synthesis* **1985**, 969-970
131. Lukyanov, S. M., Bliznets, I. V., Shorshnev, S. V., Aleksandrov, G. G., Stepanov, A. E., and Vasil'ev, A. A. (2006) Microwave-assisted synthesis and transformations of sterically hindered 3-(5-tetrazolyl)pyridines. *Tetrahedron* **62**, 1849-1863
132. Skagseth, S., Akhter, S., Paulsen, M. H., Muhammad, Z., Lauksund, S., Samuelsen, Ø., Leiros, H.-K. S., and Bayer, A. (2017) Metallo- β -lactamase inhibitors by bioisosteric replacement: Preparation, activity and binding. *European Journal of Medicinal Chemistry* **135**, 159-173
133. Yamaguchi, Y., Jin, W., Matsunaga, K., Ikemizu, S., Yamagata, Y., Wachino, J. I., Shibata, N., Arakawa, Y., and Kurosaki, H. (2007) Crystallographic investigation of the inhibition mode of a VIM-2 metallo- β -lactamase from *Pseudomonas aeruginosa* by a mercaptocarboxylate inhibitor. *Journal of Medicinal Chemistry* **50**, 6647-6653
134. Lienard, B. M. R., Garau, G., Horsfall, L., Karsisiotis, A. I., Damblon, C., Lassaux, P., Papamicael, C., Roberts, G. C. K., Galleni, M., Dideberg, O., Frere, J. M., and Schofield, C. J. (2008) Structural basis for the broad-spectrum inhibition of metallo- β -lactamases by thiols. *Organic and Biomolecular Chemistry* **6**, 2282-2294
135. Concha, N. O., Janson, C. A., Rowling, P., Pearson, S., Cheever, C. A., Clarke, B. P., Lewis, C., Galleni, M., Frère, J.-M., Payne, D. J., Bateson, J. H., and Abdel-Meguid, S. S. (2000) Crystal Structure of the IMP-1 metallo β -lactamase from *Pseudomonas aeruginosa* and its complex with a mercaptocarboxylate inhibitor: Binding determinants of a potent, broad-spectrum inhibitor. *Biochemistry* **39**, 4288-4298
136. Kurosaki, H., Yamaguchi, Y., Yasuzawa, H., Jin, W. C., Yamagata, Y., and Arakawa, Y. (2006) Probing, inhibition, and crystallographic characterization of metallo- β -lactamase (IMP-1) with fluorescent agents containing dansyl and thiol groups. *ChemMedChem* **1**, 969-980
137. Hinchliffe, P., González, M. M., Mojica, M. F., González, J. M., Castillo, V., Saiz, C., Kosmopoulou, M., Tooke, C. L., Llarrull, L. I., Mahler, G., Bonomo, R. A., Vila, A. J., and Spencer, J. (2016) Cross-class metallo- β -lactamase inhibition by bisthiazolidines reveals multiple binding modes. *Proc. Natl. Acad. Sci. U. S. A.* **113**, E3745-E3754
138. Brem, J., van Berkel, S. S., Zollman, D., Lee, S. Y., Gileadi, O., McHugh, P. J., Walsh, T. R., McDonough, M. A., and Schofield, C. J. (2016) Structural basis of

- metallo- β -lactamase inhibition by captopril stereoisomers. *Antimicrob. Agents Chemother.* **60**, 142-150
139. Mojica, M. F., Mahler, S. G., Bethel, C. R., Taracila, M. A., Kosmopoulou, M., Papp-Wallace, K. M., Llarrull, L. I., Wilson, B. M., Marshall, S. H., Wallace, C. J., Villegas, M. V., Harris, M. E., Vila, A. J., Spencer, J., and Bonomo, R. A. (2015) Exploring the role of residue 228 in substrate and inhibitor recognition by VIM metallo- β -lactamases. *Biochemistry* **54**, 3183-3196
 140. King, D. T., Worrall, L. J., Gruninger, R., and Strynadka, N. C. J. (2012) New Delhi metallo- β -lactamase: Structural insights into β -lactam recognition and Inhibition. *J. Am. Chem. Soc.* **134**, 11362-11365
 141. Hua, Y., and Flood, A. H. (2010) Click chemistry generates privileged CH hydrogen-bonding triazoles: the latest addition to anion supramolecular chemistry. *Chemical Society reviews* **39**, 1262-1271
 142. Zhou, C. H., and Wang, Y. (2012) Recent researches in triazole compounds as medicinal drugs. *Current Medicinal Chemistry* **19**, 239-280
 143. Silverman, S. M., Moses, J. E., and Sharpless, K. B. (2017) Reengineering antibiotics to combat bacterial resistance: Click chemistry [1,2,3]-Triazole Vancomycin dimers with potent activity against MRSA and VRE. *Chemistry – A European Journal* **23**, 79-83
 144. Loren, J. C., and Sharpless, K. B. (2005) The Banert Cascade: A Synthetic Sequence to Polyfunctional NH-1,2,3-Triazoles. *Synthesis* **9**, 1514-1520
 145. Weide, T., Adrian Saldanha, S., Minond, D., Spicer, T., Fotsing, J., Spaargaren, M., Frère, J.-M., Bebrone, C., Barry Sharpless, K., Hodder, P., and V. Fokin, V. (2010) *NH-1,2,3-Triazole Inhibitors of the VIM-2 metallo- β -lactamase*,
 146. Banert, K., and Hagedorn, M. (1989) First isolation of allenyl azides. *Angewandte Chemie International Edition* **28**, 1675
 147. Paetzel, M., Danel, F., de Castro, L., Mosimann, S. C., Page, M. G. P., and Strynadka, N. C. J. (2000) Crystal structure of the class D β -lactamase OXA-10. *Nature Structural and Molecular Biology* **7**, 918-925
 148. Düfert, M. A., Billingsley, K. L., and Buchwald, S. L. (2013) Suzuki-Miyaura cross-coupling of unprotected, nitrogen-rich heterocycles: Substrate scope and mechanistic investigation. *Journal of the American Chemical Society* **135**, 12877-12885
 149. Crudden, C. M., Ziebenhaus, C., Rygus, J. P. G., Ghazati, K., Unsworth, P. J., Nambo, M., Voth, S., Hutchinson, M., Laberge, V. S., Maekawa, Y., and Imao, D. (2016) Iterative protecting group-free cross-coupling leading to chiral multiply arylated structures. *Nature Communications* **7**, 11065
 150. Paul, S., Islam, M. M., and Islam, S. M. (2015) Suzuki-Miyaura reaction by heterogeneously supported Pd in water: recent studies. *Royal Society of Chemistry Advances* **5**, 42193-42221
 151. Ramgren, S. D., Hie, L., Ye, Y., and Garg, N. K. (2013) Nickel-catalyzed Suzuki-Miyaura couplings in green solvents. *Organic Letters* **15**, 3950-3953
 152. Chatterjee, A., and Ward, T. R. (2016) Recent advances in the Palladium catalyzed Suzuki-Miyaura cross-coupling reaction in water. *Catalysis Letters* **146**, 820-840
 153. Du, X., Liu, X., Xu, L., Jiang, W., Bao, M., and He, R. (2012) Chemoselective Suzuki-Miyaura coupling of Bromophenyl-substituted Bromoallenes with arylboronic acids. *Synlett* **23**, 1505-1510

154. Martin, R., and Buchwald, S. L. (2008) Palladium-catalyzed Suzuki-Miyaura cross-coupling reactions employing dialkylbiaryl phosphine ligands. *Accounts of Chemical Research* **41**, 1461-1473
155. Congreve, M., Carr, R., Murray, C., and Jhoti, H. (2003) A 'Rule of Three' for fragment-based lead discovery? *Drug Discovery Today* **8**, 876-877
156. Petrovčić, M., Alešković, M., and Mlinarić-Majerski, K. (2014) One-pot synthesis of pyrrolo[1,2]quinazolinone derivatives. *Synlett* **25**, 2769-2772
157. Puri, M., Gatard, S., Smith, D. A., and Ozerov, O. V. (2011) Competition studies of oxidative addition of aryl halides to the (PNP)Rh fragment. *Organometallics* **30**, 2472-2482
158. Caron, S., Massett, S. S., Bogle, D. E., Castaldi, M. J., and Braish, T. F. (2001) Palladium-catalyzed Suzuki-Miyaura cross-coupling reactions employing dialkylbiaryl phosphine ligands. *Organic Process Research and Development* **5**, 254
159. Dajka-Halász, B., Monsieurs, K., Éliás, O., Károlyházy, L., Tapolcsányi, P., Maes, B. U. W., Riedl, Z., Hajós, G., Dommissie, R. A., Lemièrre, G. L. F., Košmrlj, J., and Mátyus, P. (2004) Synthesis of 5H-pyridazino[4,5]indoles and their benzofurane analogues utilizing an intramolecular Heck-type reaction. *Tetrahedron* **60**, 2283
160. Itoh, T., and Mase, T. (2005) Direct synthesis of hetero-biaryl compounds containing an unprotected NH₂ group via Suzuki-Miyaura reaction. *Tetrahedron Letters* **46**, 3573
161. Thompson, A. E., Hughes, G., Batsanov, A. S., Bryce, M. R., Parry, P. R., and Tarbit, B. (2005) Palladium-Catalyzed Cross-coupling reactions of pyridylboronic acids with heteroaryl halides bearing a primary amine group: synthesis of highly substituted bipyridines and pyrazinopyridines. *The Journal of Organic Chemistry* **70**, 388
162. Schulz, T., Torborg, C., Enthaler, S., Schäffner, B., Dumrath, A., Spannenberg, A., Neumann, H., Börner, A., and Beller, M. (2009) A general palladium - catalyzed amination of aryl halides with ammonia. *Chemistry— A European Journal* **15**, 4528-4533
163. Vuoti, S., Autio, J., Laitila, M., Haukka, M., and Pursiainen, J. (2008) Palladium - catalyzed suzuki-miyaura cross - coupling of various aryl halides using ortho - alkyl - substituted arylphosphanes and (ortho - alkylphenyl)alkylphosphanes under microwave heating. *European Journal of Inorganic Chemistry*, 397
164. Youn, S. W., and Bihn, J. H. (2009). *Tetrahedron letters* **50**, 4598
165. Lund, B. A., Christopheit, T., Guttormsen, Y., Bayer, A., and Leiros, H. K. S. (2016) Screening and design of inhibitor scaffolds for the antibiotic resistance Oxacillinase-48 (OXA-48) through Surface Plasmon Resonance screening. *Journal of Medicinal Chemistry* **59**, 5542-5554
166. Himo, F., Lovell, T., Hilgraf, R., Rostovtsev, V. V., Noodleman, L., Sharpless, K. B., and Fokin, V. V. (2005) Copper(I)-catalyzed synthesis of azoles. DFT study predicts unprecedented reactivity and intermediates. *Journal of the American Chemical Society* **127**, 210-216
167. Brem, J., Struwe, W. B., Rydzik, A. M., Tarhonskaya, H., Pfeffer, I., Flashman, E., van Berkel, S. S., Spencer, J., Claridge, T. D. W., McDonough, M. A., Benesch, J. L. P., and Schofield, C. J. (2015) Studying the active-site loop movement of the São Paulo metallo-β-lactamase-1 *Chemical Science* **6**, 956-963

168. Garau, G., Bebrone, C., Anne, C., Galleni, M., Frère, J.-M., and Dideberg, O. (2005) A metallo- β -lactamase enzyme in action: Crystal structures of the monozinc carbapenemase CphA and its complex with Biapenem. *Journal of Molecular Biology* **345**, 785-795
169. Bush, K. (2013) Proliferation and significance of clinically relevant β -lactamases. *Annals of the New York Academy of Sciences* **1277**, 84-90
170. Brem, J., van Berkel, S. S., Aik, W., Rydzik, A. M., Avison, M. B., Pettinati, I., Umland, K. D., Kawamura, A., Spencer, J., Claridge, T. D., McDonough, M. A., and Schofield, C. J. (2014) Rhodanine hydrolysis leads to potent thioenolate mediated metallo- β -lactamase inhibition. *Nature chemistry* **6**, 1084-1090
171. Zervosen, A., Lu, W. P., Chen, Z., White, R. E., Demuth, T. P., Jr., and Frere, J. M. (2004) Interactions between penicillin-binding proteins (PBPs) and two novel classes of PBP inhibitors, arylalkylidene rhodanines and arylalkylidene iminothiazolidin-4-ones. *Antimicrobial Agents and Chemotherapy* **48**, 961-969
172. Zervosen, A., Sauvage, E., Frere, J. M., Charlier, P., and Luxen, A. (2012) Development of new drugs for an old target: the penicillin binding proteins. *Molecules (Basel, Switzerland)* **17**, 12478-12505
173. Grant, E. B., Guiadeen, D., Baum, E. Z., Foleno, B. D., Jin, H., Montenegro, D. A., Nelson, E. A., Bush, K., and Hlasta, D. J. (2000) The synthesis and SAR of rhodanines as novel class C β -lactamase inhibitors. *Bioorganic and Medicinal Chemistry Letters* **10**, 2179-2182
174. Spicer, T., Minond, D., Enogieru, I., Saldanha, S.A., Allais, C., Qin L., Mercer, B.A., Roush, W.R. and Hodder P. (2010). in *Probe Reports from the NIH Molecular Libraries Program*, National Center for Biotechnology Information (US), Bethesda (MD). pp
175. Mendgen, T., Steuer, C., and Klein, C. D. (2012) Privileged scaffolds or promiscuous binders: A comparative study on Rhodanines and related heterocycles in Medicinal Chemistry. *Journal of Medicinal Chemistry* **55**, 743-753
176. Zinglé, C., Tritesch, D., Grosdemange-Billiard, C., and Rohmer, M. (2014) Catechol-rhodanine derivatives: Specific and promiscuous inhibitors of *Escherichia coli* deoxyxylulose phosphate reductoisomerase (DXR). *Bioorganic & Medicinal Chemistry* **22**, 3713-3719
177. Cahill, S. T., Cain, R., Wang, D. Y., Lohans, C. T., Wareham, D. W., Oswin, H. P., Mohammed, J., Spencer, J., Fishwick, C. W., McDonough, M. A., Schofield, C. J., and Brem, J. (2017) Cyclic boronates inhibit all classes of β -lactamases. *Antimicrobial Agents and Chemotherapy* **61**
178. Vallejo, J. A., Martínez-Guitián, M., Vázquez-Ucha, J. C., González-Bello, C., Poza, M., Buynak, J. D., Bethel, C. R., Bonomo, R. A., Bou, G., and Beceiro, A. (2016) LN-1-255, a penicillanic acid sulfone able to inhibit the class D carbapenemase OXA-48. *Journal of Antimicrobial Chemotherapy* **71**, 2171-2180
179. Bush, K., and Page, M. G. P. (2017) What we may expect from novel antibacterial agents in the pipeline with respect to resistance and pharmacodynamic principles. *Journal of Pharmacokinetics and Pharmacodynamics* **44**, 113-132

Appendix

Paper 1

Paper 2

Paper 3